Effect of Thermal Fluctuations on Classical and Quantum Systems at Small Scales.

By

Shubhashis Rana

PHYS07200904002

Institute of Physics, Bhubaneswar

A thesis submitted to the

Board of Studies in Physical Sciences

In partial fulfillment of requirements

For the Degree of

DOCTOR OF PHILOSOPHY

of

HOMI BHABHA NATIONAL INSTITUTE

March, 2016

STATEMENT BY AUTHOR

This dissertation has been submitted in partial fulfillment of requirements for an advanced degree at Homi Bhabha National Institute (HBNI) and is deposited in the Library to be made available to borrowers under rules of the HBNI. Brief quotations from this dissertation are allowable without special permission, provided that accurate acknowledgement of source is made. Requests for permission for extended quotation from or reproduction of this manuscript in whole or in part may be granted by the Competent Authority of HBNI when in his or her judgment the proposed use of the material is in the interests of scholarship. In all other instances, however, permission must be obtained from the author.

Date:- 2^{nd} March 2016 (Shubhashis Rana)

CERTIFICATE

This is to certify that the thesis entitled "**Effect of thermal fluctuations on classical and quantum systems at small scales.**", which is being submitted by **Mr. Shubhashis Rana**, in partial fulfillment of the degree of **Doctor of Philosophy in Physics** of **Homi Bhabha National Institute** is a record of his own research work carried by him. He has carried out his investigations for the last six years on the subject matter of the thesis under my supervision at **Institute of Physics, Bhubaneswar**. To the best of our knowledge, the matter embodied in this thesis has not been submitted for the award of any other degree.

Signature of the Candidate **Signature of the Supervisor**

Shubhashis Rana
Institute of Physics
Bhubaneswar

Prof. Arun M. Jayannavar
Senior Professor
Institute of Physics
Bhubaneswar

Date:- 2^{nd} March 2016.

DECLARATION

I, Shubhashis Rana, hereby declare that the investigations presented in the thesis have been carried out by me. The matter embodied in the thesis is original and has not been submitted earlier as a whole or in part for a degree/diploma at this or any other Institution/University.

Date: 2^{nd} March 2016 (Shubhashis Rana)

To My Parents

Acknowledgement

It is a great pleasure for me to thank all the people who have helped me to attain the successful completion of my thesis. Firstly, I would like to express my deep sense of gratitude towards my thesis advisor, Prof. A. M. Jayannavar, who has not only guided me through the PhD course at the institute, but has encouraged and supported me in every step of my work. His critical approach towards any topic, has helped in bolstering my concepts and knowledge in several areas. His and madam's affectionate and friendly nature has also made my process of learning a pleasant one and made the atmosphere homely. I would like to extend my sincere thanks to all the members of my annual review committee, for various fruitful and illuminating discussions regarding my work. Their constructive comments and suggestions have helped me to get further insights into the problems. I have also benefited a lot from the lectures delivered by our teachers in the predoctoral course. I am grateful to Prof. G. Tripathy, Prof. M. Mahato, Prof. R. Krishnan, Dr. Sourabh Lahiri and Dr. Arnab Saha for giving their valuable time in correcting the introduction to my thesis and synopsis.

I am also thankful to all my collaborators, namely, Dr. Sourabh Lahiri, Dr. Arnab Saha. and Mr. Priyo Shankar Pal. Working with them has never allowed monotonicity to seep in, and has been a great learning experience. I would like to especially thank Dr. Sourabh Lahiri for being a good friend and for assistance in every difficulties of my work. I would like to thank Mr. Priyo Shankar Pal for being a great friend and companion throughout, ever since we have begun our collaboration.

My heartfelt gratitude goes to all my friends, seniors and juniors at IOP who have made my stay at the institute pleasant and cheerful. I always reminisce the colorful days of IOP that they have gifted.

I thank all the academic and non-academic staff members as well as the administration of IOP for helping me in many ways to complete my PhD.

I am indebted to my teachers who had taught us with ardent zeal during my School and College days. My deep regards would be ever-present for Prof. A. Nayak, Prof. P. K. Mukherjee, and Prof. M. Acharyya for their inspirational teachings that lead to choose my path toward research. I am grateful to Timir babu for his ingenious style of teaching to make our foundation in basic physics during B.Sc. days. I am

greatly indebted to our retired school teacher Pyne babu, who, in my school days, had instilled in us a deep interest in the subject.

I express my deep regards and gratitude towards my family members. Without their constructive support and scarification I may not come here. Their love and affection have always remained an invaluable source of inspiration for me. I am greatly thankful to my brother Snehashis, who has been a great friend and companion of mine throughout my life. Finally, I would like to show my deep reverence to my late grandmothers for their warmth support to put aside all the difficulties and helped me focused in my life.

Date: 2^{nd} March 2016 (Shubhashis Rana)

Contents

SYNOPSIS

Classical thermodynamics holds for macroscopic systems and is built around the concept of equilibrium states. However, the rich diverse field of non-equilibrium processes is a subject of intensive ongoing current research. In microscopic systems, fluctuations start playing a dominant role. In these systems the fluctuations of physical quantities become comparable to the relevant energy exchanges of the system. The area of stochastic thermodynamics [1] provides a framework for extending notions of classical thermodynamics to such small systems. The concepts of work, heat, and entropy are thereby extended to the level of individual system trajectories during the nonequilibrium processes. This is in contrast to the case of macroscopic systems where one can determine these thermodynamic quantities very accurately and the probability distributions reduce to a delta function.

For microscopic systems, in some trajectories one can even observe local violation of the second law of thermodynamics and these trajectories are referred to as transient second law violating trajectories. Along these trajectories the total entropy production becomes negative. For some trajectories work done on the system becomes less than the equilibrium free energy change. However, the second law continuous to be valid when averaged over all the trajectories [2].

When the microscopic systems are driven far away from equilibrium, fluctuations in physical quantities satisfy a number of strong relations. They are collectively known as fluctuation theorems [2,3,4,5,6,7]. These theorems are valid even beyond the linear response regime and replace inequalities of thermodynamic relations into equalities. From these theorems one can obtain linear and non linear response coefficients, and moreover, the second law of thermodynamics can be obtained as a corollary. These theorems also shed light on some fundamental problems such as how irreversibility arises from underlying time reversal dynamics. One of the FT was initially put forward by Jarzynski [3] in the form of the nonequilibrium work theorem, by means

of which one can extract information about equilibrium changes in free energy ΔF by measuring the nonequilibrium work W performed on a system by the external drive. The system is initially prepared in equilibrium, and then driven away from equilibrium using some predetermined protocol $\lambda(t)$ which runs from $t = 0$ to $t = \tau$. The Jarzynski Equality is given by

$$\langle e^{-\beta W} \rangle = e^{-\beta \Delta F}. \tag{0.1}$$

The work W, depends on trajectory of the system, whose initial state is sampled from equilibrium distribution. $\beta = 1/k_B T$, T being the temperature of the bath. The angular brackets denote averaging over an ensemble of such trajectories and the free energy differences $\Delta F = F(\lambda(\tau)) - F(\lambda(0)$. A stronger fluctuation theorem was provided by Crooks [4, 5] in the form

$$\frac{P_f(W)}{P_r(-W)} = e^{\beta(W - \Delta F)}, \tag{0.2}$$

$P_f(W)$ and $P_r(W)$ being the work probability densities generated under the forward protocol $\lambda(t)$ and the reverse protocol $\lambda(\tau - t)$, respectively. Later a more general fluctuation theorem was put forward by Seifert which contains Jarzynski and Crooks theorems as special cases [6, 7] taking arbitrary initial distribution. The Seifert fluctuation theorem states that the ratio of the probability of a phase space trajectory along forward process to that of the corresponding reverse phase space trajectory in the reverse process is equal to exponential of total entropy production along the forward trajectory. In particular total entropy production Δs_{tot} obeys integral fluctuation theorems, $\langle e^{-\Delta s_{tot}} \rangle = 1$.

Fluctuation theorems constrain the performance characteristics of engines/molecular motors at nano-scales and has proved successful in understanding the micro and the nano world. With the improvement of technology one can monitor micron/nano sized

objects such as RNA, single atom, molecular motor etc. Several fluctuation theorems are verified experimentally.

In this thesis, We have mainly focused on the extensions of these fluctuation theorems to different scenarios. These include fluctuation relations for heat engines in steady state, generalized fluctuation theorems in presence of measurement and feedback for quantum systems, and fluctuation theorems for inhomogenious system. We have also studied the effect of confinement on stochastic resonance. In the following we describe our work in brief.

A fluctuation relation for heat engines (FRHE) has been derived recently [8]. We take a simple model [9], where the system is connected periodically with two heat baths. The protocol is as follows. In the beginning, the system is in contact with the cooler bath. The system is then coupled to the hotter bath and the external parameters are changed cyclically, eventually bringing the system back to its initial state, once the coupling with the hot bath is switched off. In this work, we lift the condition of initial thermal equilibrium and derive a new fluctuation relation for the central system (heat engine) being in a time-periodic steady state (TPSS). Carnots inequality for classical thermodynamics follows as a direct consequence of this fluctuation theorem even in TPSS. For the special case of the absence of hot bath we obtain the integral fluctuation theorem for total entropy and for the case of no extraction of work we get the generalized exchange fluctuation theorem. Recently micro-sized heat engines have been realized experimentally [10] in the TPSS. We numerically simulate the same model and verify our proposed theorems.

In another work, we study the stochastic thermodynamics of small scale heat engines [11]. They operate in presence of highly fluctuating input and output energy fluxes and are therefore much better characterized by fluctuating efficiencies. Finite time stochastic thermodynamics provides us with a consistent framework for small scale systems operating arbitrary far from equilibrium. Using this framework we

have carried out an extensive analysis of single particle heat engines by manipulating a Brownian particle in a time dependent harmonic potential with time-dependent coupling to two heat baths. Different cyclic protocols with and without inertia are considered. Thermodynamic quantities such as work, heat and stochastic efficiency exhibit strong fluctuations in time periodic steady states. The fluctuations of stochastic efficiency dominates over the mean value even in the quasi-static regime. The phase diagrams for system operations are qualitatively different for inertial and over-damped regimes. This is supported by our analytical results in the quasi-static regime. In time periodic steady state there are several realizations where the system does not work as a heat engine. Such transient second law violating realizations decrease as we increase cycle time. Hence for larger cycle times our system works more reliably as an engine. Some of our results differ qualitatively from earlier claims in the literature. We have also verified fluctuation relations for heat engines in time periodic steady state.

We have generalized the fluctuation theorems in presence of feedback and measurements for quantum systems [12]. Intermediate measurements on the system leads to information gain that can be used to extract more work from the system by driving it using appropriate feedback. We have derived the Jarzynski equality (JE) for an isolated quantum system in three different cases: (i) the full unitary evolution with no intermediate measurements, (ii) with intermediate measurements of arbitrary observables and (iii) with intermediate measurements whose outcomes are used to modify the external protocol (feedback). Our treatment is based on path probability in state space for each realization. This is in contrast to the formal approach based on projection operators and density matrices. We have found that the JE remains unaffected in the second case, but gets modified in the third case where the mutual information between the measured values with the actual eigenvalues must be incorporated into the relation.

In an another work, using same trajectory dependent path probability formalism in state space, we have also derived generalized entropy production fluctuation relations for a quantum system in the presence of measurement and feedback [13]. We have obtained these results for three different cases: (i) system evolving in isolation from its surroundings; (ii) system weakly coupled to a heat bath; and (iii) system in contact with a reservoir using quantum Crooks fluctuation theorem. In the case (iii), we have followed the treatment carried out in [14], where a quantum trajectory has been defined as a sequence of alternating work and heat steps. The obtained entropy production fluctuation theorems retain the same form as in the classical case. The inequality of second law of thermodynamics gets modified in the presence of information. These fluctuation theorems are robust against intermediate measurements of any observable performed with respect to von Neumann projective measurements as well as weak or positive operator valued measurements.

In a separate work, we compare the fluctuation relations for work and entropy in underdamped and overdamped systems, when the friction coefficient of the medium is space-dependent [15]. We find that these relations remain unaffected in both cases. However, for the overdamped system, the analysis is more involved and a blind application of normal rules of calculus would lead to inconsistent results.

Stochastic resonance (SR) is a phenomenon in which a feeble input signal applied to a bistable potential gets magnified at a particular noise strength. In this phenomenon noise plays a constructive role. It has previously been shown that the average injected energy to the system is the best quantifier of SR. Using this quantifier, we have observed bistability as a necessary but not a sufficient condition for observing SR [16]. SR is observed in superharmonic (hard) potentials, but is not observed in subharmonic (soft) potentials, even through the potential is bistable. However, in both soft and hard potentials, we have observed resonance phenomenon as a function of driving frequency. Some subtleties in the dynamics of particle in the

two different types of potentials are analyzed based on the probability distributions of work done on the system over a period.

Bibliography

[1] K. Sekimoto, Prog. Theor. Phys. Suppl. **130**, 17 (1998).

[2] U. Seifert, Rep. Prog. Phys. **75**, 126001 (2012)

[3] C. Jarzynski, Phys. Rev. Lett. **78**, 2690 (1997).

[4] G. E. Crooks, J. Stat. Phys. **90**, 1481 (1998).

[5] G. E. Crooks, Phys. Rev. E **60**, 2721 (1999).

[6] U. Seifert, Phys. Rev. Lett. **95**, 040602 (2005).

[7] U. Seifert, Eur. Phys. J. B **64**, 423 (2008).

[8] N. A. Sinitsyn, J. Phys. A: Math theor **44**, 405001 (2011).

[9] S. Lahiri, S. Rana and A. M. Jayannavar, J. Phys. A: Math theor **45**, 465001 (2012)

[10] V. Blickle and C. Bechinger, Nature Phys. **8**,143 (2012).

[11] S. Rana, P. S. Pal, A. Saha and A. M. Jayannavar, Phys. Rev. E **90**, 042146 (2014).

[12] S. Rana, S. Lahiri and A. M. Jayannavar, Pramana **79**, 233 (2012).

[13] S. Rana, S Lahiri and A. M. Jayannavar. Pramana **80**, 207 (2013).

[14] H. T. Quan and H. Dong, arxiv/cond-mat: 0812.4955

[15] S. Lahiri, S. Rana and A. M. Jayannavar, Physics Letters A **378**, 979 (2014).

[16] S. Rana, S. Lahiri and AM Jayannavar, Eur. Phys. J. B **84**, 323 (2011).

Publications:

1. ** The role of soft versus hard bistable systems on stochastic resonance using average cycle energy as a quantifier,
   S. Rana, S. Lahiri and AM Jayannavar,
   The European Physical Journal B **84**, 323 (2011).

2. Fluctuation theorems in presence of information gain and feedback,
   S. Lahiri, **S. Rana** and A. M. Jayannavar,
   J. Phys. A: Math. Theor. **45**, 065002 (2012).

3. ** Quantum Jarzynski equality with multiple measurement and feedback for isolated system,
   S. Rana, S. Lahiri and A. M. Jayannavar,
   Pramana **79**, 233 (2012).

4. ** Fluctuation relations for heat engines in time-periodic steady states.
   S. Lahiri, **S. Rana** and A. M. Jayannavar
   J. of Phys. A: Math. and Theor. **45**, 465001 (2012)

5. ** Generalized entropy production fluctuation theorems for quantum systems,
   S. Rana, S Lahiri and A. M. Jayannavar,
   Pramana **80**, 207 (2013).

6. ** Fluctuation theorems in inhomogenious media under coarse graining,
   S. Lahiri, **S. Rana** and A. M. Jayannavar,
   Physics Letters A **378**, 979 (2014).

7. Extracting work from a single heat bath - A case study on Brownian particle under external magnetic field in presence of information,
   P. S. Pal, **S. Rana**, A. Saha and A. M. Jayannavar,
   Phys. Rev. E **90**, 022143 (2014).

8. ** Single Particle Stochastic Heat Engine,
   S. Rana, P. S. Pal, A. Saha and A. M. Jayannavar,
   Phys. Rev. E **90**, 042146 (2014).

9. Anomalous Brownian Refrigerator,
   S. Rana, P. S. Pal, A. Saha and A. M. Jayannavar,
   ArXiv: 1503.02559.

Here, ∗∗ denotes the papers on which my thesis is based.

Chapter 1

Introduction

1.1 Introduction

'Thermo' means heat and 'dynamics' means motion and thermodynamics is the science of flow of heat. It is about the study of energy and its transformation into different forms [1]. Usually, thermodynamics deals with systems having large ($\sim 10^{23}$) number of particles without giving much importance to their individual microscopic properties. Therefore, it can describe macroscopic physical properties of matter generically. For example, thermodynamics tells us physical properties like pressure, volume, temperature of $\sim 10^{23}$ number of gas molecules at high temperatures and low density can be related in a simple way as $\frac{PV}{T}$ = constant, which is a result that is independent of the microscopic properties of individual gas molecules. On the other hand, if we want to describe the system from microscopic point of view, we need the help of statistical mechanics [2, 3].

Any typical macroscopic system contains large number of molecules and this has large ($\sim 10^{23}$) degrees of freedom. For classical systems these molecules obey simple Newton's equations of motion in some force field with appropriate boundary conditions. Now, it is impossible to know all the initial coordinates and momenta of each individual molecule/atom. Moreover, available techniques to solve dynamical equations are incapable to handle such huge number of equations. However, if we coarse grain our observation, we find that these positions and momenta obey some probability laws. Indeed, the thermodynamic variables such as energy, volume, pressure, etc. can be described probabilistically.

It can be shown that relative fluctuations for fixed intensive quantities (temperature, pressure etc.), extensive quantities (volume, energy etc.) are proportional to $1/\sqrt{N}$ where N is the number of particles. For macroscopic systems, as the system size is large, one simply recovers the classical thermodynamics observation. It can be mentioned that depending on boundary, the system can be described in terms of

microcanonical, canonical or grand canonical ensembles. For isolated system, microcanonical statistical mechanics is applicable. For this case, each micro-state has equal probability. For canonical system, energy exchange (thermal or mechanical) with the surroundings is allowed. Grand canonical system is more general in which both energy and particle exchange is possible. Gibbs, Maxwell and Boltzmann developed the concepts of equilibrium statistical mechanics more than a century ago. The formalism of equilibrium statistical mechanics is that we first have to find the equilibrium distribution of occupation of the energy states of the system and determine the partition function. Free energy can then be calculated from the partition function. Other thermodynamic variables like average energy, specific heat, entropy, magnetic moment, susceptibility, conductance etc. can be found by taking appropriate derivatives of the free energy. Hence, statistical mechanics describes the macroscopic phenomena of the system statistically, by observing the properties of the individual molecules and builds a bridge between mechanics with the thermodynamics where the typical time scale of observation is much larger than atomic time scale.

It is easy to describe the system in equilibrium where the thermodynamic variables do not change in time and they are related to each other. This relationship is called equation of state. Equation of state of a system is the only system specific input which classical thermodynamics requires. If we shift our focus away from the equilibrium state, we come across the rich and diverse domain of non-equilibrium processes. The system goes out of equilibrium in the presence of some drive and the principle of detailed balance is broken. Take an example of a rod connecting two thermal baths. When the two baths are kept at same temperature, the rod will be in equilibrium with the baths. Now, if the rod is connected to two baths at different temperatures, heat will flow through the rod from hot to the cold bath and rod will be out of equilibrium. Actually we are surrounded by these noneqilibrium systems. Examples include biological systems, driven colloids, flow of fluids, mechanical and biological

transport, spreading of species, traffic movement, stock market, social network etc. Although, equilibrium statistical mechanics can be used to describe the systems close to equilibrium, linear response theory connects response functions for small drives to equilibrium fluctuations. In this regime one obtains celebrated Onsagar reciprocal relation and fluctuation dissipation relation. It can not be applied when the system is far away from equilibrium. Indeed, there is no common prescription to deal with such systems. Depending on the problem, some of the techniques can be applied to describe the dynamical properties of the system in this regime. These include diffusion equation [4], Fokker Planck equation [4, 5, 7, 6, 8], Boltzmann transport equation [9], Cahn-Hilliard equation [10] etc. It is important to note that all these equations are irreversible in time although the underlying microscopic dynamics is time reversible. This is quite surprising and a long standing paradox is that how individual particle, obeying time reversible equations of motion, when moving collectively, show time-irreversibility. In this respect, Arthur Eddington first introduced the concepts of arrow of time. This can be understood by a simple example. Take a box which is divided into two parts by a partition and fill one part of it with ideal gas. Now, if the partition is removed, the gas will fill the full box and after some time it reaches equilibrium. But we do not observe the reverse process spontaneously, i.e., if initially the gas is in equilibrium in the full box after some time we do not find all the gas molecules in one half of the box. Although it is microscopically possible, as the microscopic dynamics obey simple Newton's laws of motion. If we reverse the velocities of all the molecules at the full box in equilibrium, theoretically we can observe the reverse process. However, in practice it does not happen because to reach this initial condition in equilibrium it may take a time that is more than the age of the universe. The concept of irreversibility is directly related to entropy. The second law states that entropy always increases with time. Entropy is a measure of disorder. System always chooses a path in which disorder (number of accessible configurations) increases. For

isolated systems at equilibrium, the disorder is maximum. That's why we do not observe the reverse process.

For macroscopic systems, the effect of thermal fluctuations are negligible. One can hardly observe any deviation of physical quantities from their means except in some special cases such as near a phase transitions. At the critical point fluctuations become so large that they become evident to macroscopic observations [1]. As soon as the system size becomes macroscopic fluctuations start playing dominant role. In this limit, the thermal fluctuations $k_BT \approx 4 \times 10^{-21} J$ at room temperature (300 K) are comparable to the relevant energy exchanges of the system. To describe the thermodynamics at this scale a new framework of stochastic energetics [12,11,13] has evolved in the last two decades. Indeed, the concepts of input work, heat dissipation, entropy production etc. have been extended to the level of individual phase space trajectories. These thermodynamic quantities now become path dependent variables and evolve along with the phase space evolution of the system. Moreover, for a single trajectory it is possible to observe a rare event such as the decreasing of total entropy over a short time interval. However, if we take ensemble of such trajectories by repeating the same experiment again and again, the second law is obeyed on average.

Research in this area has given birth to a group of exact and powerful theorems that dictate the behavior of such systems. They are commonly referred to as the *Fluctuation Theorems* (FTs) [15,16,17,18,19,20,21,22,23,24,25,26,27,13,28,29,30], and these theorems are valid even far from equilibrium, well beyond the scope of the linear response theory. These theorems have been derived for different scenarios such as for deterministic dynamics, stochastic dynamics and even for quantum dynamics [31, 32, 33, 34, 35]. Different FTs hold when the system is in the transient regime or in non-equilibrium steady state (NESS). The FTs provide quantitative relations that measure the probability to observe rare events concerning the work performed by the system [23, 29] or the entropy production [22] and also shed new light on

the fundamental problem of how irreversibility arises from underlying time reversal symmetries. Moreover the second law is obtained as a corollary from these theorems.

With the improvement of technology in last two decades, it has been possible to manipulate and measure physical systems at the micro and nano scale. This opens up vast new areas for new experiments and gives us an opportunity to improve our understanding of the micro/nano world. Tiny biological systems, provide a natural setting for applying the tools of non-equilibrium statistical mechanics. Several such set-ups include bio-polymers like DNA, RNA etc. manipulated by optical tweezers [37,38], molecular motors driven by chemical gradients [39]etc. FTs have already been verified in those set-ups including other experiments like colloidal particle driven by optical traps [40].

If a macroscopic system is initially at equilibrium with a single heat bath, it is impossible to extract energy from the bath and perform some useful work during a cyclic protocol. For non cyclic process that means input work W (i.e, extracted work W_{ext}= -W) is always greater than the free energy change of the system ΔF. However, for mesoscopic systems one may observe for few realizations, $W < \Delta F$. These trajectories are termed as transient second law violating trajectories [42]. However, one recovers the second law on average i.e., $\langle W \rangle > \Delta F$. Here the angular brackets represent the ensemble average. Now, if a measurement is performed on the system and a proper feedback is applied depending on the acquired information, then one can extract energy even on average from a single heat bath in a cyclic process (for a non cyclic process this is equivalent to $\langle W \rangle < \Delta F$). Szilard engine is a prime example in this regard [43]. In recent studies [44, 45, 46, 47]it has been shown that when feedback is applied, the second law gets modified and the total entropy gets bounded below by the acquired information. Motivated by this, in Chapter 4 and 5 of this thesis, we have generalized the fluctuation theorems to quantum systems for multiple measurement and feedback. In this respect it can be mentioned that, due to performance of

measurement, entropy of the system may get reduced. But, this reduction of entropy should be compensated by the increase of entropy of the measurement device [48, 49]. Indeed, it is possible to do measurement without energy lost. However, one always needs to do work to erase the information, which was stored in the memory, to make the process complete. Thus, if we take the system, the bath and the measurement device (memory) together as the universe second law is restored [49, 50].

FT for heat engine has recently been derived [51] and it is found Carnot efficiency must be the upper bound on average. However, for single trajectory the efficiency (stochastic efficiency) may violate this law. Last two years have witnessed growing interest in this new area and it is observed that the distribution of stochastic efficiency displays power law behavior [52]. In Chapter 3 we have shown that depending on system parameters, during a single protocol of an engine one can observe different phase space regions including a refrigerator region.

Before going into the details of our findings, we would like to go through the basic concepts used in the rest of the thesis.

1.1.1 Langevin equation and fluctuation-dissipation theorem

When the system size are micron size or smaller, fluctuation play a dominant role. One prime example is the Brownian motion which describes the random motion of a micron size particle immersed into a liquid. This motion occurs due to random kicks received from the liquid molecules. If we try to describe this motion by Newton's Law, we have to keep track of the motion of every single molecule in the liquid, including the Brownian particle, at every moment. To resolve this issue simply, Langevin came forward with an idea. He determined the total force acting on the Brownian particle of mass m and velocity v at any time t and wrote the equation of motion as [7]

$$m\dot{v} = -\gamma v + \xi(t), \tag{1.1}$$

which is known as Langevin equation. Here, the over-head dot represents time derivative. The deterministic force (first part) will be obviously the macroscopic frictional force which is related to Stokes' law and arises due to moving body inside a crowd (liquid particles). This force always oppose to the motion of the Brownian particle and is proportional to its velocity v. For a spherical particle of radius a, moving in a fluid of viscosity η, frictional coefficient will be $\gamma = 6\pi\eta a$. The second term $\xi(t)$ represents the fluctuating force due to the random kicks of the liquid molecules on the Brownian particle. This random force must obey certain properties. First of all, as there is no preferential direction of the kicks, average will vanish, i.e.,

$$\langle \xi(t) \rangle = 0. \tag{1.2}$$

Here, angular bracket represents ensemble average at any time. Now, as there is no correlation between two successive kicks the second moment will follow

$$\langle \xi(t)\xi(t') \rangle = 2D\delta(t - t'), \tag{1.3}$$

with D a constant to be determined. Note that, the Fourier transform of delta function is independent of frequency. Hence corresponding noise is called white noise. Solving eq.(1.1) one gets velocity of the particle at any time t, from given initial velocity, v_0 as

$$v(t) = e^{-\gamma t/m} v_0 + \frac{1}{m} \int_0^t e^{-\gamma(t-t')/m} \xi(t'). \tag{1.4}$$

Thus, the average velocity goes to zero at long time, for any initial velocity. It is expected because, in equilibrium, there will not be any preferential direction of a Brownian motion. In this limit, average mean square velocity must satisfy the relation $\langle v^2 \rangle_{eq} = \frac{k_B T}{m}$. Here, k_B is the Boltzmann constant, T is temperature of the medium.

Using this relation, one can determine the constant

$$D = \gamma k_B T, \tag{1.5}$$

which is known as fluctuation-dissipation theorem. It relates the strength D of the fluctuating force with the dissipation force having frictional coefficient γ.

1.1.2 Stochastic energetics

The evolution of the phase-space trajectory for mesoscopic systems become stochastic in nature [12, 11]. All the thermodynamic quantities such as work, heat etc. become stochastic and depend on this phase space trajectory. If a particle of mass m is confined in a time dependent effective potential $V(x,t)$ (which include effective potential arises due to any external time dependent conservative force). The corresponding Langevin equation contains an extra term:

$$m\dot{v} = -\frac{\partial V(x,t)}{\partial x} - \gamma v + \xi(t). \tag{1.6}$$

The total force acting on the particle from its surrounding(bath) is $-\gamma v+\xi(t)$. Hence, the reaction force of the particle will be $-(-\gamma v + \xi(t))$. If the particle moves at an amount dx, Sekimoto defined the heat dissipated to bath [12] as

$$dQ = -(-\gamma v + \xi(t))dx = -\left(m\dot{v} + \frac{\partial V(x,t)}{\partial x}\right)dx \tag{1.7}$$

where we have used eq.(1.6) to rearrange the force term. Now, we have $dV(x,t) = \frac{\partial V(x,t)}{\partial x}dx + \frac{\partial V(x,t)}{\partial t}dt$. Then,

$$
\begin{aligned}
dQ &= -m\dot{v}dx - dV(x,t) + \frac{\partial V(x,t)}{\partial t}dt \\
&= -mvdv - dV(x,t) + \frac{\partial V(x,t)}{\partial t}dt \\
&= -d(\frac{1}{2}mv^2 + V(x,t)) + \frac{\partial V(x,t)}{\partial t}dt \\
&= -dE + \delta W. \qquad (1.8)
\end{aligned}
$$

In second line we have used Stratonivich type calculus. The first term in eq.(1.8) represents the change in internal energy which is defined as $E = \frac{1}{2}mv^2 + V(x,t)$. Then one can identify work done on the system [23] as

$$dW = \frac{\partial V(x,t)}{\partial t}dt. \qquad (1.9)$$

Eq.(1.8) represents first law for this small increment of time. For a stochastic trajectory upto time τ total heat goes to bath and work done on the system is defined as

$$Q(\tau) = -\int_0^\tau (-\gamma v + \xi(t))\dot{x}dt = -\int_0^\tau \left(m\dot{v} + \frac{\partial V(x,t)}{\partial x}\right) vdt, \qquad (1.10)$$

$$W(\tau) = \int_0^\tau \frac{\partial V(x,t)}{\partial t}dt \qquad (1.11)$$

respectively and depend on the particular realization of the stochastic trajectory. While internal energy is a state function and depend on the beginning and end point of the path, $\Delta E(\tau) = \frac{1}{2}mv_\tau^2 + V(x_\tau,\tau) - \frac{1}{2}mv_0^2 - V(x_0,0)$, where (x_τ, v_τ) and (x_0, v_0) represent initial and final phase space point respectively.

Overdamped case

When the relaxation time of velocity, m/γ, becomes much smaller compared to the typical time scale of the change position variable (or in other way round the typical time scale of our interest Δt, is such that $\Delta t \gg m/\gamma$), one can ignore the inertia term and rewrite the Langevin equation as

$$\gamma v = -\frac{\partial V(x,t)}{\partial x} + \xi(t). \tag{1.12}$$

In this overdamped limit, one similarly defines the above mentioned thermodynamic variables for a particular stochastic trajectory as

$$\begin{aligned} Q(\tau) &= -\int_0^\tau \frac{\partial V(x,t)}{\partial x}\dot{x}dt \\ W(\tau) &= \int_0^\tau \frac{\partial V(x,t)}{\partial t}dt \\ \Delta E(\tau) &= V(x_\tau,\tau) - V(x_0,0). \end{aligned} \tag{1.13}$$

If the time dependency of the system can be realized by changing the time-dependent potential $V(x,\lambda)$ and non-conservative force $f(x,\lambda)$ through a protocol $\lambda(t)$, the overdamped equation becomes

$$\gamma\dot{x} = -\frac{\partial V(x,\lambda)}{\partial x} + f(x,\lambda) + \xi(t). \tag{1.14}$$

For this case, the definition of work [30] is then modified to

$$W(\tau) = \int_0^\tau \frac{\partial V(x,\lambda)}{\partial t}dt + \int_0^\tau f(x,\lambda)\dot{x}dt \tag{1.15}$$

The drift coefficient is denoted as $b(x,t) = \frac{1}{\gamma}(-\frac{\partial V(x,\lambda)}{\partial x} + f(x,\lambda))$. If $P(x,t)$ denotes the probability of finding the particle at x in time t, corresponding Fokker-Planck

equation [7] will be

$$\frac{\partial P(x,t)}{\partial t} = -\frac{\partial J(x,t)}{\partial x}, \tag{1.16}$$

where the current is

$$J(x,t) = b(x,t)P(x,t) - \frac{k_B T}{\gamma}\frac{\partial P(x,t)}{\partial x}. \tag{1.17}$$

The local mean velocity of the particle at x at any time t is defined as

$$\mathcal{V}(x,t) = \frac{J(x,t)}{P(x,t)} = b(x,t) - \frac{k_B T}{\gamma}\frac{\partial \ln P(x,t)}{\partial x}. \tag{1.18}$$

If there is no drive, i.e., $f(x,\lambda) = 0$ and the particle is kept at fixed potential $V(x,\lambda)$, the total current will be zero and the system will reach equilibrium with probability distribution

$$P_{eq}(x,\lambda) = e^{-\beta[V(x,\lambda)-F(\lambda)]} \tag{1.19}$$

where $F(\lambda)$ is the equilibrium free energy defined as $e^{-\beta F(\lambda)} = \int dx e^{-\beta V(x,\lambda)}$.

When the system is driven by a fixed λ, the total current become constant and the system will reach a time independent NESS with probability distribution

$$P_{ss}(x,\lambda) = e^{-\phi(x,\lambda)}, \tag{1.20}$$

where $\phi(x,\lambda)$ is the nonequilibrium potential. The steady state current now becomes

$$J_{ss}(x,\lambda) = b(x,\lambda)P_{ss}(x,\lambda) - \frac{k_B T}{\gamma}\frac{\partial P_{ss}(x,\lambda)}{\partial x}. \tag{1.21}$$

and the mean local velocity at steady state becomes

$$\mathcal{V}_{ss}(x,\lambda) = b(x,\lambda) + \frac{k_B T}{\gamma}\frac{\partial \phi(x,\lambda)}{\partial x}. \tag{1.22}$$

The idea of decomposing the total heat into two parts namely 'house-keeping heat' and 'excess heat' for the the system in time periodic steady state (TPSS), was put forward by Oono and Paniconi [53] and made explicit in Langevin system by Hatano and Sasa [54]. The dissipated heat now can be rewritten as

$$\begin{aligned} Q(\tau) &= -\int_0^\tau (-\gamma v + \xi(t))\dot{x}dt \\ &= \gamma \int_0^\tau b(x,\lambda)\dot{x}dt \\ &= \gamma \int_0^\tau \mathcal{V}_{ss}(x,\lambda)\dot{x}dt - k_B T \int_0^\tau \frac{\partial \phi(x,\lambda)}{\partial x}\dot{x}dt. \end{aligned} \tag{1.23}$$

The house-keeping heat is the part which is required just to maintain the steady state and is defined as

$$Q_{hk}(\tau) = \gamma \int_0^\tau \mathcal{V}_{ss}(x,\lambda)\dot{x}dt. \tag{1.24}$$

On the other hand, excess heat is the heat that is produced on top of the house-keeping heat, such that $Q(\tau) = Q_{hk}(\tau) + Q_{ex}(\tau)$.

$$\begin{aligned} Q_{ex}(\tau) &= -k_B T \int_0^\tau \frac{\partial \phi(x,\lambda)}{\partial x}\dot{x}dt \\ &= k_B T \left[-\Delta\phi + \int_0^\tau \frac{\partial \phi(x,\lambda)}{\partial \lambda}\dot{\lambda}dt \right], \end{aligned} \tag{1.25}$$

as $d\phi = \frac{\partial \phi(x,\lambda)}{\partial x}dx + \frac{\partial \phi(x,\lambda)}{\partial \lambda}d\lambda$. For equilibrium system, $Q_{hk} = 0$ due to $\mathcal{V}_{ss}(x,\lambda) = 0$ and hence Q_{ex} reduced to the total heat Q.

1.2 Second law at mesoscopic scales

For classical thermodynamics the second law states that for any thermodynamic process the total entropy change is always positive [1], i.e.,

$$\Delta S_{tot} \geq 0 \tag{1.26}$$

The total entropy consists of two parts, the system entropy change ΔS and the bath entropy change ΔS_m. Hence,

$$\Delta S_{tot} = \Delta S + \Delta S_m. \tag{1.27}$$

Now, if the system is connected to only one bath at temperature T, then bath entropy change ΔS_m will be $\frac{Q}{T}$, where Q is the heat goes to the bath during the process. Using first law $W = \Delta E + Q$ we can rewrite the second law as

$$\begin{aligned} \Delta S + \Delta S_m &\geq 0 \\ \Delta S + \frac{Q}{T} &\geq 0 \\ T\Delta S - \Delta E + W &\geq 0. \end{aligned} \tag{1.28}$$

Using the definition of Helmholtz Free energy $F = E - TS$ the above equation reduces to

$$W - \Delta F \geq 0. \tag{1.29}$$

This is another form of second law and equality sign holds only during a reversible process. The above inequality states that, among all processes taking place between any two given thermodynamic states, the work done on the system is minimum for a reversible process and is equal to the free energy change of the corresponding states. The excess work done on the system during a process over the free energy change is

called dissipated work $W_{diss} = W - \Delta F$, as this amount of work will be dissipated into the bath. Hence, dissipated work is always non-negative, i.e., $W_{diss} \geq 0$.

However, for mesoscopic systems one may find few trajectories for which they violate the above mentioned laws and are known as transient second law violating trajectories. But, it can be shown that the second law is obeyed on average [23, 27],

$$\langle \Delta s_{tot} \rangle \geq 0 \qquad\qquad \langle W \rangle - \Delta F \geq 0. \tag{1.30}$$

Here, the angular bracket represents the ensemble average of given thermodynamic quantity over large number of realizations of a process.

1.3 Fluctuation theorems

In the last couple of decades a lot of work has been directed towards nonequilibrium statistical mechanics, and has given birth to several exact and unexpected relations that are valid even when the system is far from equilibrium. These results, although in principle valid quite generally, are in practice relevant mostly for mesoscopic systems for which the fluctuations are substantial. These are called *fluctuation theorems*(FTs) [20, 21, 23, 28, 29]. They transform classical thermodynamic inequalities into equalities. These theorems also shed new light on some fundamental problems such as how irreversibility arises from underlying time-reversible dynamics. Moreover, these theorems have important implications for nanotechnology and nano physics. Advances in experimental techniques have made dramatic progress in the area of single-molecule manipulation and nanotechnology have led to experimental verification of the various fluctuation theorems [41, 18]. FTs are the universal properties of the probability distribution $P(\Omega)$ for functional $\Omega[x(t)]$, like work, heat, entropy etc., evaluated along the stochastic trajectories from ensembles with well specified initial distributions $p_0(x_0)$. In the following, we will classify various FTs in brief.

1.3.1 Integral fluctuation theorem

Any non-dimensionalized functional $\Omega[x(t)]$ with probability distribution $P(\Omega)$ obey Integral Fluctuation Theorem (IFT) [30] if

$$\langle \exp(-\Omega) \rangle = \int P(\Omega) \exp(-\Omega) = 1. \tag{1.31}$$

From the convexity of exponential function one can obtain the following inequality

$$\langle \Omega \rangle \geq 0. \tag{1.32}$$

Sometime this inequality represents a well known thermodynamic law. In this respect, it should be mentioned that, classical thermodynamics is valid for macroscopic systems and ignores any fluctuations in any thermodynamic variable. However, this is not true for meso/ microscopic systems. The number of realizations for which $\Omega < 0$ can be characterized as 'violating' the corresponding thermodynamic law at trajectory level. The probability for obtaining $\Omega < -\omega$ with $\omega \geq 0$ can be easily calculated and can be given by

$$prob[\Omega < -\omega] \leq \int_{-\infty}^{-\omega} d\Omega P(\Omega) e^{-\omega-\Omega} \leq e^{-\omega}. \tag{1.33}$$

From the above expression it is revealed that the violation is of the order of 1. Now, for an N dimensional system, Ω will be typically order of NK_BT. Thus, the violation is exponentially small for large systems and restores the classical result (as shown in figure 1.1).

If the distribution $P(\Omega)$ is Gaussian, IFT gives a constraint on the width of the

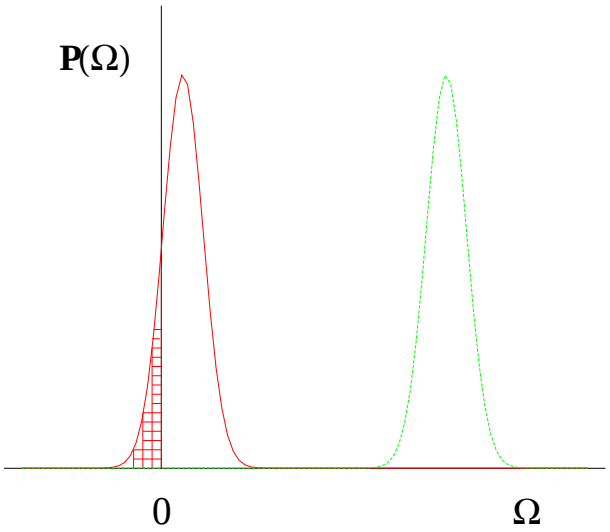

Figure 1.1: The distribution at the right is that of a thermodynamic variable Ω in a macroscopic system (diagram is not to scale). Obviously, because of the large value of the mean, there would be negligible probability of observing a process in which Ω is negative. On the other hand, the distribution for the mesoscopic system (left) may have an appreciable part of the distribution on the negative side (shaded part).

distribution and its mean and they are related by [55]

$$\langle(\Omega - \langle\Omega\rangle)^2\rangle = 2\langle\Omega\rangle. \tag{1.34}$$

The above equation referred to as fluctuation-dissipation relation.

1.3.2 Detailed fluctuation theorem

The detailed fluctuation theorem (DFT) is stronger than the IFT and relate the positive part of any distribution to its negative part by

$$\frac{P(-\Omega)}{P(\Omega)} = \exp(-\Omega). \tag{1.35}$$

From DFT one can trivially gets corresponding IFT but the reverse is not true. Here, DFT (eq.(1.35)) is for a steady state.

1.3.3 Generalized Crooks fluctuation theorems

These relation relate any distribution $P(\Omega)$ of the original process with the distribution $P^{\dagger}(\Omega)$ of same physical variable in the corresponding conjugate process and is given by

$$\frac{P^{\dagger}(-\Omega)}{P(\Omega)} = \exp(-\Omega). \tag{1.36}$$

As $P^{\dagger}(\Omega)$ is normalized it implies IFT but not DFT. Next, we will discuss various well known FTs in detail.

1.3.4 Crooks fluctuation theorem

Consider a system driven by a protocol $\lambda(t)$ from time $t = 0$ to $t = \tau$. This leads to evolution of the phase space variable of the system x_t at any time t. The initial and final value of the protocol is $\lambda(0) = \lambda_A$ and $\lambda(\tau) = \lambda_B$ respectively. For simplicity we restrict the motion of the system in one dimension only and corresponding $x_t = (x, v, t)$ where x, v represent position and velocity of the system (take for an example of a single particle) at time t. One can easily extend the same treatment to the multidimensional space. In the reverse process, the protocol would start from λ_B and would go to λ_A and corresponding time reverse protocol of the forward process is simply denoted as $\tilde{\lambda}(t) = \lambda(\tau - t)$. Note that, one can get reverse trajectory if the particle travels through the same position with exactly equal but opposite velocity.

If $\tilde{x}_t$ denotes time reversed phase space point of x_t then $\tilde{x}_t = (x, -v, t)$. Note that in the reverse process the actual time of elapse is $\tau - t$ instead of t. In figure 1.2, we have shown the evolution of a typical forward trajectory $X(t)$ in phase space and corresponding reverse trajectory $\tilde{X}(t)$. In discrete time step, consider a typical trajectory $X = x_0 \to x_1 \to x_2 \to .... \to x_\tau$ then corresponding reverse trajectory would be $\tilde{X} = \tilde{x}_0 \leftarrow \tilde{x}_1 \leftarrow \tilde{x}_2 \leftarrow .... \leftarrow \tilde{x}_\tau$. Crooks [28, 29] showed that in the

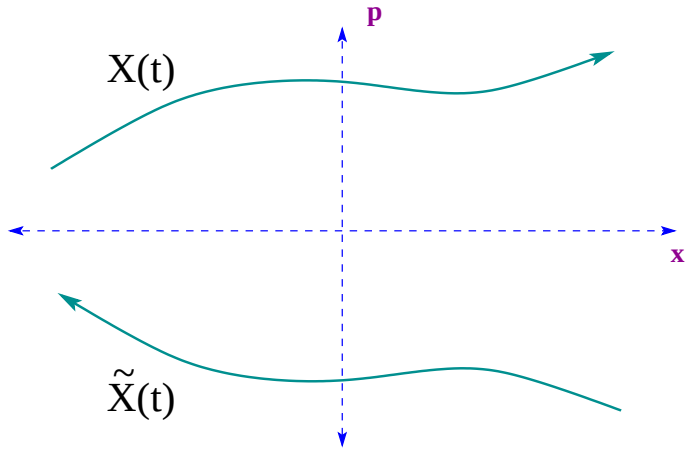

Figure 1.2: The figure shows a typical forward trajectory $X(t)$ in phase space and its corresponding reverse trajectory $\tilde{X}(t)$. The momentum coordinates (p) are inverted in the case of the reverse trajectory, while the position coordinates (x) remain the same.

trajectory picture,

$$\frac{\tilde{P}[\tilde{X}|\tilde{x}_\tau]}{P[X|x_0]} = \exp(-\beta Q), \tag{1.37}$$

where Q is the total heat flowing into the bath in the forward evolution and $\beta = 1/k_B T$. Here, $P[X|x_0]$ denotes the conditional probability to observe trajectory X in the forward process for given initial phase space point x_0. While, $\tilde{P}[\tilde{X}|\tilde{x}_\tau]$ represents the conditional probability to observe the trajectory $\tilde{X}$ for given initial phase space point $\tilde{x}_\tau$ when the protocol is followed in reverse order. Now, let the system start initially from equilibrium distribution for fixed initial protocol λ_A, then

$$p(x_0) = e^{-\beta[H(x_0,\lambda_A)-F_A]}, \tag{1.38}$$

where $H(x_0, \lambda_A)$ denotes the Hamiltonian of the system. Corresponding equilibrium free energy is given by $F_A = -k_B T \ln Z_A$ with partition function $Z_A = \int dx_0 \exp^{-\beta[H(x_0,\lambda_A)]}$. Before the beginning of the the reverse process, one makes sure that the system is in canonical distribution with the initial protocol of the reverse process $\tilde{\lambda}(0) = \lambda(\tau) =$

λ_B, which is the final protocol corresponding to the forward process. Then

$$p_1(\tilde{x}_\tau) = e^{-\beta[H(\tilde{x}_\tau,\lambda_B)-F_B]}, \tag{1.39}$$

where, $H(\tilde{x}_\tau, \lambda_B)$ and F_B represents corresponding Hamiltonian and free energy of the system in the reverse process for fixed protocol λ_B. Then Crooks shows [28, 29] that the probability to observe the froward trajectory to that of the corresponding reverse trajectory is simply related by

$$\frac{\tilde{P}[\tilde{X}]}{P[X]} = \frac{\tilde{P}[\tilde{X}|\tilde{x}_\tau]p_1(\tilde{x}_\tau)}{P[X|x_0]p(x_0)} = \exp[-\beta(W - \Delta F)]. \tag{1.40}$$

where $\Delta F = F_B - F_A$. Using the above relation one can easily derive the Crooks Fluctuation theorem (CFT) which relates the pdf of work $P(W)$ in the forward process is under a protocol $\lambda(t)$ to the corresponding pdf $\tilde{P}(W)$ in the time reverse process, driven by the protocol $\tilde{\lambda}(t) = \lambda(\tau - t)$ and is given by

$$\frac{\tilde{P}(-W)}{P(W)} = \exp[-(W - \Delta F)/T]. \tag{1.41}$$

This implies that ΔF can be obtained by locating the crossing point of the two distributions.

1.3.5 Jarzynski equality

Simply by cross multiplying and integrating the CFT one can obtain

$$\langle e^{-\beta W}\rangle = \int dW P(W) e^{-\beta W} = e^{-\beta\Delta F} \int dW \tilde{P}(-W) = e^{-\beta\Delta F}. \tag{1.42}$$

This is the celebrated Jarzynski Equality (JE) [23] which relates the nonequilibrium work done on the system with the equilibrium free energy difference and provide

a tool to calculate free energy change from the ensemble of work done on the system due to a particular protocol. Using Jensen's inequality $\langle e^{-x} \rangle \geq e^{-\langle x \rangle}$, we can write $e^{-\beta \langle W \rangle} \leq \langle e^{-\beta W} \rangle = e^{-\beta \Delta F}$; which leads to the second law,

$$\langle W \rangle \geq \Delta F. \tag{1.43}$$

In this respect, it is mentioned that, for macroscopic system W is always greater than ΔF. But, for any microscopic system there may be many realizations that violate this. These realizations are known as transient second law violating trajectories. However, second law is valid on average which comes as a direct consequence of JE. A more general FT was put forward by Seifert [13] which contains the Jarzynski and the Crooks theorems as special cases.

1.3.6 Seifert's Integral fluctuation theorem

Before going further in the fluctuation theorems now we give basic concepts of entropy in small systems. Entropy in general is a concept valid in equilibrium. The nonequlibrium entropy of a system with probability $p(x,t)$ is defined as

$$S(t) = -k_B \int dx p(x,t) \ln p(x,t). \tag{1.44}$$

However, Seifert [27] first introduced the concepts of entropy for individual trajectory. In this trajectory picture he defined entropy as

$$s(t) = -k_B \ln p(x,t). \tag{1.45}$$

A system which is in contact with a heat bath, is initially prepared in some arbitrary distribution $p(x_0)$ of phase space points and is perturbed by varying an external parameter $\lambda(t)$ up to time $t = \tau$. In the reverse process, the system evolves from

some other initial distribution $p_1(\tilde{x}_\tau)$ under the time-reversed protocol $\lambda(\tau - t)$. The Seifert's FT states that, the probability of a phase space trajectory along the forward process, $P[X]$ is related to that along the reverse process, $\tilde{P}[\tilde{X}]$, as

$$\frac{\tilde{P}[\tilde{X}]}{P[X]} = \frac{\tilde{P}[\tilde{X}|\tilde{x}_\tau]p_1(\tilde{x}_\tau)}{P[X|x_0]p(x_0)} = e^{-\beta Q}\frac{p_1(\tilde{x}_\tau)}{p(x_0)}. \tag{1.46}$$

If, in particular, the distribution $p_1(x_\tau)$ in the final distribution at time τ as dictated by dynamics, satisfy $p_1(x_\tau) = p_1(\tilde{x}_\tau)$, we can write the system entropy change on this particular forward trajectory as

$$\Delta s = -k_B \ln \frac{p_1(x_\tau)}{p(x_0)} = -k_B \ln \frac{p_1(\tilde{x}_\tau)}{p(x_0)}. \tag{1.47}$$

The entropy change of the bath is defined as $\Delta s_B = \frac{Q}{T}$, where Q is heat absorbed by the bath. Hence the total entropy production along this particular trajectory consists of two parts

$$\Delta s_{tot} = \Delta s + \Delta s_B = -k_B \ln \frac{p_1(\tilde{x}_\tau)}{p(x_0)} + \frac{Q}{T}. \tag{1.48}$$

Taking $k_B = 1$, we can rewrite the Seifert FT in trajectory picture as

$$\frac{\tilde{P}[\tilde{X}]}{P[X]} = e^{-\Delta s_{tot}}. \tag{1.49}$$

Simply cross multiplying the above equation we get Δs_{tot} obey

$$\langle e^{-\Delta s_{tot}} \rangle = 1. \tag{1.50}$$

This is the celebrated integral fluctuation theorem (IFT) given by Seifert [27, 13]. Applying Jensen's inequality one obtains

$$\langle \Delta s_{tot} \rangle \geq 0. \tag{1.51}$$

This is a statement of second law of thermodynamics, expressed in the form of inequality for the average change in total entropy.

1.3.7 Steady state FT (SSFT)

In NESS, a stronger FT holds for Δs_{tot} for arbitrary time τ [27] and corresponding SSFT can be stated as

$$\frac{P(-\Delta s_{tot})}{P(\Delta s_{tot})} = \exp(-\Delta s_{tot}). \tag{1.52}$$

IFT follows from this DFT. Earlier it was thought this theorem is valid only in the long time limit. But, as we included the system entropy change for individual trajectory in Δs_{tot}, DFT hold for any arbitrary time.

1.3.8 Hatano-Sasa relation

When the system is in NESS, we already decomposed the total heat into two parts, the house keeping heat q_{hk} the heat needed to maintain the steady state and excess heat q_{ex} which is produced on top of q_{hk}.

When the system undergoes a transition between two steady states it follows the Hatano-Sasa relation [54] ,

$$\langle \exp[-\Delta\phi + \beta q_{ex}] \rangle = 1. \tag{1.53}$$

Here $\Delta\phi$ is the change in nonequilibrium potential during this transition. This relation is the generalization of Jarzynski equality in the time periodic steady state. It follows

the inequality

$$\langle \Delta\phi \rangle \geq -\beta \langle q_{ex} \rangle. \tag{1.54}$$

As q_{ex} is bounded and the inequality becomes equality for the quasistatic process while total heat dissipation q scales with time. Hence the above inequality is stronger than the Clausius inequality $\langle \Delta s \rangle \geq -q/T$. When the system is given time to relax to its final λ_t, $\Delta\phi$ will be reduced to Δs and one obtains the inequality

$$\langle \Delta s \rangle \geq -\beta \langle q_{ex} \rangle. \tag{1.55}$$

This relation is the nonequilibrium steady state version of Clausius inequality.

The housekeeping heat q_{hk} also obeys the following IFT [56]

$$\langle \exp[-q_{hk}/T] \rangle = 1, \tag{1.56}$$

for arbitrary initial state, driving and length of trajectories. The corresponding inequality

$$\langle q_{hk} \rangle \geq 0. \tag{1.57}$$

1.4 Information and entropy

Maxwell in his famous gedanken experiment illustrated, only knowing velocity of each individual gas molecules, a demon can monitor the gas particles and separate them into hot and cold part. This seemed to be violation of the second law as there is no energy cost for this action. Its resolution, for the first time, revealed the relationship of information and entropy.

In 1921, Szilard formulated an engine that can extract energy from a heat bath and convert it into useful work in presence of information. In his original derivation, he considered a single gas molecule confined in a box of volume V and the box is

connected to a bath with temperature T. A demon is placed to monitor the system and extract energy. First the demon inserts a partition quickly in the middle and separates the box into two equal parts. The gas molecule would be confined into any of the two parts. Then it measures in which part the molecule is in. Depending on the measurement the partition is moved isothermally to the end of the box, such that $k_B T \ln 2$ work is extracted. Finally the partition is removed and the system goes to its original state. Classically, insertion and removal of the partition do not need any energy. Hence, one can extract energy from heat bath repeatedly which was a bit surprising and was termed as a perpetual machine. However, it is unfair to treat a single particle, kicking randomly to the wall of the box, as an ideal gas. But, any system that undergoes a phase-space splitting can be used as a working system to harness energy. The importance of Szilard Engine and Maxwell demon are that they put information on the same footing as entropy that will be discussed below in more detail.

1.4.1 Shannon entropy, non-equilibrium free energy and second law

In information theory [43], the Shannon entropy of a random variable X with probability density matrix at any time $\rho(x,t)$, is defined as

$$\mathcal{H}(X,t) = -\mathrm{Tr}\ \rho(x,t) \ln \rho(x,t). \tag{1.58}$$

Shannon entropy denotes the uncertainty of a random variable and measures the amount of information needed to describe the random variable. When X represents the microscopic state of a physical system one can define the non-equilibrium entropy as

$$S(t) = k_B \mathcal{H}(X,t) = -k_B \mathrm{Tr}\ \rho(x,t) \ln \rho(x,t), \tag{1.59}$$

where k_B is the Boltzmann constant. Let us consider a system connected to a bath of temperature T and $H(t)$ denotes corresponding time dependent Hamiltonian. The system energy at any time is given by

$$E(t) = \text{Tr } \rho(t)H(t). \tag{1.60}$$

Corresponding nonequilibrium free energy is defined as [57]

$$\mathcal{F}(t) = E(t) - TS(t). \tag{1.61}$$

Now, the instantaneous equilibrium density matrix of the system can be defined as

$$\rho^{eq}(t) = e^{-\beta(H(t)-F(t))}, \tag{1.62}$$

with $\beta = 1/k_BT$ the inverse bath temperature and the partition function $Z(t) = e^{-\beta F(t)} = \text{Tr } e^{-\beta H(t)}$. Then the non-equilibrium entropy coincides with the corresponding equilibrium entropy and one can recover the usual relation $F = \text{Tr } \rho^{eq}H - TS$ with F as equilibrium free energy.

Suppose the system evolves from time 0 to upto time τ and $W(\tau)$ and $Q(\tau)$ represent the work done on the system and heat input to the bath. Then according to the first law of thermodynamics, the internal energy change of the system during this evolution becomes

$$\Delta E(\tau) = W(\tau) - Q(\tau). \tag{1.63}$$

The change in nonequilibrium system entropy consists of two terms,

$$\Delta S(\tau) = \Delta S_{tot}(\tau) - \Delta S_B(\tau). \tag{1.64}$$

The first term, the total entropy production $\Delta S_{tot}(\tau) \geq 0$, is a positive quantity. The second one, the entropy flow to the bath, is defined as $\Delta S_B = Q/T$. Using first law and definition of nonequilibrium free energy one gets

$$T\Delta S_{tot}(\tau) = W(\tau) - \Delta\mathcal{F}(\tau) \geq 0, \tag{1.65}$$

which implies the extractable work $-W(\tau)$ is always bounded by decrease of nonequilibrium free energy difference $-\Delta\mathcal{F}(\tau)$. The difference between $\mathcal{F}(t)$ and $F(t)$ is always positive and can be written as

$$\mathcal{F}(t) - F(t) = TI(t) = TD[\rho(t)||\rho^{eq}(t)] \geq 0. \tag{1.66}$$

Here, $I(t)$ represents the information needed to specify the noneqilibrium state from the corresponding equilibrium state. One can rewrite the second law under the form of nonequilibrium Landauer principle

$$W_{irr}(\tau) = W(\tau) - \Delta F(\tau) = T\Delta S_{tot}(\tau) + T\Delta I(\tau), \tag{1.67}$$

$$\Rightarrow W_{irr}(\tau) \geq T\Delta I(\tau). \tag{1.68}$$

If $\Delta I(\tau)$ is negative, then we can extract more work than the equilibrium free energy difference. However for reversible process $\Delta S_{tot}(\tau) = 0$ and this inequality becomes

$$W_{irr}(\tau) = T\Delta I(\tau). \tag{1.69}$$

Now, if the system reaches finally an equilibrium distribution. i.e., no information is left in the final distribution ($I(\tau) = 0$), one can reach the minimum bound of the

$W_{irr}(\tau)$ and the value will be

$$W_{irr}^{min}(\tau) = -TI(0). \tag{1.70}$$

For this case, the total information in the initial state ($I(0)$) is completely used to extract work from the system $W_{ext}^{max} = -W_{irr}^{min}(\tau) = TI(0)$.

1.4.2 Relative entropy and mutual information

In Information theory, the relative entropy or Kullback Leibler distance measures the distance between two distributions and defined as

$$D(p||q) = \sum_x p(x) \ln \frac{p(x)}{q(x)}. \tag{1.71}$$

It measures the inefficiency of taking the distribution $q(x)$ while actual distribution is $p(x)$ and $\mathcal{H}(p) + D(p||q)$ is the number of bits required on average to describe the random variable in terms of $q(x)$. However, it is not true distance as the function is not symmetric [43]. If the two distributions coincide, $p(x) = q(x)$ then relative entropy vanishes. Using the property, $\ln(x) \leq 1 - x$ for $x \geq 0$ we have

$$\begin{aligned} D(p||q) \quad &= \sum_x p(x) \ln \frac{p(x)}{q(x)} \\ &= -\sum_x p(x) \ln \frac{q(x)}{p(x)} \\ &\geq \sum_x p(x) \left[1 - \frac{q(x)}{p(x)}\right] = \sum_x [p(x) - q(x)] = 1 - 1 = 0, \end{aligned} \tag{1.72}$$

this means, relative entropy is always positive. The mutual information between two random variables U and V is defined as

$$I(U;V) = \sum_{u,v} \rho(u,v) \ln \frac{\rho(u,v)}{\rho(u)\rho(v)} = \mathcal{H}(U) + \mathcal{H}(V) - \mathcal{H}(U,V). \tag{1.73}$$

Mutual information is basically the relative entropy between the joint distribution of the two random variables with their product distribution. Note that, unlike relative entropy, mutual information is symmetric i.e, $I(U;V) = I(V;U)$. This $I(U;V)$ is always positive and vanishes only when these two random variables U and V are statistically independent i.e., there is no correlation between them. One can rewrite $I(U;V)$ as (see figure 1.3)

$$I(U;V) = \mathcal{H}(U) - \mathcal{H}(U|V) = \mathcal{H}(V) - \mathcal{H}(V|U). \tag{1.74}$$

Where $\mathcal{H}(U|V) = -\sum_{u,v} \rho(v)\rho(u|v) \ln(u|v)$ denotes the conditional entropy. Hence, mutual information denotes the reduction of uncertainty of one random variable due to the knowledge of another.

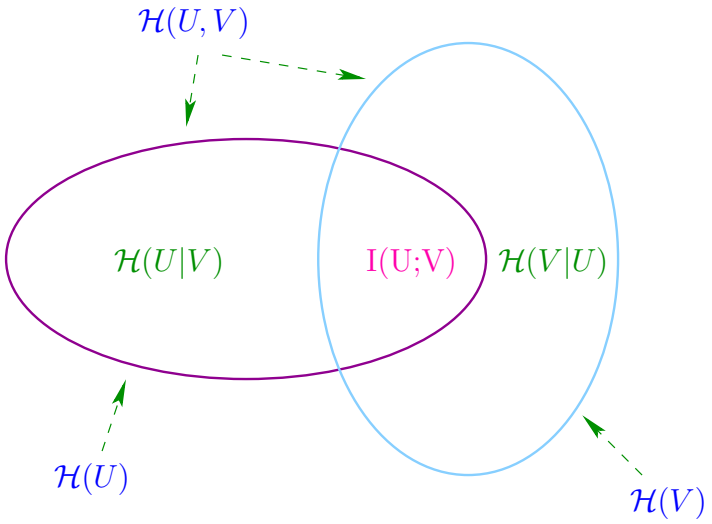

Figure 1.3: a simple diagram to describe mutual information $I(U;V)$

.

1.4.3 Measurement and entropy

Next, we will discuss the effect of measurement in the original system with probability density $\rho(x)$. Now, a measurement is performed and m is the outcome like left or right in the Szilard engine. The probability density will be updated to $\rho(x|m)$ after this measurement. If the system is initially in equilibrium due to the performance of measurement, $\rho(x|m)$ will not be in canonical. That means measurement leads the system to a nonequilibrium states although there is no energy cost. The change in nonequilibrium entropy due to measurement is $S(\rho(x|m) - S(\rho(x))$. Taking the average over all possible outcomes with probability p_m, this noneqilibrium entropy change becomes

$$\Delta S_{meas} = k_B(\mathcal{H}(X|M) - \mathcal{H}(X)) = -k_B I(X;M). \tag{1.75}$$

Note that, in measurement process neither the Hamiltonian nor the micro-state of the system are affected. That means the average energy of the system does not change due to measurement. Hence the nonequilibrium free energy change becomes,

$$\Delta\mathcal{F}_{meas} = \sum_m p_m \mathcal{F}(\rho(x|m);\mathcal{H}) - \mathcal{F}(\rho(x);\mathcal{H}) = -T\Delta S_{meas} = k_B T I(X;M). \tag{1.76}$$

As, $I(X;M) \geq 0$ there is always increase in nonequilibrium free energy which can be eventually used to extract work at a latter time isothermally.

1.4.4 Landauer principle and memory

Information seems to be an abstract quantity at first glance. However, it is not. When a measurement is performed, the obtained information is being stored in a piece of paper or in the hard-disk etc. In this perspective Landauer shed new light in his famous article 'Information is physical' [58]. Any physical system with multiple

distinguishable meta-stable states can be used to store the information. However, these states should have long enough lifetimes and should not be affected by the environmental fluctuations or any external constraints. Then only a system can act reliably as memory in desired time. It means ergodicity must be broken or effectively broken in the timescale when memory is reliable. The total phase space Γ is split into several ergodic regions Γ_m for each memory outcome m. Magnetization in a small ferromagnetic domain of a standard magnetic memory or high free barrier separating microscopic degrees of freedom in single electron memory are few examples in this regard.

Let p_m denotes the probability to be in the ergodic region Γ_m of the memory. now if the memory is in local equilibrium, one can take E_m and S_m as average energy and non-equilibrium entropy of the corresponding ergodic region. The nonequilibrium free energy of the memory is [49]

$$\mathcal{F}(M) = \sum_m p_m F_m - k_B T \mathcal{H}(M), \tag{1.77}$$

where, $F_m = E_m - TS_m$ and $\mathcal{H}(M) = -\sum_m p_m \ln p_m$ is the Shannon entropy of the informational states. Note that, total entropy of the memory is sum of Shannon entropy $\mathcal{H}(M)$ and the individual internal entropies S_m. Now after manipulation of the memory, we assume that the Hamiltonian of the system reaches its initial Hamiltonian. Then we need to be concerned about only the expression of p_m for particular memory state. Suppose, during measurement, the state changes from M' with probability p'_m to the state M with probability p_m. The change in free energy for the memory for this case will be $\Delta\mathcal{F}^{mem}_{meas} = \mathcal{F}(M) - \mathcal{F}(M')$. Similarly for resetting the memory to its original state M' the free energy change will be $\Delta\mathcal{F}^{mem}_{reset} = \mathcal{F}(M') - \mathcal{F}(M)$ and work done to reset the memory must obey

$$W_{reset} \geq \Delta\mathcal{F}^{mem}_{reset}. \tag{1.78}$$

In this respect, if one takes symmetric memory $F_0 = F_1 = F_2 = ...$ the free energy change will be reduced to only the Shannon entropy change $\Delta\mathcal{F}^{mem}_{reset} = -k_BT(\mathcal{H}(M) - \mathcal{H}(M'))$. Now if we reset the state to a standard state such that $p'_0 = 1$ and all other $p'_m = 0$ then $\mathcal{H}(M') = 0$. and get $\Delta\mathcal{F}^{mem}_{reset} = -k_BT\mathcal{H}(M)$. Finally, if the memory consists of only two states and for random bit $p_0 = p_1 = 1/2$, one obtains the celebrated Landauer's limit

$$W_{reset} \geq k_BT \ln 2, \tag{1.79}$$

while equality holds for a reversible process. This is the famous Landauer's principle which states that the minimum work needed to erase one bit of information is $k_BT \ln 2$.

1.5 Stochastic resonance

Resonance occurs when the internal frequency of a system matches with the frequency of an applied periodic force. During resonance there is a periodic transfer of energy from this applied force to the system. Take an example of a swing which moves in a particular frequency. Now as soon as the swing reaches its highest point a small force is applied. As a result, it will reach to a higher position in the opposite side. Thus the amplitude of the swing would increase in each step if one performs the same process again and again.

On the other hand in stochastic resonance(SR) [59, 60, 62, 61], a feeble signal is amplified due to the presence of optimum noise. Generally, noise is unwanted and hampers the accuracy of a device. However, some time an extra dose of noise can improve the performance of the devices. In 1981, this phenomenon was first introduced to explain occurrence of the ice ages. Recently, it has attracted much interest in the field of physics, chemistry, biological science and engineering.

To explain SR, let us take a particle of mass m, placed in a thermal bath in temperature T and confined in an one dimensional double well potential $V(x)$ as

shown at figure 1.4.

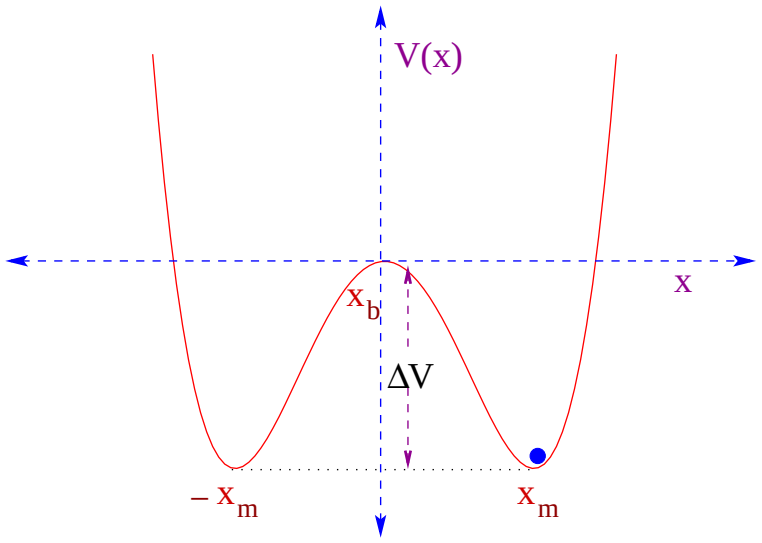

Figure 1.4: A typical bistable potential showing the positions of maxima at x_b; two minima at x_m and $-x_m$. The barrier height is ΔV.

The particle follows the overdamped Langevin equation. Due to presence of thermal noise particle may hop from one well to the other with Kramers escape rate [7]

$$r_k = \frac{(|V_b''||V_m''|)^{\frac{1}{2}}}{2\pi m\gamma} \exp\left[-\frac{\Delta V}{k_B T}\right]. \tag{1.80}$$

Here ΔV is the height of the barrier $\Delta V = V_b - V_m$ and γ is the frictional coefficient of the medium.

If a time dependent external force $A\sin(\omega t)$ with frequency ω is applied to the system then, it swings the potential in such a manner that in first half of the cycle, the potential in one well become lower than the other (as shown in figure 1.5). In second half, the effect is just the opposite. However, this force is too small to make the particle cross the barrier. Hence, if the noise strength is very small the particle will be confined in one well. On the other hand, for very high noise strength the particle may not see the barrier and randomly jump from one well to the another. However in the intermediate noise strength if the average waiting time $1/r_k$ is comparable to half of

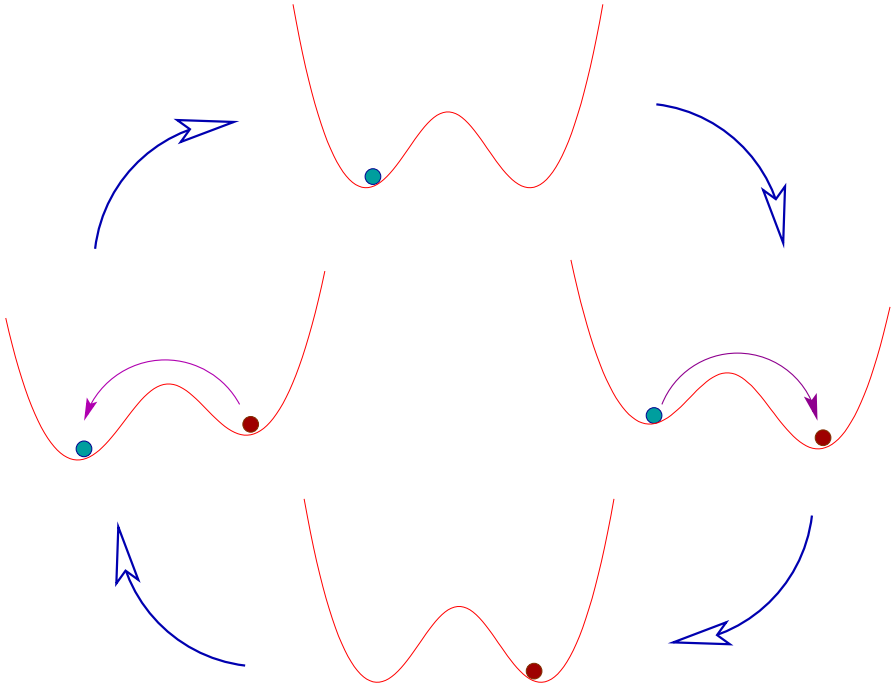

Figure 1.5: Schematic diagram for synchronization of particle hopping with the drive frequency at stochastic resonance

the time period of the external drive π/ω, the particle hopping will be synchronized with the external drive. This phenomena is known as SR and occurs due to perfect matching of these two time scales $1/r_k = \pi/\omega$.

There are different quantifiers of SR such as signal to noise ratio, spectral power amplification, and hysteresis loop area etc [59,63]. However, work done on the system (absorbed energy) may be an appropriate quantifier [64].

1.6 Plan of the thesis

The plan of the thesis is as follows. In **Chapter 2**, we have derived fluctuation relations for heat engines in TPSS. In the beginning, the system is in contact with the cooler bath. The system is then coupled to the hotter bath and external parameters are changed cyclically, eventually bringing the system back to its initial state, once

the coupling with the hot bath is switched off. We lift the condition of initial thermal equilibrium and derive a new fluctuation relation for the central system (heat engine) being in a TPSS. Carnot's inequality for classical thermodynamics follows as a direct consequence of this FT even in TPSS. For the special cases of the absence of hot bath and no extraction of work, we obtain the IFT for total entropy and the generalized exchange FT, respectively. Recently microsized heat engines have been realized experimentally in the TPSS. We numerically simulate the same model and verify our proposed theorems.

In **Chapter 3**, we have performed an extensive analysis of a single particle stochastic heat engine constructed by manipulating a Brownian particle in a time dependent harmonic potential. The cycle consists of two isothermal steps at different temperatures and two adiabatic steps similar to that of a Carnot engine. The engine shows qualitative differences in inertial and overdamped regimes. All the thermodynamic quantities, including efficiency, exhibit strong fluctuations in a TPSS. The fluctuations of stochastic efficiency dominate over the mean values even in the quasistatic regime. Interestingly, our system acts as an engine provided the temperature difference between the two reservoirs is greater than a finite critical value which in turn depends on the cycle time and other system parameters. This is supported by our analytical results carried out in the quasistatic regime. Our system works more reliably as an engine for large cycle times. By studying various model systems we observe that the operational characteristics are model dependent. Our results clearly rules out any universal relation between efficiency at maximum power and temperature of the baths. We have also verified fluctuation relations for heat engines in TPSS.

In **Chapter 4**, we derive the JE for an isolated quantum system for three different cases: (i) the full evolution is unitary with no intermediate measurements, (ii) with intermediate measurements of arbitrary observables being performed, and (iii) with intermediate measurements whose outcomes are used to modify the external protocol

(feedback). We assume that the measurements will involve errors that are purely classical in nature. Our treatment is based on path probability in state space for each realization. This is in contrast to the formal approach based on projection operator and density matrices. We find that the JE remains unaffected in the second case, but gets modified in the third case where the mutual information between the measured values with the actual eigenvalues must be incorporated into the relation.

Based on trajectory dependent path probability formalism in state space, in **Chapter 5**, we derive generalized entropy production fluctuation relations for a quantum system in the presence of measurement and feedback. We have obtained these results for three different cases: (i) the system is evolving in isolation from its surroundings; (ii) the system being weakly coupled to a heat bath; and (iii) system in contact with reservoir using quantum CFT. In case (iii), we build on the treatment carried out in [65], where a quantum trajectory has been defined as a sequence of alternating work and heat steps. The obtained entropy production FTs retain the same form as in the classical case. The inequality of second law of thermodynamics gets modified in the presence of information. These FTs are robust against intermediate measurements of any observable performed with respect to von Neumann projective measurements as well as weak or positive operator valued measurements.

In **Chapter 6**, we compare the fluctuation relations for work and entropy in underdamped and overdamped systems, when the friction coefficient of the medium is space-dependent. We find that these relations remain unaffected in both cases. We have restricted ourselves to Stratonovich discretization scheme for the overdamped case.

Using the input energy per cycle as a quantifier of SR, in **Chapter 7** we show that SR is observed in superharmonic (hard) potentials. However, it is not observed in subharmonic (soft) potentials, even though the potential is bistable. These results are consistent with recent observations based on amplitude of average position as a

quantifier. In both soft and hard potentials, we observe resonance phenomenon as a function of the driving frequency. The nature of probability distributions of average work are qualitatively different for soft and hard potentials.

Chapter 2

Fluctuation relations for heat engines in TPSS

2.1 Introduction

In this chapter we derive fluctuation relations for heat engines (FRHE) in time periodic steady state. As a corollary we prove the existence of a bound on efficiency for engine, similar to Carnot result. However our bound is valid for arbitrary cycle time. This fluctuation theorem put constrains on the operation characterization of engine.

Fluctuation theorems [20, 21, 23, 28, 29] are exact relations that remain valid even for systems driven far away from thermal equilibrium. They transform classical thermodynamic inequalities into equalities. Advances in experimental techniques have made dramatic progress in the area of single-molecule manipulation and nanotechnology have led to experimental verification of the various fluctuation theorems [41, 18]. Recently another equality is added to the class of fluctuation theorems, namely, FRHE [51]. Initially the system is in thermal equilibrium with a cold thermal reservoir at temperature T_c, and then coupled to a hot thermal reservoir at temperature $T_h > T_c$. At this stage, the parameters driving the working substance (our system of interest) are changed cyclically so that at the end of the cycle all the parameters attain their initial values, and the interaction with the hot reservoir is switched off, and the system is coupled to the cold reservoir. The equality reads

$$\left\langle \exp\left[-Q_h\left(\frac{1}{T_c}-\frac{1}{T_h}\right)+\frac{W}{T_c}\right]\right\rangle = 1. \tag{2.1}$$

Here, $\langle\cdots\rangle$ denotes averaging over many realizations of the cycle. Q_h is the heat *absorbed* from the hot bath and W is the work *extracted* from the system in a cycle.

2.2 Derivation from Seifert's theorem

We provide here a derivation slightly different from that given in [51, 18], by using the Seifert's integral fluctuation theorem [27, 13], $\langle e^{-\Delta s_{tot}}\rangle = 1$ (in presence of multiple

baths). Using first law of thermodynamics, the internal energy change of the system

$$\Delta E = Q_h - Q_c - W. \tag{2.2}$$

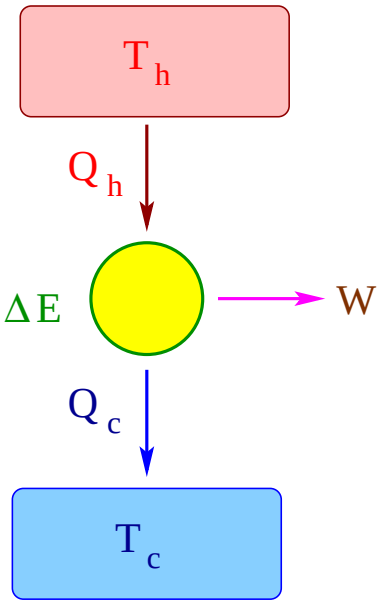

Figure 2.1: During one cycle, energy flow in a heat engine as dictated by first law $\Delta E = Q_h - Q_c - W$.

Here Q_c denotes the heat dissipated to the cold bath. Figure 2.1 denotes the schematic diagram of the energy flow over a cycle. The total entropy production being given by

$$\Delta s_{tot} = \Delta s_h + \Delta s_c + \Delta s. \tag{2.3}$$

Δs_h, Δs_c and Δs are the entropy changes of the hot bath, the cold bath and of the central system, respectively. Denoting the initial and final distributions for the forward process by $p_0(x_0)$ and $p_1(x_\tau)$, we have [27, 13]

$$\Delta s_h = -\frac{Q_h}{T_h}; \qquad \Delta s_c = \frac{Q_c}{T_c}; \tag{2.4}$$

$$\Delta s = \ln \frac{p_0(x_0)}{p_1(x_\tau)} = \ln \left[\frac{e^{-E(x_0)/T_c}}{Z_0} \cdot \frac{Z_\tau}{e^{-\beta E(x_\tau)/T_c}} \right] = \frac{\Delta E}{T_c}, \tag{2.5}$$

where $\Delta E = E(x_\tau) - E(x_0)$, and we have made use of the fact that for a cyclic process, $Z_0 = Z_\tau$. Using the first law, eq. (2.2), we have $Q_c = Q_h - W - \Delta E$. Thus, Δs_{tot} becomes

$$\begin{aligned} \Delta s_{tot} &= -\frac{Q_h}{T_h} + \frac{Q_c}{T_c} + \frac{\Delta E}{T_c} \\ &= -\frac{Q_h}{T_h} + \frac{Q_h - W - \Delta E}{T_c} + \frac{\Delta E}{T_c} \\ &= Q_h \left(\frac{1}{T_c} - \frac{1}{T_h} \right) - \frac{W}{T_c}. \end{aligned} \tag{2.6}$$

Seifert's theorem then gives eq. (2.1). Equality (2.1), together with the Jensen's inequality gives

$$\left\langle Q_h \left(\frac{1}{T_c} - \frac{1}{T_h} \right) - \frac{W}{T_c} \right\rangle \geq 0, \tag{2.7}$$

which can be rewritten as

$$\frac{\langle W \rangle}{\langle Q_h \rangle} \leq \eta_c, \tag{2.8}$$

η_c being the Carnot efficiency given by $\eta_c \equiv 1 - \frac{T_c}{T_h}$. This is then, the Carnot's theorem for maximum efficiency applied to a mesoscopic heat engine. Now, instead of taking the averaged quantities, one can also define the efficiency for each individual trajectory, $\eta \equiv W/Q_h$, which is, of course, a fluctuating quantity. Consequently, there may be trajectories along which $\eta > \eta_c$, which will be termed as the *atypical trajectories* (trajectories that seem to flout the behaviour dictated by the second law). In fact, η can also become negative, in which case, along a cycle, the system does not perform as a heat engine (for example, when heat is absorbed by the system, but work is being done *on* the system). In next chapter it will be discussed in detail.

2.3 Derivation of the FRHE for a time-periodic steady state

Recently the Carnot engine has been investigated experimentally in the time-periodic steady state (TPSS) [66]. In a TPSS, the probability density of system state, $p_{ss}(x,t)$, is periodic in time, $p_{ss}(x,t+\tau) = p_{ss}(x,t)$, where τ is the time-period of the external drive. The occupation probabilities of a motor in a TPSS, consisting of a two-level system, has been studied in [67]. In a TPSS, the probability density for the system state can be written as $p_{ss}(x,\lambda) = e^{-\phi(x,\lambda)}$, λ being the external time-dependent protocol, and $\phi(x,\lambda)$ is an effective potential. In such a case, the condition of initial equilibration of the working substance with the cold bath ought to be lifted. Once again, in a part of the cycle, the system is connected to the cold bath, while in the other part, it is connected to the hot bath. In this case, the change in system entropy during a cycle is given by $\Delta\phi$, and the change in the total entropy becomes

$$\begin{aligned}
\Delta s_{tot} &= -\frac{Q_h}{T_h} + \frac{Q_c}{T_c} + \Delta\phi \\
&= -\frac{Q_h}{T_h} + \frac{Q_h - W - \Delta E}{T_c} + \Delta\phi \\
&= Q_h\left(\frac{1}{T_c} - \frac{1}{T_h}\right) - \frac{W + \Delta E}{T_c} + \Delta\phi. \qquad (2.9)
\end{aligned}$$

Let X denote the short form for a trajectory in phase space: $\{x_0 \to x_1 \to x_2 \to \cdots \to x_\tau\}$, and let $\tilde{X}$ denote the time-reversed path: $\{x_0 \leftarrow x_1 \leftarrow x_2 \leftarrow \cdots \leftarrow x_\tau\}$, the subscripts denoting discretized time. According to the detailed fluctuation theorem for total entropy [27, 13], we then have the following ratio between the probability densities for the forward and reverse trajectories, represented by $P[X]$ and $\tilde{P}[\tilde{X}]$, respectively:

$$\frac{P[X]}{\tilde{P}[\tilde{X}]} = e^{\Delta s_{tot}} = \exp\left[Q_h\left(\frac{1}{T_c} - \frac{1}{T_h}\right) - \frac{W + \Delta E}{T_c} + \Delta\phi\right], \qquad (2.10)$$

whose integrated form is given by the new equality

$$\left\langle \exp\left[-Q_h\left(\frac{1}{T_c}-\frac{1}{T_h}\right)+\frac{W+\Delta E}{T_c}-\Delta\phi\right]\right\rangle = 1. \tag{2.11}$$

We next derive a detailed fluctuation theorem for the joint probability distribution for work, heat, change in internal energy and system entropy.

2.4 Fluctuation theorem for the joint probability distribution

Using eq. (2.10), we obtain a relation for the joint probability density for Q_h, W, ΔE and $\Delta\phi$. These quantities are odd under time-reversal.

$$\begin{aligned}
&P(Q_h, W, \Delta E, \Delta\phi) \\
&= \int \mathcal{D}[X]\ P[X]\ \delta(Q_h - Q_h[X])\ \delta(W - W[X]) \\
&\qquad\qquad \times\delta(\Delta E - \Delta E(x_0, x_\tau))\ \delta(\Delta\phi - \Delta\phi(x_0, x_\tau))
\end{aligned}$$

$$\begin{aligned}
&= \int \mathcal{D}[X]\ P[\tilde{X}] \exp\left[-Q_h\left(\frac{1}{T_c}-\frac{1}{T_h}\right)+\frac{W+\Delta E}{T_c}-\Delta\phi\right]\ \delta(Q_h - Q_h[X]) \\
&\qquad \times\delta(W - W[X])\ \delta(\Delta E - \Delta E(x_0, x_\tau))\ \delta(\Delta\phi - \Delta\phi(x_0, x_\tau)).
\end{aligned}$$

Here, $\mathcal{D}[X] = \mathcal{D}[\tilde{X}] = dx_0 dx_1 \cdots dx_\tau$, where $\tilde{x}$ is the time-reversed state of x. We now now perform a change of variables from x to $\tilde{x}$. Then,

$$\begin{aligned} P(Q_h, W, \Delta E, \Delta\phi) &= \exp\left[Q_h\left(\frac{1}{T_c} - \frac{1}{T_h}\right) - \frac{W + \Delta E}{T_c} + \Delta\phi\right] \\ &\quad \times \int \mathcal{D}[X]\ \delta(Q_h + \tilde{Q}_h[\tilde{X}])\ \delta(W + \tilde{W}[\tilde{X}]) \\ &\quad \times\ \delta(\Delta E + \Delta\tilde{E}(\tilde{x}_0, \tilde{x}_\tau))\ \delta(\Delta\phi + \Delta\tilde{\phi}(\tilde{x}_0, \tilde{x}_\tau)) \\ &= \tilde{P}(-Q_h, -W, -\Delta E, -\Delta\phi) \\ &\quad \times\ \exp\left[Q_h\left(\frac{1}{T_c} - \frac{1}{T_h}\right) - \frac{W + \Delta E}{T_c} + \Delta\phi\right]. \end{aligned} \tag{2.12}$$

Here, $\tilde{P}(-Q_h, -W, -\Delta E, -\Delta\phi)$ is the joint probability density for $-Q_h$, $-W$, $-\Delta E$ and $-\Delta\phi$, along the reverse process. Noting that in a TPSS, P and $\tilde{P}$ have the same functional forms, we can write

$$\frac{P(Q_h, W, \Delta E, \Delta\phi)}{P(-Q_h, -W, -\Delta E, -\Delta\phi)} = \exp\left[Q_h\left(\frac{1}{T_c} - \frac{1}{T_h}\right) - \frac{W + \Delta E}{T_c} + \Delta\phi\right]. \tag{2.13}$$

Eq. (2.13) readily leads to eq. (2.11), which in turn gives rise to the inequality

$$\langle Q_h\rangle\left(\tfrac{1}{T_c} - \tfrac{1}{T_h}\right) - \tfrac{\langle W\rangle + \langle\Delta E\rangle - T_c\langle\Delta\phi\rangle}{T_c} \geq 0. \tag{2.14}$$

In the TPSS, we have, $\langle\Delta E\rangle = 0$, and $\langle\Delta\phi\rangle = 0$. Then we arrive, even for the TPSS, to the Carnot's theorem, namely,

$$\frac{\langle W\rangle}{\langle Q_h\rangle} \leq \eta_c. \tag{2.15}$$

For $T_c = T_h$ (system is in contact with a single bath), we retrieve the Seifert's integral fluctuation theorem from eq. (2.11) for a system in contact with a bath at

temperature T_c [27, 13]:

$$\left\langle \exp\left[\frac{W+\Delta E}{T_c}-\Delta\phi\right]\right\rangle = \left\langle \exp\left[-\frac{Q_c}{T_c}-\Delta\phi\right]\right\rangle = \langle e^{-\Delta s_{tot}}\rangle = 1. \tag{2.16}$$

We have used the first law for system in contact with only the cold bath, $\Delta E = -W - Q_c$, the first step. If no work is extracted from the system, then the system effectively acts as a heat conductor between the two heat baths, giving rise to the generalized exchange fluctuation theorem [68] in TPSS:

$$\left\langle \exp\left[-Q_h\left(\frac{1}{T_c}-\frac{1}{T_h}\right)+\frac{\Delta E}{T_c}-\Delta\phi\right]\right\rangle = 1. \tag{2.17}$$

An example of the above case (eq. (2.17)) would be a particle in a harmonic potential coupled to a bath whose temperature changes periodically in time, while no other parameters of the harmonic oscillator are changed, and consequently work extracted is zero. This model should be experimentally realizable.

To verify our proposed theorem, eq. (2.11), we study a simple heat engine which has been experimentally realized recently. Some related points have been clarified through the simulations of the distribution functions of physical quantities appearing in our theorems.

2.5 The model and numerical results

In this section, we verify eq. (2.11) numerically. For this purpose, we choose the model used in [66], namely, the mesoscopic realization of a Stirling engine. Each cycle in its operation consists of the following steps:

1. **Step 1**: an overdamped colloidal particle is initially trapped in a harmonic potential with a spring constant k_{min} (state A): $V(x,0) = \frac{1}{2}k_{min}x^2$. The particle is in contact with a medium of temperature T_c. Without breaking contact with

the heat bath, the stiffness constant is subsequently changed, via a prescribed time-dependence of this constant $k(t)$, until it reaches a value k_{max} (state B) after a time τ. The potential function now is given by $V(x,\tau) = \frac{1}{2}k_{max}x^2$.

2. **Step 2**: the bath temperature is suddenly switched to $T_h > T_c$ (state C). The distribution of states of the system does not change during this instantaneous jump.

3. **Step 3**: now the spring constant follows a separate time dependence due to which its value changes from k_{max} to k_{min} (state D) over a time τ.

4. **Step 4**: in the last step, the temperature of the medium is once again instantaneously switched back to its initial value T_c and the system returns to state A. The full cycle is then repeated.

Since in steps 2 and 4, the stiffness constant is held fixed, the work done is identically equal to zero in these two steps. We choose the functional dependence for the stiffness constant during the transition state $A \rightarrow$ state B to be linear and of the following form:

$$k(t) = k_{min} + q\left(\frac{t}{\tau}\right). \tag{2.18}$$

According to this equation, after time τ, the system reaches $k_{max} = k(\tau) = k_{min} + q$. Similarly, during the transition state $C \rightarrow$ state D, the form of $k(t)$ is given by

$$k(t) = k_{max} - q\left(\frac{t}{\tau} - 1\right). \tag{2.19}$$

We find that when the full cycle is complete, i.e. $t = 2\tau$, we get back the initial spring constant $k_{min} = k(2\tau) = k_{max} - q$. In our simulation, we choose the values of the constants (in dimensionless units) to be $k_{min} = 1$, $k_{max} = 2$, $T_c = 0.1$ and $T_h = 0.4$. Initially, as a consistency check, we verify that for a very slow process (time of observation large compared to the relaxation period of the system to its

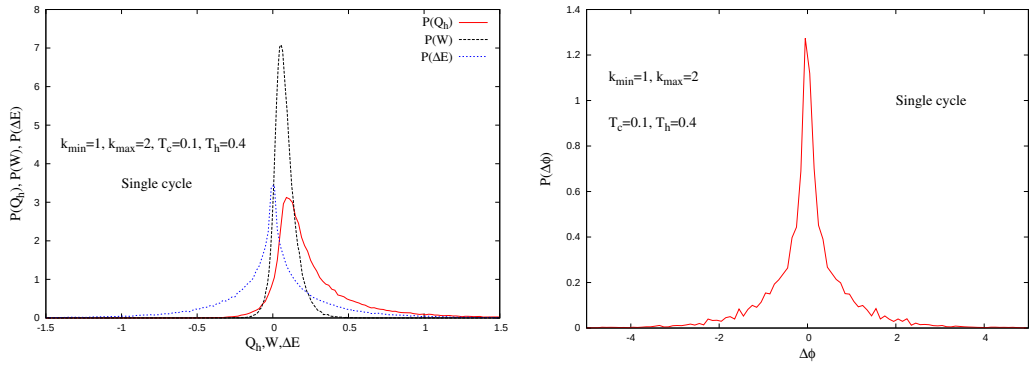

(a) (b)

Figure 2.2: (a) Distribution of Q_h, W and ΔE for a single cycle of the heat engine in a steady state, for $\tau = 5$. (b) Distribution of $\Delta\phi$ for the same parameters.

equilibrium state), the average work done on the system equals the change in its free energy (quasi-static process). In our simulation, we have used Heun's method of integration and have generated $\sim 10^5$ state space trajectories. The changes in free energy during the steps 1 and 3 are

$$\Delta F_{A\to B} = \frac{T_c}{2} \ln \frac{k_{max}}{k_{min}} \tag{2.20}$$

and

$$\Delta F_{C\to D} = \frac{T_h}{2} \ln \frac{k_{min}}{k_{max}}, \tag{2.21}$$

respectively. For our chosen parameters, we get $\Delta F_{1\to 2} = 0.035$ and $\Delta F_{3\to 4} = -0.139$. From our simulation, we obtain the average works done in steps 1 and 3 reach these values as we increase the time of observation. For $\tau = 50$, we obtain $\langle W\rangle_{A\to B} = 0.036$ and $\langle W\rangle_{C\to D} = -0.138$, respectively, which match with the theoretical results, within our numerical accuracy.

For reaching the time-periodic steady state, we leave out several initial cycles to skip the transient regime. For this TPSS, we have chosen $\tau = 5$, and we obtain the value of eq. (2.11) to be 1.083, which is very close to unity. Thus, the above relation is verified in our numerical simulations.

Now we study the behaviour of Δs_{tot} (eq. (2.9)) when each realization of the experiment consists of a large number of cycles. It apparently seems that since ΔE and $\Delta\phi$ are state functions, while Q_h and W scale with time of observation, in the limit of a large number of cycles, we will have vanishing contribution from the state functions to the fluctuation theorem. To verify this numerically, in figure 2.2(a), we have plotted the distributions for Q_h, W and ΔE for a single cycle of the heat engine. ΔE being a state function is symmetric about the $\Delta E = 0$ axis. In figure 2.2(b), the distribution for change in system entropy, $\Delta\phi$, is plotted for a single cycle.

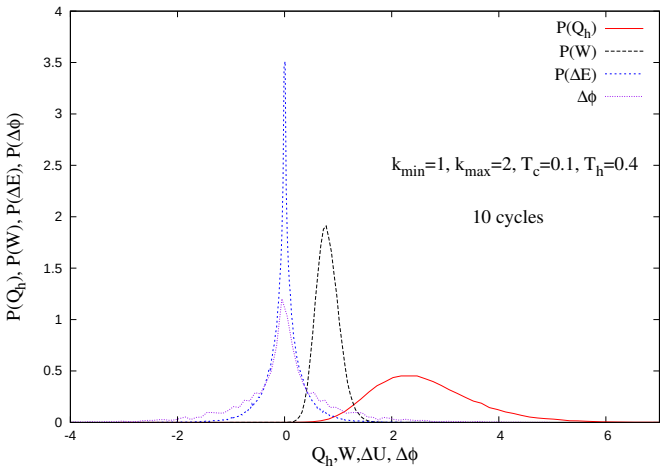

Figure 2.3: Distribution of Q_h, W and ΔE for 10 cycles of the heat engine in a steady state, with the half observation time $\tau = 5$ for each cycle.

In figure 2.3, we have plotted the distribution functions for Q_h, W, ΔE and $\Delta\phi$ for 10 cycles in the steady state. As expected, we find that the distributions for Q_h and W tend towards a Gaussian and shift towards right, but those for ΔE and $\Delta\phi$ remain similar to the case of a single cycle.

In figure 2.4, we have plotted distributions of $R \equiv Q_h(1/T_c - 1/T_h) - W/T_c$ (which is the extensive part of Δs_{tot}) and of Δs_{tot} itself. In figure 2.4(a), we find that the two quantities follow distributions that are slightly different from each other. In figure 2.4 (b), we find that when we take a large number of cycles, the distributions begin to coincide. This is because the contribution from the distributions of state functions

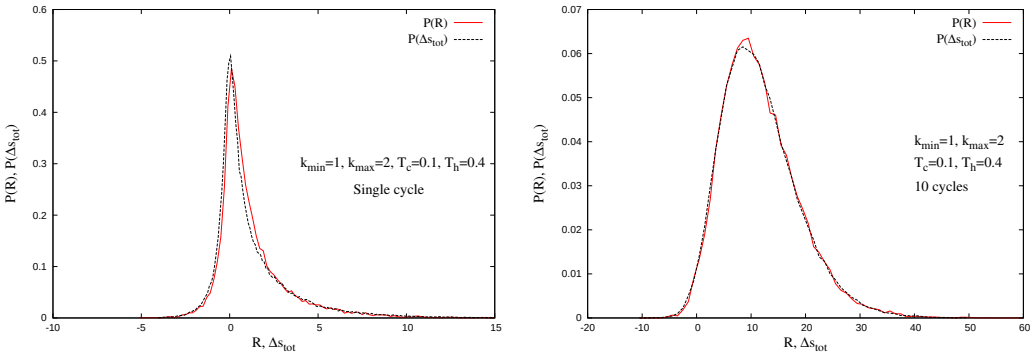

(a) (b)

Figure 2.4: (a) Distribution of the $R \equiv Q_h(1/T_c - 1/T_h) - W/T_c$, which is the extensive part of Δs_{tot} and of Δs_{tot} itself, for a single cycle in steady state. (b) Same distributions for 10 cycles, and we still find an appreciable difference between the two.

become small as compared to the contributions from the extensive quantities in the limit of large number of cycles. However, it may be noted that the intensive quantities do contribute in the extreme tails of the distributions (large deviation). To see this contribution we need very high precision simulation in the tail region, which is beyond the accuracy of our simulation. This point also arises in the case of heat and work theorems. Work obeys a fluctuation theorem. However, due to the contribution from the internal energy change, heat does not follow a fluctuation theorem, even in the limit of large observation time [36, 25].

2.6 Conclusion

In conclusion, we have generalized the fluctuation relation for heat engines to time-periodic steady states, which leads to the Carnot's theorem. Generalized FRHE leads to, in different limits, to the Seifert's theorem, and the generalized exchange fluctuation theorem. Our FRHE has been verified numerically in a simple realistic heat engine. It would be interesting to check whether the steady state distribution $p_{ss}(x,t)$ in the special case specified below eq. (2.17) can be calculated analytically, for example, by generalizing the method given for time-independent steady state in [69].

Also, the work distribution for a system starting from equilibrium and trapped in a harmonic potential of time-dependent stiffness constant has been studied in [70]. It would be interesting to see whether this procedure can be generalized to deduce the steady state distributions of different thermodynamic quantities for the heat engine considered in section 2.5.

Chapter 3

Single Particle Stochastic Heat Engine

3.1 Introduction

Motivated by the recent experimental observation on micro-size heat engines [66], we have performed an extensive analysis of single particle stochastic heat engine. We showed that nano-scale heat engine operate on different principles than their macroscopic counterpart.

Thermodynamic heat engines convert heat into useful work. They work cyclically between two thermal reservoirs kept at different temperatures T_l and T_h ($T_h > T_l$). The second law of thermodynamics restricts their efficiency to the Carnot limit [1], $\eta_C = 1 - \frac{T_l}{T_h}$. However, this efficiency can only be achieved in the quasistatic limit where transitions between thermodynamic states occur infinitesimally slowly and hence the power output vanishes. Curzon and Ahlborn (C-A) [71] showed that for finite time endoreversible heat engines, efficiency at maximum power is given by $\eta_{CA} = 1 - \sqrt{\frac{T_l}{T_h}}$. As yet there is no consensus on this result ([30, 72, 73, 74, 75]).

With the advances in nano-technology, a few-micrometer-sized Stirling heat engine has been experimentally realized [66]. This microscopic heat engine operates in conditions where typical changes in their energies are of the order of the thermal energy per degree of freedom [38]. An appropriate theoretical framework to deal with these systems has been developed during the past decades within the context of stochastic thermodynamics [11, 12, 76, 77, 78]. This formalism of stochastic energetics provides a method to calculate work, heat and entropy even for a single particle along a microscopic trajectory. One can obtain average quantities after averaging over respective ensembles. The averaged thermodynamic quantities, work and entropy, obey second law. Using this formulation various single particle heat engines have been studied in the literature [72, 79, 80, 14, 52]. Fluctuation relations for heat engines (FRHE) [51, 81, 82] operating in a time periodic steady state (TPSS) have recently been obtained [81]. FRHE are in the form of equality and Carnot's inequality for efficiency η_c follows as a direct consequence of this theorem.

In this chapter we have studied in detail a simple model for a stochastic heat engine described by Langevin equation. Both underdamped and overdamped regimes are explored and qualitative differences are pointed out. We emphasize on fluctuations of thermodynamic variables including the engine efficiency. We show that fluctuations dominate the mean values even in quasistatic regime. Therefore in such situations one needs to study the full probability distribution of the physical variable for the proper analysis of the system.

In section 3.2, we describe the model of our system and the protocol. In section 3.3, we obtain analytical results for relevant average thermodynamic quantities in the quasistatic regime for the underdamped case. In section 3.4, engine with finite time cycle in the inertial regime is studied numerically, in detail. The system driven by time asymmetric cycles and various other model systems are also explored. We have verified FRHE in this section. Sections 3.5 and 3.6 are devoted to the analytical and numerical studies of the system in the overdamped limit. Finally, we conclude in section 3.7. Each section is self contained.

3.2 The Model

The single particle stochastic heat engine consists of a Brownian particle having position x and velocity v at time t, confined in a one dimensional harmonic trap. The stiffness of the trap $k(t)$ varies periodically in time as shown in figure 3.1. For the underdamped case, the equation of motion for the particle is given by [7, 83]

$$m\dot{v} = -\gamma v - k(t)x + \sqrt{\gamma T}\xi(t). \tag{3.1}$$

In overdamped limit the equation reduces to

$$\gamma\dot{x} = -k(t)x + \sqrt{\gamma T}\xi(t). \tag{3.2}$$

In our further analysis, we set mass of the particle m, the Boltzmann constant k_B and the frictional coefficient γ to be unity. T is the temperature of the thermal bath. All physical parameters are made dimensionless. The noise is Gaussian with zero mean, $\langle \xi(t) \rangle = 0$ and is delta correlated, $\langle \xi(t_1)\xi(t_2) \rangle = 2\delta(t_1 - t_2)$. The internal energies of the particle in the underdamped and the overdamped limit are given by $u(x, v) = \frac{1}{2}k(t)x^2 + \frac{1}{2}mv^2$ and $u(x) = \frac{1}{2}k(t)x^2$, respectively.

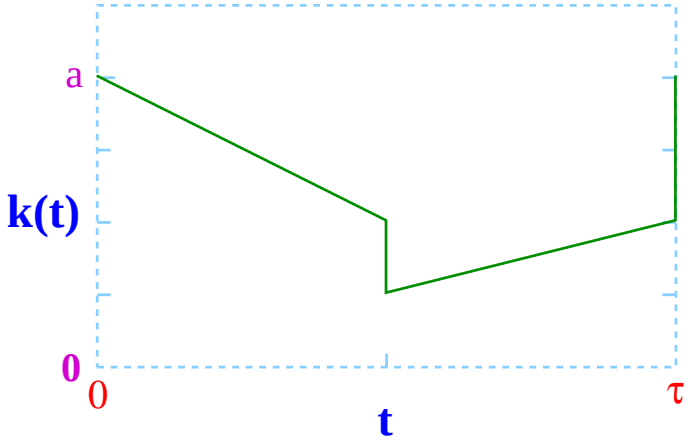

Figure 3.1: Stochastic heat engine in a harmonic potential: the time dependence of our periodically driven stiffness constant (protocol) k(t) for the full cycle ($0 \leq t \leq \tau$).

Operation of the system consists of four steps - two isotherms and two adiabatics. In the first step, the system undergoes an isothermal expansion, during which it is connected to a hot bath at temperature T_h and the stiffness constant is varied linearly with time as

$$k(t) = a\left(1 - \frac{t}{\tau}\right) = k_1(t), \tag{3.3}$$

for $0 < t < \tau/2$. Here τ is the period of the cycle and a is the initial value of the stiffness constant. In the second step, the potential undergoes an instantaneous expansion (adiabatic) by decreasing the stiffness constant from $a/2$ to $a/4$. As the process is instantaneous the distribution before and after expansion will not change and heat absorption will be zero. In the third step, the system is connected to a cold bath with lower temperature T_l and isothermal compression of the trap is carried out

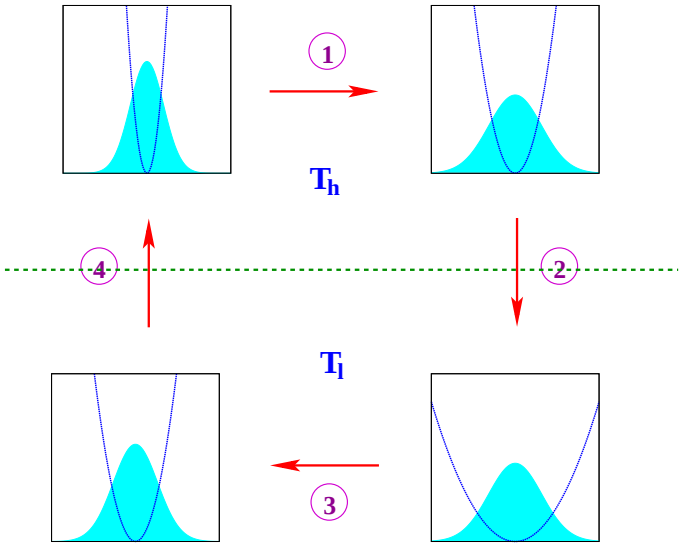

Figure 3.2: Schematic representation for a cyclic process of stochastic heat engine operating between two reservoirs kept at temperatures T_h and T_l. The cycle consists of two isothermal steps and two adiabatic steps according to the time varying protocol k(t). The blue line denotes a one dimensional potential V(x,t) and the filled region denote the corresponding steady state distribution.

by changing the stiffness as

$$k(t) = a\frac{t}{2\tau} = k_2(t), \tag{3.4}$$

for $\tau/2 < t < \tau$. In the last step, we carry out instantaneous adiabatic compression by varying the stiffness constant from $a/2$ to a and simultaneously connecting the system to the hot bath. This cycle is then repeated . The time dependence of the protocol is given in figure 3.1 and a schematic representation of the system within a cycle at its various stages is depicted in figure 3.2.

The described protocol differs from those used in earlier studies. In the experimental set up [66] two adiabatic steps are absent. Work optimized protocol is used by Schmiedl and Seifert [72] whereas the protocol based on the concept of shortcut to adiabaticity is used by Tu [80]. However, their emphasis is on the possible correlation between efficiency at maximum power and C-A bound. Our main motivation, namely to study the fluctuation of physical quantities, is different from earlier studies

as mentioned in the introduction.

3.3 Underdamped quasistatic limit

In this section, we analytically calculate the average thermodynamic quantities of our model system in the quasistatic limit. In this limit, the duration of the protocol is much larger than all the relevant time scales, including the relaxation time. Hence as protocol is changed, the system immediately adjusts to the equilibrium state corresponding to the value of protocol at that instant. First, we calculate the average work done on the particle in all the four steps of a cycle and the heat absorbed by it in the first isothermal step. Finally, we calculate efficiency in the quasistatic limit.

In the first isothermal process, average work done on the particle is the same as the free energy change (ΔF_h) before and after the expansion, i.e.,

$$W_1 = \Delta F_h = \frac{T_h}{2} \ln \frac{k_1(\tau/2)}{k_1(\tau)} = \frac{T_h}{2} \ln \frac{1}{2}. \tag{3.5}$$

At $t = \tau/2$, the system is in equilibrium with the bath at T_h with stiffness constant $a/2$. The second step being instantaneous, no heat will be dissipated and the phase space distribution remains unaltered. Correspondingly the average work done on the particle is equal to the change in its internal energy:

$$\begin{aligned} W_2 &= N_1 \int_{-\infty}^{\infty} dxdv \left(\frac{a}{4} - \frac{a}{2}\right) \frac{x^2}{2} e^{-\frac{ax^2}{4T_h} - \frac{v^2}{2T_h}} \\ &= -\frac{T_h}{4}, \end{aligned} \tag{3.6}$$

where $N_1 = \frac{1}{2\pi T_h}\sqrt{\frac{a}{2}}$, is the normalization constant. Similarly in the third step (i.e., isothermal compression step) the average work done on the particle in the quasistatic

limit is

$$W_3 = \Delta F_l = \frac{T_l}{2} \ln \frac{k_2(\tau)}{k_2(\tau/2)} = \frac{T_l}{2} \ln 2. \tag{3.7}$$

The average work done in the last step (i.e., second adiabatic step) is given as

$$\begin{aligned} W_4 &= N_2 \int_{-\infty}^{\infty} dx dv (a - \frac{a}{2}) \frac{x^2}{2} e^{-\frac{ax^2}{4T_l} - \frac{v^2}{2T_l}} \\ &= \frac{T_l}{2}, \end{aligned} \tag{3.8}$$

with $N_2 = \frac{1}{2\pi T_l} \sqrt{\frac{a}{2}}$. Hence, the average total work done in the full cycle of the heat engine in the quasistatic process is

$$\begin{aligned} W_{tot} &= W_1 + W_2 + W_3 + W_4 \\ &= \frac{T_h}{2} \ln \frac{1}{2} - \frac{T_h}{4} + \frac{T_l}{2} \ln 2 + \frac{T_l}{2}. \end{aligned} \tag{3.9}$$

To obtain the heat absorption in the first step (i.e., isothermal expansion), we calculate the average change of internal energy and use the first law. During this process, the particle stays in contact with hot bath at temperature T_h. However, it is to be noted that at time $t = 0^-$, the system was in contact with low temperature bath at T_l, whereas at $t = 0^+$ the system is in contact with hot bath at T_h. Thus the system has to relax into new equilibrium after sudden change in temperature. The time taken for this relaxation process is assumed to be negligible compared to the cycle time τ. This relaxation leads to an additional heat flow which accounts for the change in the internal energy during the relaxation process. One can readily obtain the internal energy at $t = 0^+$ as $3T_l/2$ while after the relaxation it is T_h. Hence, the average internal energy change in the first step is

$$\Delta U_1 = T_h - \frac{3T_l}{2}. \tag{3.10}$$

Now using the first law, the average heat absorption from the hot bath for the first step is

$$-Q_1 = \Delta U_1 - W_1 = T_h - \frac{3T_l}{2} - \frac{T_h}{2}\ln\frac{1}{2}. \tag{3.11}$$

Hence efficiency of the engine for the underdamped case in the quasistatic limit is given by

$$\begin{aligned}\bar{\eta}_q &= \frac{-W_{tot}}{-Q_1} = -\frac{\frac{T_h}{2}\ln\frac{1}{2} - \frac{T_h}{4} + \frac{T_l}{2}\ln 2 + \frac{T_l}{2}}{T_h - \frac{3T_l}{2} - \frac{T_h}{2}\ln\frac{1}{2}} \\ &= -\frac{T_h\ln\frac{1}{2} - \frac{T_h}{2} + T_l\ln 2 + T_l}{2T_h - 3T_l - T_h\ln\frac{1}{2}}.\end{aligned} \tag{3.12}$$

Here we would like to emphasize that $\bar{\eta}$ is defined ignoring fluctuations and the subscript q denotes the quasistatic limit. We will show later that fluctuations play an important role even in the quasistatic regime. Work done during the cycle w and heat absorbed during the first step q_1 are fluctuating quantities. Stochastic efficiency is defined as $\eta = \frac{w}{q_1}$ [52] and hence its average $\langle\eta\rangle = \langle\frac{w}{q_1}\rangle$ is not the same as $\bar{\eta} = \frac{\langle w\rangle}{\langle q_1\rangle}$ which is given in eq.(3.12) for quasistatic limit. This will be discussed in detail in subsequent sections. In our notation, the thermodynamic quantities are denoted by capital letters only for quasistatic limit, whereas, small letters are used to denote those quantities for finite time cycles.

According to our convention negative work done on the system implies extraction of work; while, negative heat means that heat enters into the system. It is important to note from eq.(3.11) that in quasistatic limit heat flows from the bath to the system provided

$$\begin{aligned}&2T_h - 3T_l - T_h\ln\frac{1}{2} \geq 0 \\ &\Rightarrow \frac{T_l}{T_h} \leq \frac{2+\ln 2}{3} = 0.898\end{aligned} \tag{3.13}$$

and similarly from eq.(3.9) work can be extracted from the system if

$$T_h \ln\frac{1}{2} - \frac{T_h}{2} + T_l \ln 2 + T_l \leq 0$$
$$\Rightarrow \frac{T_l}{T_h} \leq \frac{0.5 + \ln 2}{1 + \ln 2} = 0.705. \tag{3.14}$$

Therefore, in quasistatic regime our model system operates in three different modes of operation depending on the ratio of the temperatures of the thermal baths. First, when $0 < \frac{T_l}{T_h} \leq 0.705$ is maintained, work can be extracted and heat is absorbed from hot bath and it acts as an engine. Second, when $0.705 \leq \frac{T_l}{T_h} \leq 0.898$ is set, heat is absorbed from the bath but we cannot extract work. And finally when we have $\frac{T_l}{T_h} \geq 0.898$ neither heat is absorbed nor the work is extracted. In this case work done on the system heats up the hot bath. Therefore, there is a particular regime in parameter space where the system act as an engine. This is in contrast to the Carnot engine which works for arbitrary temperature difference between two baths. The above mentioned condition is only valid in the quasistatic limit. For finite time cycle the operational condition for heat engine depends on cycle time apart from T_h and T_l, which will be shown in our simulation. Our exact expression of W_{tot} and Q_1 are in complete agreement with our numerical results in the quasistatic limit. Thus these analytical calculations act as a check for our numerical simulation.

3.4 finite cycle time engine in inertial regime

For finite-cycle-time we study our system numerically. When the Langevin system is driven periodically it is known that after initial transients, the system will settle down to a TPSS. The joint probability distribution $P_{ss}(x, v, t)$ of position and velocity of the particle is periodic in time, i.e., $P_{ss}(x, v, t) = P_{ss}(x, v, t + \tau)$.

For numerical simulations we evolve our system with a time periodic protocol (as shown in figure 3.1. We have used Heun's method for integrating the basic Langevin

equation [84] with time step $dt = 0.0002$. We make sure that the system is in the TPSS by going beyond the initial transient regime. We then consider at least 10^5 cycles of operations and physical quantities are averaged over all these cycles. For rest of the paper we keep m, a, γ fixed at $m = 1.0$, $a = 5.0$, $\gamma = 1.0$.

We now make use of the concepts of stochastic energetics [11, 12, 76, 77, 78] to calculate work, heat and internal energy for a given trajectory. The thermodynamic work done on the particle during first part of the cycle, in each computational step dt, is given by

$$dw_1(t_i) = \frac{\partial u_1(t_i)}{\partial k_1(t_i)} \dot{k}_1(t_i) dt. \tag{3.15}$$

with $u_1(t_i) = \frac{1}{2}k_1(t_i)x^2(t_i) + \frac{1}{2}v^2(t_i)$ and $t_i = i.dt$. Now, $w_1 = \sum_{i=0}^{N} dw_1(t_i)$ where $N = \frac{\tau}{2dt}$. The internal energy is a thermodynamic state function and hence its change during the isothermal process is given by $du_1 = \frac{1}{2}k_1(\tau/2)x^2(\tau/2) + \frac{1}{2}v^2(\tau/2) - \frac{1}{2}k_1(0)x^2(0) - \frac{1}{2}v^2(0)$. The heat absorption by the bath is $q_1 = w_1 - du_1$ using the first law of thermodynamics. The second step which is adiabatic is instantaneous and hence the particle does not get any chance to evolve. Thus work done is only instantaneous change in internal energy, i.e., $w_2 = \frac{1}{2}[k_2(\tau/2) - k_1(\tau/2)]x^2(\tau/2)$. Similarly, for step three, work done is given by

$$dw_3(t_i) = \frac{\partial u_2(t_i)}{\partial k_2(t_i)} \dot{k}_2(t_i) dt \tag{3.16}$$

and $w_3 = \sum_{i=N}^{2N} dw_3(t_i)$; internal energy change $du_2 = \frac{1}{2}k_2(\tau)x^2(\tau) + \frac{1}{2}v^2(\tau) - \frac{1}{2}k_2(\tau/2)x^2(\tau/2) - \frac{1}{2}v^2(\tau/2)$; and heat delivered to the cold bath is $q_2 = w_3 - du_2$. For the last adiabatic process, work done on the particle is $w_4 = \frac{1}{2}[k_1(0) - k_2(\tau)]x^2(\tau)$. The total work done on the system in a cycle is $w = w_1 + w_2 + w_3 + w_4$. It should be noted that each w_i (i=1,2,3,4) is a fluctuating quantity and their values depend on a particular phase space trajectory.

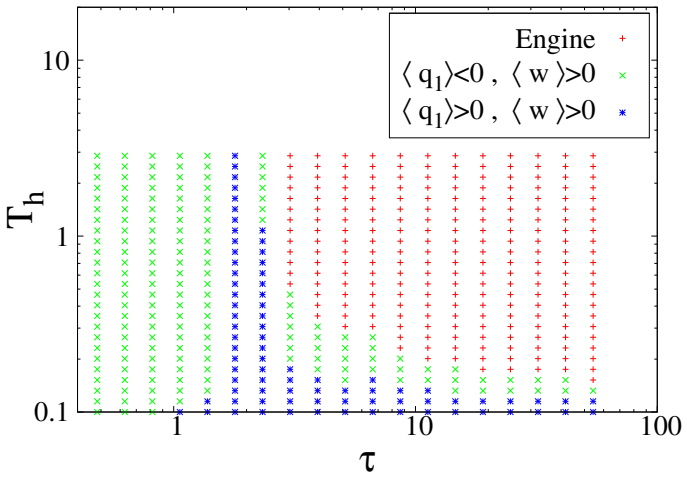

Figure 3.3: Phase diagram for different T_h and τ but for fixed $T_l = 0.1$.

In figure 3.3, we have shown the phase diagram of the operation of our system. Here we have varied T_h and cycle time τ keeping T_l fixed at 0.1. There are three distinct regimes. The system acts as an engine when $\langle w \rangle < 0$ and $\langle q_1 \rangle < 0$. The angular bracket $\langle . \rangle$ indicates average over several realizations. In the other two regimes the system ceases to work as a heat engine altogether($\langle w \rangle > 0$). For $\langle w \rangle > 0$ we have two distinct domains with $\langle q_1 \rangle < 0$ and $\langle q_1 \rangle > 0$. The latter implies work is done on the system which heats up the hot bath. In the large cycle time limit numerical results are consistent with our analytical predictions made in last section. We re-emphasize that the system works as a heat engine provided there is a minimal difference between T_h and T_l which depends on cycle time τ and other physical parameters. From the Phase diagram it is apparent that, as we decrease τ for fixed T_h, there exists a lower bound below which the system does not perform as an engine, as it only consumes work.

In figure 3.4, we have plotted $\langle w \rangle$, $\langle q_1 \rangle$ and $\langle q_2 \rangle$ with respect to cycle time τ. We have fixed $T_h = 0.5$ and $T_l = 0.1$ for all subsequent figures. Starting from zero, $\langle w \rangle$ initially increases and reaches a peak value. Then it starts decreasing and finally saturates to a negative value (-0.214), which is close to our theoretical result (from

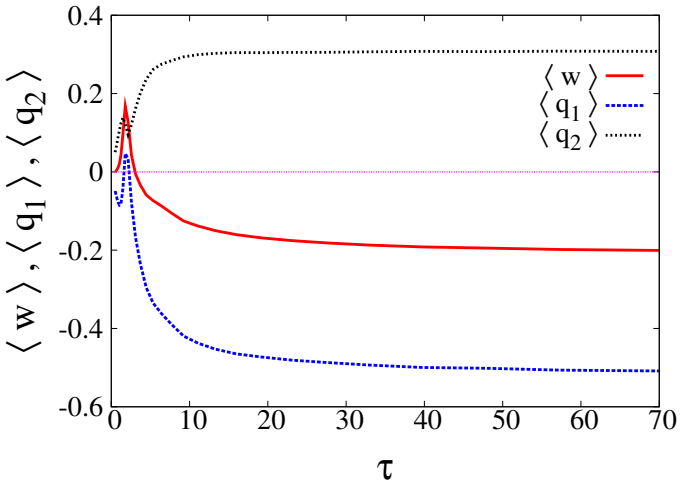

Figure 3.4: Variation of$\langle w\rangle$, $\langle q_1\rangle$ and $\langle q_2\rangle$ with cycle time τ.

eq.(3.9)). The work can be extracted in the region where it becomes negative. As we increase cycle time, $\langle q_1\rangle$ changes dramatically. It has a positive region sandwiched between two negative regions. When $\langle q_1\rangle > 0$ heat is released to the hot bath while work is done on the particle. In the quasistatic limit it saturates at the theoretical value -0.523(from eq.(3.11)). In contrast to $\langle q_1\rangle$, $\langle q_2\rangle$ is always positive, i.e., heat is always released to the cold bath. Internal energy being a state function, $\langle \Delta u\rangle$ is zero over a cycle in TPSS and hence $\langle w\rangle = \langle q_1\rangle + \langle q_2\rangle$. Using the saturation value of $\langle w\rangle$ and $\langle q_1\rangle$ we immediately get $\langle q_2\rangle$ to be equal to 0.310 which is close to our numerical result.

We now study the nature of stochastic efficiency η and engine power $p = -\frac{w}{\tau}$ as a function of cycle time. The engine is in TPSS where probability distributions of system variables are periodic in time. However, for a given realization of a cycle, state of the system (position and velocity) does not come back to its initial state. Thus for each cycle thermodynamic quantities will depend on the particular microscopic trajectory and hence w, q_1, q_2, η and p are all fluctuating quantities from cycle to cycle. The average efficiency is defined as $\langle\eta\rangle = \langle\frac{w}{q_1}\rangle$. Due to fluctuation in w and q_1, it is to be noted that $\langle\eta\rangle = \langle\frac{w}{q_1}\rangle \neq \frac{\langle w\rangle}{\langle q_1\rangle} = \bar{\eta}$. Fluctuation theorems [51, 81, 82] put

stringent condition on $\frac{\langle w \rangle}{\langle q_1 \rangle}$ which is bounded by the Carnot efficiency i.e., $\frac{\langle w \rangle}{\langle q_1 \rangle} \leq 1 - \frac{T_l}{T_h}$. However, no such bound exist for $\langle \eta \rangle$ [82].

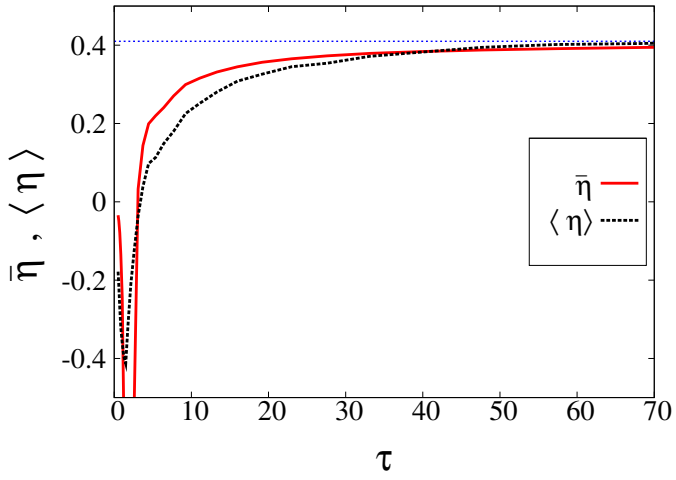

Figure 3.5: Variation of $\langle \eta \rangle$ and $\bar{\eta}$ with cycle time τ.The doted blue line denotes the quasistatic limit for $\bar{\eta}$.

The first law for any microscopic realization of cycle can be written as

$$w = \Delta u + q_1 + q_2. \tag{3.17}$$

The change in the internal energy Δu is unbounded. It is zero only on the average. Similarly q_1, q_2 and w take values in the range $(-\infty, \infty)$ but are constrained by first law. Hence it is not surprising that η can take values between $-\infty$ to ∞.

In figure 3.5 we have plotted efficiencies $\langle \eta \rangle$ and $\bar{\eta}$ as a function of cycle time. Initially for small τ, our system doesn't work as an engine. Due to large dissipation work cannot be extracted ($\langle w \rangle \geq 0$). In this regime, efficiency is negative. On further increasing τ, efficiency becomes positive and it monotonically increases. For large τ, $\langle \eta \rangle$ and $\bar{\eta}$ saturate. The saturation value for $\bar{\eta}$ is 0.41 which can be obtained analytically in quasistatic regime. In general $\langle \eta \rangle \neq \bar{\eta}$. We find both $\langle \eta \rangle$ and $\bar{\eta}$ are less than the Carnot efficiency $\eta_c = 0.8$.

In figure 3.6, average power $\langle p \rangle$ is plotted as a function of τ. There is a negative

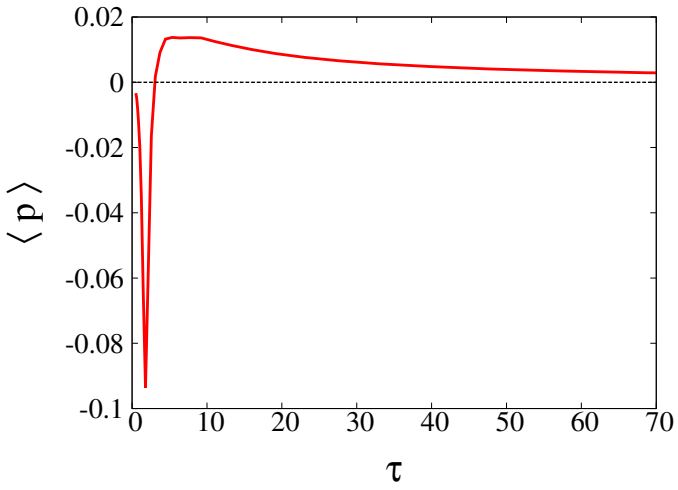

Figure 3.6: Variation of average power $\langle p \rangle$ with cycle time τ.

region for low cycle time. Beyond the critical value of $\tau \simeq 3.0$, power becomes positive and exhibits a peak and finally tends to zero in the large τ limit. The efficiencies $\langle \eta \rangle$ and $\bar{\eta}$ at maximum power are given by 0.16 and 0.25 respectively. Both of these values are less than $\eta_{CA} = 0.554$.

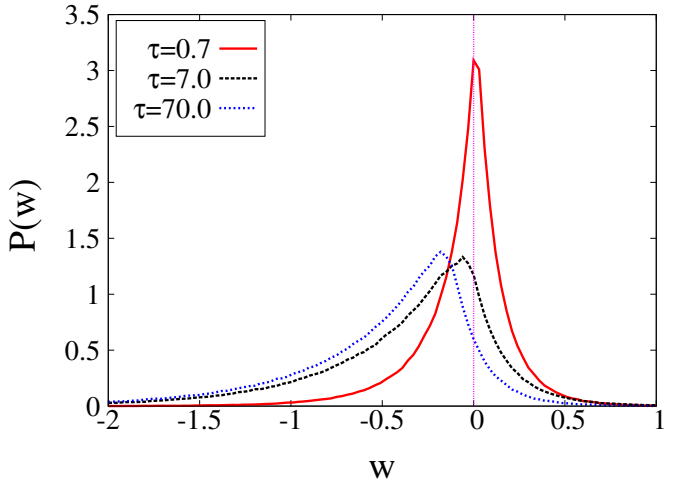

Figure 3.7: Distribution of w for different cycle times (τ=0.7, 7.0, 70.0).

As mentioned earlier, physical quantities q_1, w and η are strongly fluctuating variables. To study these fluctuations we focus on probability distribution of these quantities $P(q_1)$, $P(w)$ and $P(\eta)$. In figures 3.7, 3.8 and 3.9 we have plotted them

for three different time periods. For $\tau = 0.7$, distribution of w and q_1 are sharply peaked around zero with $\langle w \rangle = 0.005$, $\langle q_1 \rangle = -0.065$. As we increase the cycle time $P(w)$ and $P(q_1)$ become broad, asymmetric and shift towards negative side. For large negative value of arguments the distributions exhibit long tail. For large positive values of w and q_1 the distribution falls off exponentially or faster [85]. The trajectory responsible for positive values are atypical and sometimes referred to as transient second law violating trajectories [17, 86, 42]. Strong fluctuations in heat and work persist even in the quasistatic limit($\tau = 70$). These fluctuations in work are mainly attributed to two adiabatic processes, while fluctuations of q_1 result from relaxation process when the system, in contact with low temperature bath, is brought in direct contact with high temperature reservoir.

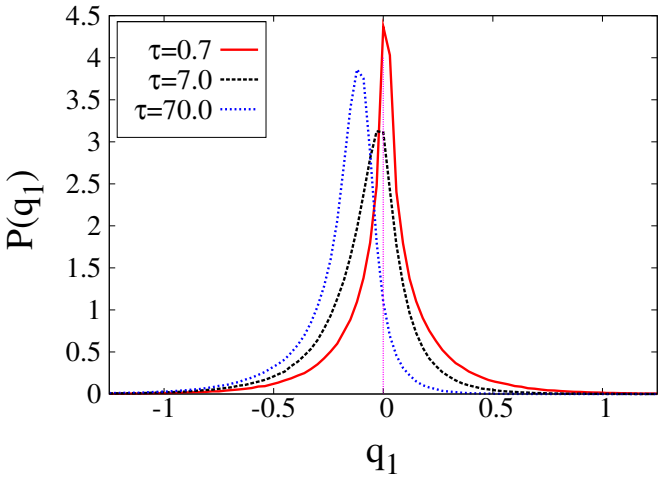

Figure 3.8: Distribution of q_1 for different cycle times.

For $\tau = 0.7$, $\langle \eta \rangle$ is negative (-0.26). The distribution $P(\eta)$ is asymmetric and there is a broad shoulder on the negative side. As we increase τ, distribution shifts towards positive side. It is not surprising to see the finite weight for values $\eta < 0$ and $\eta > 1$ [82]. Moreover, we have noticed (see inset of figure(3.9)) that the tail of $P(\eta)$ decays as a power law (η^{α}) for several decades. The exponent α depends on the system and protocol parameters (e.g., τ) and are given in figure captions. It is

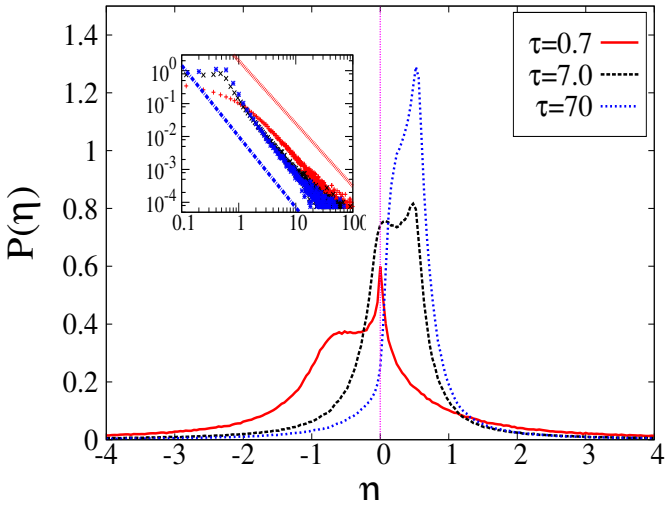

Figure 3.9: Distribution of η for different cycle times. Inset shows positive tails of the distributions plotted in log scale. They behave as η^{α}. For τ= 0.7, α =-1.906 $\pm$ 0.005; for τ= 7.0, α =-2.018 $\pm$ 0.006 and for τ= 70, α =-2.158 $\pm$ 0.007.

not clear whether this power extends indefnitely for large values of η. However, given our numerical data we can calculate variance which is finite. As we increase the cycle time the standard deviation of η (σ_η), becomes smaller. However, it remains larger compared to mean values. For example, $\langle\eta\rangle = 0.161$ and corresponding $\sigma_\eta = 1.32$ at $\tau = 7.0$ and $\langle\eta\rangle = 0.406$ whereas $\sigma_\eta = 1.11$ for $\tau = 70.0$. We would like to emphasize that mean is dominated by fluctuations even in the quasistatic regime. Any physical quantity with relative variance larger than one, is referred to as non-self averaging quantity. For such cases mean ceases to be a good physical variable and one has to resort to the analysis for full probability distribution. This is one of our main result. Non-self averaging quantities arises mainly in physics of quenched disordered systems.

Note that, η becomes positive if both w and q_1 are positive or both of them are negative. η becomes negative when w and q_1 have opposite signs. In order to have a better understanding of our system we have plotted the joint distributions of w and q_1 for different τ in figure 3.10. For a given cycle, the system acts as an engine when both w and q_1 are negative i.e, in the third quadrant of the plot. Using our numerical

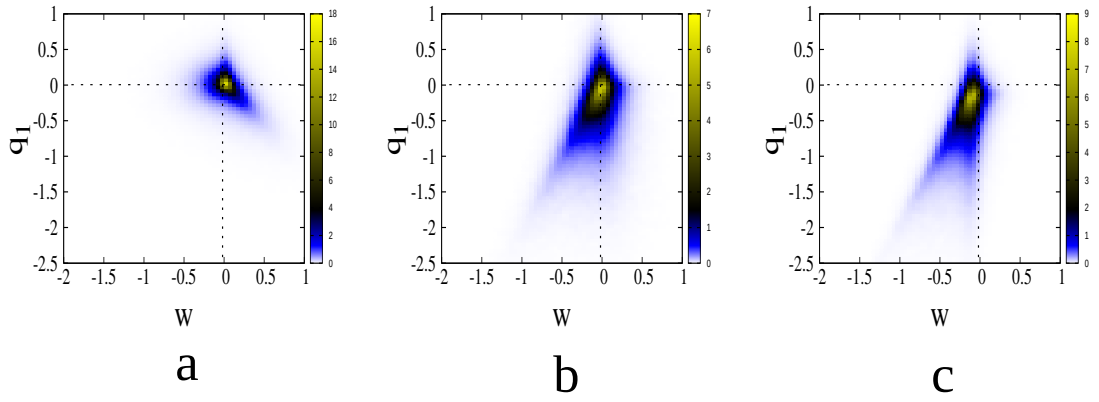

Figure 3.10: Joint distribution of w and q_1 for different τ. In a) $\tau = 0.7$, in b) $\tau = 7.0$, in c) $\tau = 70$.

results we have calculated the ratio of the total number of realizations falling in the third quadrant to the total number of realizations. These fractions for $\tau = 0.7$, 7.0 and 70.0 are calculated to be 0.226, 0.583 and 0.858, respectively. It is clear from this that for large cycle times the reliability of the system working as an engine increases. Though we observe that even in quasistatic regime there are realizations for which the system does not act as an engine. This is due to strong fluctuations in work and heat as discussed earlier. In the following table we have sumarized our numerical results for a comparision.

Table 3.1: For Underdamped case

Cycle time	$\langle w \rangle$	$\langle q_1 \rangle$	$\langle p \rangle$	$\bar{\eta}$	$\langle \eta \rangle$	σ_η	acts as engine
0.7	0.005	-0.065	-0.007	-0.074	-0.260	2.09	22.6%
7.0	-0.095	-0.375	0.014	0.254	0.161	1.32	58.3 %
70.0	-0.201	-0.508	0.003	0.395	0.406	1.11	85.8 %

In TPSS the joint probability density $P_{ss}(x, v, t)$ is periodic in time: $P_{ss}(x, v, t + \tau) = P_{ss}(x, v, t)$. For simplicity we write $P_{ss}(x, v, t) = e^{-\phi(x,v,t)}$. From the definition of stochastic entropy [27, 13, 87] of the system S_{sys}, the change in the system entropy for a trajectory over a cycle is given by $\Delta S_{sys} = \Delta\phi = \phi(x_2, v_2, \tau) - \phi(x_1, v_1, 0)$

where (x_1, v_1) and (x_2, v_2) are the initial and final phase space points for a particular realization of the cycle. To calculate $\Delta\phi$ we evaluate $P_{ss}(x, v, 0)$ at the initial point of the cycle which also coincide at the end point $t = \tau$. In figure 3.11 we have plotted joint phase space distribution at TPSS for three different values of $\tau = 0.7$, 7.0 and 70.0. We see that for $\tau = 0.7$ and $\tau = 7.0$ phase space distributions are not symmetric and there exist strong correlation between x and v which was ignored in the earlier literature [80]. Only in the large τ limit the distribution becomes symmetric (see figure 3.11c). The cross-correlation between position and velocity disappears and the distribution $P_{ss}(x, v)$ becomes uncorrelated Gaussian in the quasistatic limit. Due to correlation, the width of the distribution become larger as we decrease cycle time τ.

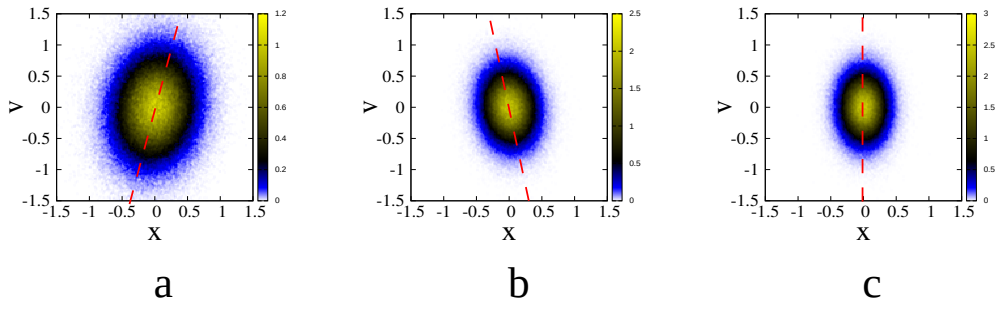

Figure 3.11: Initial phase space distribution at different cycle times τ. In a)$\tau = 0.7$, in b) $\tau = 7.0$, in c)$\tau = 70$. The asymmetric position of red broken line along the major axis of the elliptical Gaussian distribution for lower values of τ (=0.7 and 7.0) indicates nonzero $\langle xv \rangle$. This correlation becomes zero for larger τ (=70), where the position of the major axis also becomes symmetric.

Recently, FRHE in TPSS has been derived [81]. It extends the total entropy production fluctuation theorem of Seifert [27,13,88] applied to heat engine. The total entropy production ΔS_{tot} over a cycle is a stochastic variable and in our present case is given by

$$\Delta S_{tot} = \Delta\phi + \frac{q_1}{T_h} + \frac{q_2}{T_l}. \tag{3.18}$$

Using the first law (eq.3.17)

$$\Delta S_{tot} = \Delta\phi + \frac{q_1}{T_h} + \frac{w - q_1 - \Delta u}{T_l}. \tag{3.19}$$

The second law which is valid on average, can be stated as $\langle \Delta S_{tot} \rangle \geq 0$. In TPSS, $\langle \Delta u \rangle = \langle \Delta\phi \rangle = 0$, which implies $\bar{\eta} = \frac{\langle w \rangle}{\langle q_1 \rangle} \leq 1 - \frac{T_l}{T_h} = \eta_c$. Thus the second law puts the constraint on efficiency which is defined as $\frac{\langle w \rangle}{\langle q_1 \rangle}$. It should be noted that this constraint is valid for any finite time cycle in TPSS, unlike the Carnot which is valid for macroscopic engines in the quasistatic regime. However, it does not put any constraint on the average efficiency ($\langle \frac{w}{q_1} \rangle$). The fluctuation theorem for heat engine replaces the inequality relation of the second law by the equality relation, namely [81],

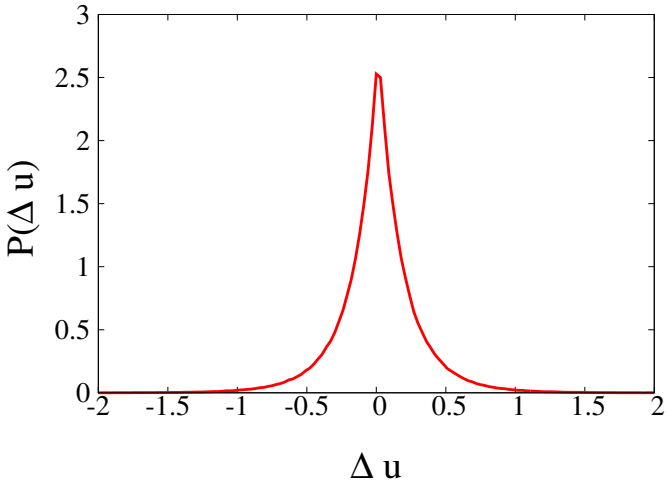

Figure 3.12: Distribution of the internal energy change in one cycle for underdamped steady state for τ=7.0.

$$\langle e^{-\Delta S_{tot}} \rangle = \langle e^{-(\Delta\phi + \frac{q_1}{T_h} + \frac{w - q_1 - \Delta u}{T_l})} \rangle = 1 \tag{3.20}$$

eq.(3.20) is FRHE in TPSS. By calculating all the relevant stochastic variables w, q_1, $\Delta\phi$, Δu over all trajectories for finite τ we have verified eq.(3.20) in the TPSS. We have obtained the value to be 0.96 for $\tau = 7.0$, which is well within our numerical

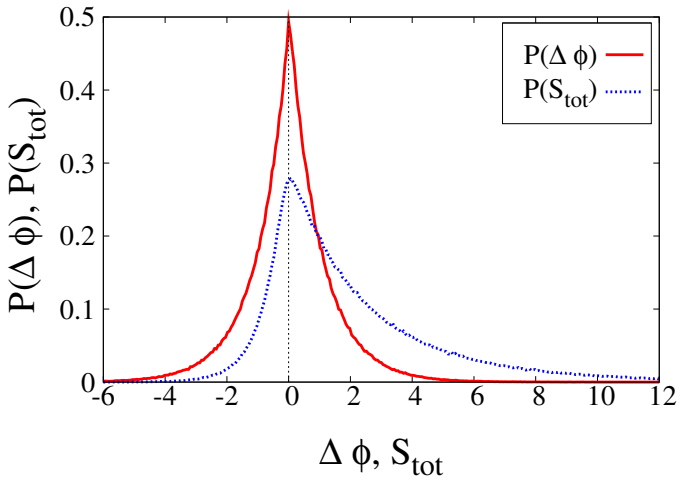

Figure 3.13: Distribution of system entropy change and total entropy production in one cycle for underdamped steady state for τ=7.0

.

accuracy. We would like to emphasize that, in eq.(3.20), four stochastic variables appear in the exponent. Small changes in these values affect the exponential function by a large amount. Given this fact, our observed value of $\langle e^{-\Delta S_{tot}} \rangle$ is quite satisfactory.

For the same parameter value $\tau = 7.0$, in figure 3.12 we have plotted the probability distribution, $P(\Delta u)$, as a function of Δu. In figure 3.13, we have plotted the probability distribution of change of system entropy $P(\Delta\phi)$ and total entropy $P(\Delta S_{tot})$ as a function of their arguments. It is clear that as u and ϕ are state functions, $P(\Delta u)$ and $P(\Delta\phi)$ are symmetric with zero mean. However, the distribution $P(\Delta S_{tot})$ is asymmetric with a long tail for positive large ΔS_{tot}. There is also a finite weight towards negative ΔS_{tot}. This contribution arises due to transient second law violating periodic cycles [17, 42]. However, $\langle \Delta S_{tot} \rangle$ remains positive as demanded by the second law.

Till now we concentrated on symmetric cycle, i.e., equal contact times of the system with hot and cold bath. Naturally, the question arises what will happen if the cycle is time asymmetric. To the best of our knowledge this question has

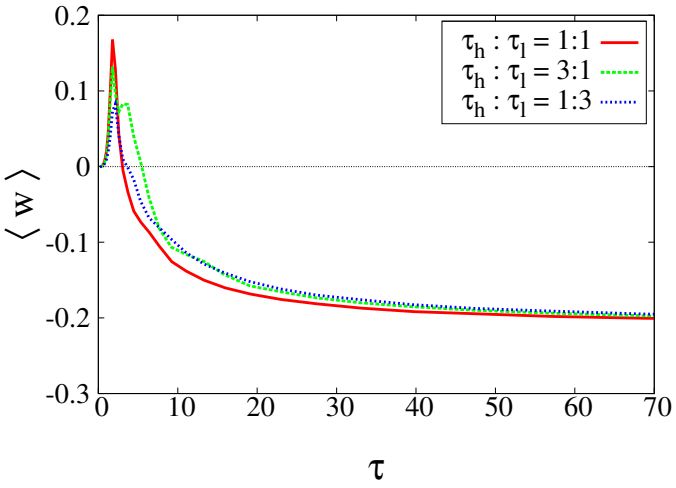

Figure 3.14: Variation of $\langle w \rangle$ vs τ for symmetric as well as asymmetrical cycles. Here τ_h and τ_l are contact times of the particle with hot and cold bath respectively. Thus, $\tau = \tau_h + \tau_l = 7.0$ for our case.

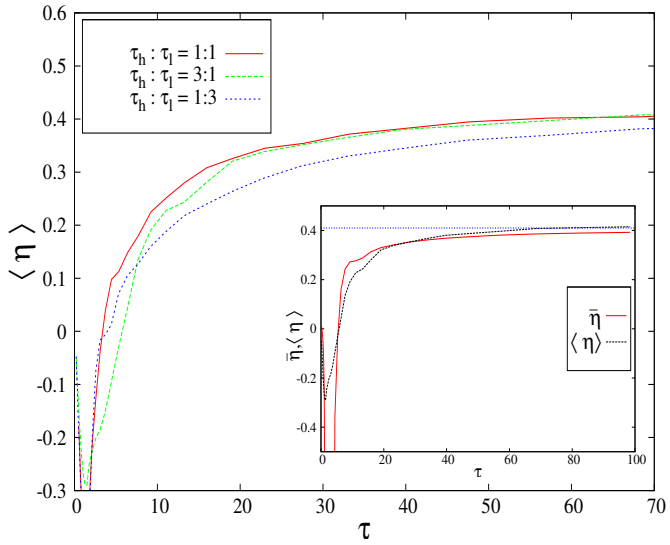

Figure 3.15: (Color online) Variation of $\langle \eta \rangle$ vs τ for symmetric as well as asymmetrical cycles. inset: comparision of $\langle \eta \rangle$ with $\bar{\eta}$ for $\tau_h : \tau_l = 3 : 1$.

not been addressed in earlier literature. If the contact time of one bath is different from that of the other, it can affect work output, heat dissipation to each bath, power and efficiency. However, in the quasistatic limit there should not be any effect of this asymmetry. This is clear from figure 3.14 that the average work, for three different asymmetric cycles, asymptotically approach each other in the quasistatic

limit. In the non-quasistatic limit, work extracted by the engine for asymmetric cycles is small compared to symmetric cycle. From figure 3.15 it is seen that $\langle\eta\rangle$ is lower for asymmetrical cycles. The inset shows even in quasistatic limit $\langle\eta\rangle \neq \bar{\eta}$ for $\tau_h : \tau_l = 3 : 1$. We have verified separately that asymmetry also decreases the power. Thus asymmetry in the cycle degrades the performance characteristics of the engine.

We now briefly compare the nature of power and efficiency of our system when the confining potential is different. We have taken the confining potential $\frac{1}{2}k(t)x^n$ with n=2,4,6. For n=4,6 the confining potentials are referred to as hard potential. The equilibrium distributions for hard potentials are no longer Gaussian and hence in the quasistatic limit, the average work, heat dissipation etc., will be different from those for the harmonic potential.

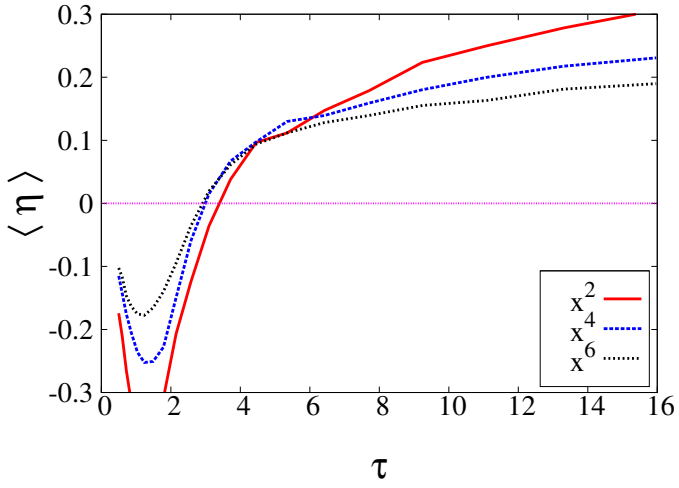

Figure 3.16: Variation of $\langle\eta\rangle$ with τ for different types of potentials.

In figure 3.16 and 3.17 we have plotted $\langle\eta\rangle$ and $\langle p\rangle$ as a function of cycle time for different potentials. Average efficiency $\langle\eta\rangle$ for large τ decreases as potential becomes harder and thereby degrading the performance. $\langle\eta\rangle$ saturates at the higher value of τ (not shown in the figure). From figure 3.17 we observe that harder the potential smaller will be the critical time τ above which the system acts as an engine. For large cycle time the power decreases as the potential becomes harder. However, we

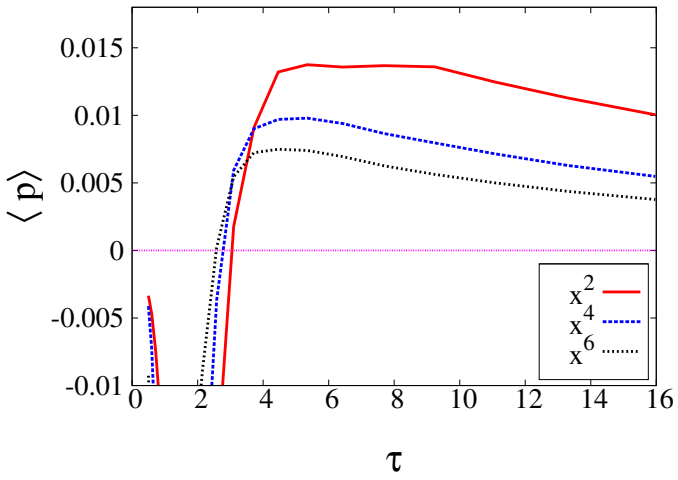

Figure 3.17: Variation of power $\langle p \rangle$ with τ for different types of potentials.

see clearly that there are three values of efficiencies $\langle \eta \rangle$ and $\bar{\eta}$ at maximum power 0.16, 0.10, 0.08 and 0.25, 0.16, 0.13 for n=2,4,6 respectively. It is apparent that the efficiency at maximum power is model dependent and decreases as the potential becomes harder. Even the saturation value is different and it is lower for harder potential. Clearly, these two figures indicate that operational characteristics of our system are model dependent. Thus we do not expect any universal relation involving only the average efficiency at maximum power and temperatures of the reservoirs.

So far we have studied our system in detail in the underdamped regime which is a general case. From now on we restrict to the overdamped regime and highlight some qualitative differences.

3.5 Overdamped quasistatic case

In the overdamped limit, dynamics of the system follows Langevin eq.(3.2), where inertial effects are ignored. This approximation is valid when the time steps of the observation are much larger than m/γ. The internal energy of the system is given only in terms of potential energy. For this case equilibrium distribution of a particle

in a static harmonic potential is given by $P_{eq}(x) = Ne^{-\frac{kx^2}{2k_BT}}$ from which one can easily obtain the free energy. The analytical calculation for average thermodynamic quantities in quasistatic limit are similar to the underdamped case. The total average work done on the particle during the entire cycle is given by as

$$\begin{aligned} W_{tot} &= \Delta F_h + W_2 + \Delta F_l + W_4 \\ &= \frac{T_h}{2}\ln\frac{1}{2} - \frac{T_h}{4} + \frac{T_l}{2}\ln 2 + \frac{T_l}{2}. \end{aligned} \tag{3.21}$$

Interestingly, the expression for W_{tot} remains the same as for the case of the inertial system discussed earlier and the system extracts work provided $\frac{T_l}{T_h} < 0.705$. Using same arguments similar to the underdamped case and keeping in mind only the fact that there is only one phase space variable, namely position, the average internal energy change in the overdamped limit in the first step can be expressed as

$$\Delta U_1 = \frac{T_h}{2} - T_l. \tag{3.22}$$

Using the first law the average heat absorption from the hot bath during the first step is

$$-Q_1 = \Delta U_1 - \Delta F_h = \frac{T_h}{2} - T_l - \frac{T_h}{2}\ln\frac{1}{2}. \tag{3.23}$$

The expression for efficiency in the overdamped case is

$$\bar{\eta}_q = \frac{-W_{tot}}{-Q_1} = -\frac{\frac{T_h}{2}\ln\frac{1}{2} - \frac{T_h}{4} + \frac{T_l}{2}\ln 2 + \frac{T_l}{2}}{\frac{T_h}{2} - T_l - \frac{T_h}{2}\ln\frac{1}{2}}, \tag{3.24}$$

which is different from the earlier case. In quasistatic limit, from eq.(3.23) heat flows from the bath to the system provided $\frac{T_l}{T_h} < \frac{1+\ln 2}{2} = 0.846$. This ratio $\frac{T_l}{T_h}$ differs from that obtained for the underdamped case. From Eqs.(3.21) and (3.23), the system acts as an engine for the same condition ($\frac{T_l}{T_h} < 0.705$) as for the underdamped case. A

finite temperature difference between hot and cold bath is required so that the system can act as a heat engine.

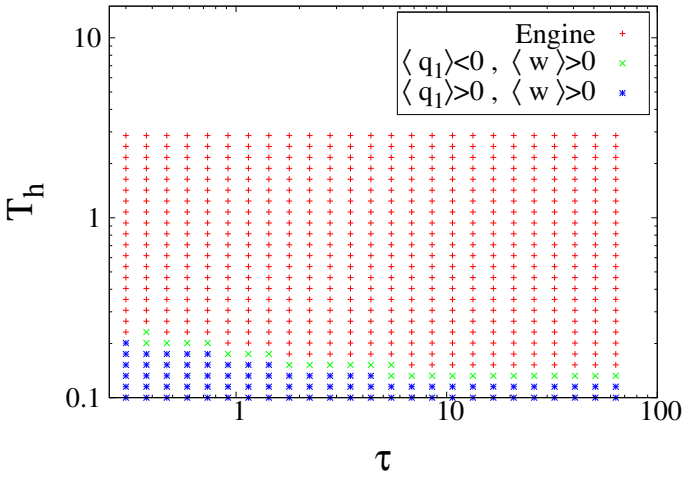

Figure 3.18: Phase diagram for different T_h and τ but for fixed $T_l = 0.1$.

3.6 finite cycle time engine in the Overdamped regime

Analysis for finite time cycle is carried out by numerical methods as discussed earlier. For a better understanding in the overdamped regime, all the parameters have been kept same as in the underdamped case. In figure 3.18, we have plotted the phase diagram for the overdamped case keeping T_l fixed at 0.1. For large τ (quasistatic limit) we observe, from phase diagram, that the system operates as a heat engine provided T_h is greater than a critical value. This critical value is close to the theoretical value of 0.142 obtained from the bounds determined in quasistatic calculation. The phase diagram shows a qualitative difference from the underdamped phase diagram (figure 3.3). The system always acts as an engine in $\tau \to 0$ limit provided we are above a critical value of T_h, which is not the case for the underdamped engine. This is clear from figure 3.19, where we have plotted average work done on the system $\langle w \rangle$ and

average heat released to each bath with $\langle q_1 \rangle$ and $\langle q_2 \rangle$ as a function of τ. Note that the observed anomalous part for $\langle w \rangle$ and $\langle q_1 \rangle$ in the underdamped case for small τ regime is absent in this regime. The quantities $\langle w \rangle$, $\langle q_1 \rangle$ and $\langle q_2 \rangle$ show monotonic behavior and saturate at large cycle time to their analytical limits -0.214, -0.324 and 0.110, respectively. Unlike the underdamped case here, $\langle w \rangle$ and $\langle q_1 \rangle$ are always negative.

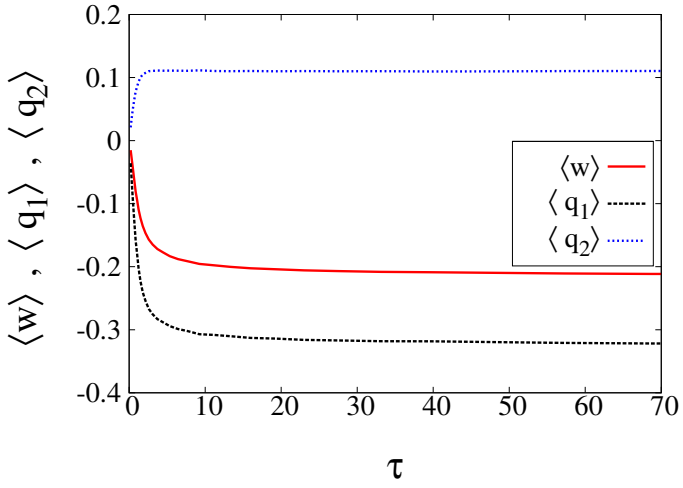

Figure 3.19: Variation of $\langle w \rangle$, $\langle q_1 \rangle$ and $\langle q_2 \rangle$ with cycle time τ.

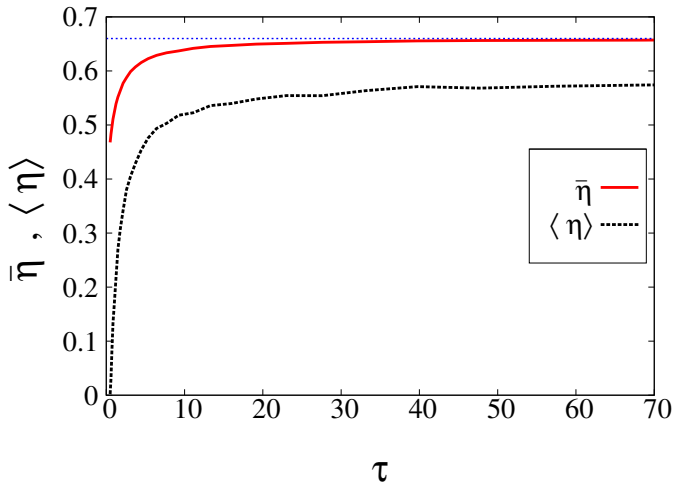

Figure 3.20: Variation of $\langle \eta \rangle$ and $\bar{\eta}$ with cycle time τ. The doted blue line denotes the quasistatic limit for $\bar{\eta}$.

In figure 3.20 we have plotted the average of efficiency $\langle \eta \rangle$ and $\bar{\eta}$ as a function of τ. Both the efficiencies increase monotonically from zero and saturate for large τ.

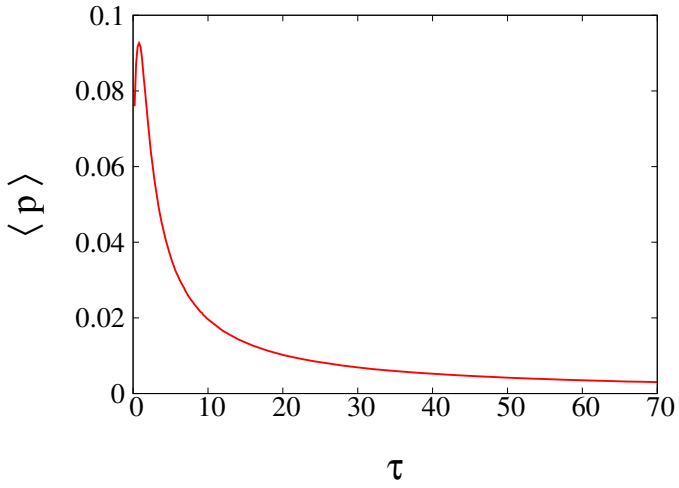

Figure 3.21: Variation of $\langle p \rangle$ with cycle time τ.

The saturation value of $\bar{\eta}$ is close to the theoretically predicted value of 0.660. The saturation value of $\langle \eta \rangle$ is found numerically to be 0.571 which is much less than the corresponding value of $\bar{\eta}$. Both these values are less than the Carnot value $\eta_c = 0.8$. It is clear that $\langle \eta \rangle \neq \bar{\eta}$ due to the strong correlation between fluctuating variables w and q_1 for all τ.

From figure 3.21, we see that power exhibits a sharp peak at $\tau = 0.8$. Corresponding efficiencies $\langle \eta \rangle$ and $\bar{\eta}$ at maximum power are equal to 0.11 and 0.51 which are less than the C-A result ($\eta_{CA} = 0.554$).

To study the nature of fluctuations in the overdamped regime we have plotted the distribution $P(w)$, $P(q_1)$ and $P(\eta)$ in figures 3.22, 3.23 and 3.24 respectively. The qualitative nature of the distributions of $P(w)$ and $P(q_1)$ remain the same for different values of τ as in the underdamped case. The fluctuations are smaller compared to the underdamped case. The distribution $P(\eta)$ shows a double peak behavior for $\tau = 0.7$ with $\langle \eta \rangle = 0.086$ and standard deviation $\sigma_\eta = 1.688$. For $\tau = 7.0$, $\langle \eta \rangle = 0.496$ and $\sigma_\eta = 1.287$. For $\tau = 70$, $\langle \eta \rangle = 0.571$ and $\sigma_\eta = 1.234$. We observe that even in the quasistatic regime, fluctuations of η dominate over the mean value. Thus η is a non self averaging quantity. We have also seen that the fraction of the realizations for

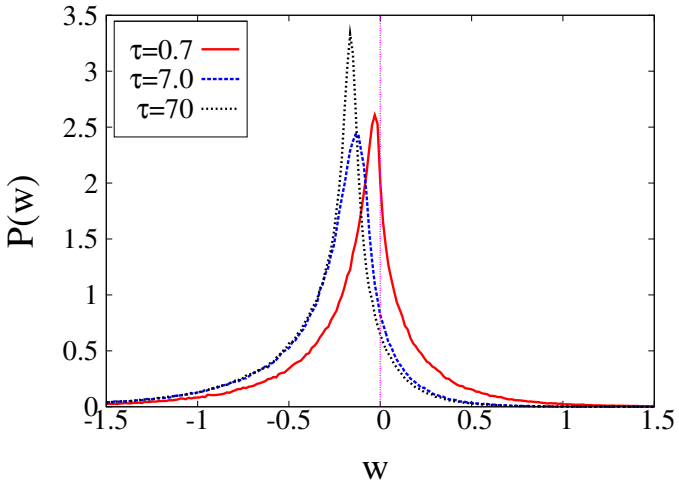

Figure 3.22: Distribution of w for different cycle times in the overdamped case.

which the system acts as an engine, increases with cycle time τ. Numerical values for these fractions are 0.488, 0.817 and 0.861, for $\tau = 0.7$, 7.0 and 70.0, respectively. Hence, finite fraction of realization does not act as an engine even in quasistatic limit. Similar to the underdamped case, the reliability of the system to act as an engine increases with τ. We sumarize our numerical results in the following table:

Table 3.2: For Overdamped case

Cycle time	$\langle w \rangle$	$\langle q_1 \rangle$	$\langle p \rangle$	$\bar{\eta}$	$\langle \eta \rangle$	σ_η	acts as engine
0.7	-0.064	-0.131	0.092	0.493	0.086	1.688	48.8 %
7.0	-0.190	-0.302	0.027	0.631	0.496	1.287	81.7 %
70.0	-0.210	-0.319	0.003	0.658	0.571	1.234	86.1 %

Finally, we discuss the performance characteristics of our system in the overdamped regime using an experimental protocol [66]. The experimental protocol consists of only two steps, in which the two adiabatic steps of figure 3.1 are absent. In the quasistatic regime the system acts as an engine for any temperature difference and there is no bound on T_h unlike our four step protocol [66]. This suggests that the phase diagram will depend on the nature of protocol as well as on system parameters and is not unique. As discussed earlier, most of the work fluctuations specially in

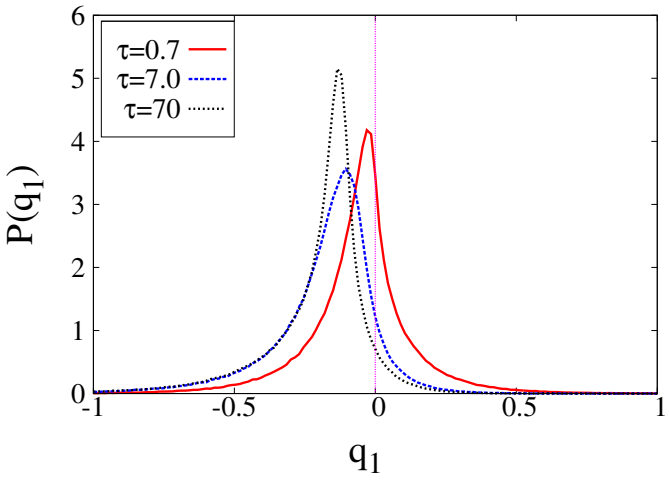

Figure 3.23: Distribution of q_1 for different cycle times in the overdamped case.

quasistatic regime arise from two adiabatic steps. In the absence of these two steps, we have observed in our simulation that in the quasistatic regime, work distribution $P(w)$ is sharply peaked like a delta function at $W = -\frac{1}{2}(T_h - T_l)\ln 2$ (analytical result) [66]. However, fluctuations in q_1 persist even in the quasistatic regime as a result of the relaxation process that follows when the system, in contact with the cold bath, is brought in direct contact with high temperature reservoir. The distribution of stochastic efficiency $P(\eta)$ exhibits a qualitative differences. It has almost zero weight for $\eta < 0$ in large τ limit and shows a broad double peak feature which is confined in the region $0 < \eta < 1$. Beyond $\eta > 1$ a long tail is observed. For $\tau = 70$ we have numerically calculated $\langle\eta\rangle = 0.579$ and $\sigma_\eta = 0.903$. Even for this protocol we notice that fluctuations dominates over the mean value.

3.7 Summary

We summarise our results in this section. We have carried out an extensive analysis of a single particle stochastic heat engine by manipulating a Brownian particle in a harmonic trap with a periodically time dependent stiffness constant as a protocol.

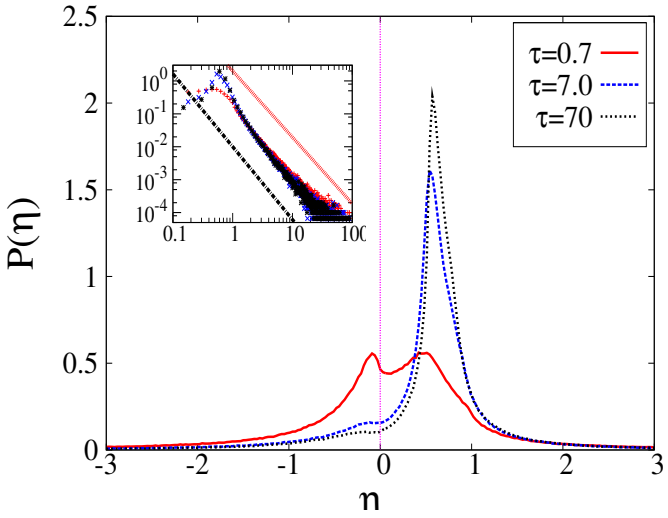

Figure 3.24: Distribution of η for different cycle times in the overdamped case. Inset shows positive tails of the distributions plotted in log scale. Slopes of the straight lines indicate the exponents. For τ= 0.7, 7.0 and α =-2.013 $\pm$ 0.004, -2.186 $\pm$ 0.005 and -2.213 $\pm$ 0.006 respectively.

The cycle consists of two isothermal steps and two adiabatic steps similar to that of Carnot engine. The proposed model is studied taking into account both the inertial and overdamped Langevin equations. Thermodynamic quantities, defined over microscopic phase space trajectory of our system, fluctuate from one cycle of operation to another. Their magnitude depends on the trajectory of the particle during the cycle. This is done by using the methods of stochastic energetics. Average value of thermodynamic quantities and their distribution functions have been calculated numerically in TPSS. Analytical results of average thermodynamic quantities have been obtained in the quasistatic regime. These results are consistent with the corresponding numerical results. We have reported several new results which were not addressed in earlier literature.

The full phase diagram for operation of a system is given in both inertial and high friction regime. They differ from each other qualitatively. In both cases it is also shown that system acts as an engine provided the temperature difference is greater than a critical value (unlike Carnot engine). This critical value depends on system

parameters and is consistent with analytical results in quasistatic limit. Moreover, for fixed bath temperatures and system parameters there should be a critical cycle time above which the system acts as an engine.

The mean of the stochastic efficiency is dominated by its fluctuations ($\langle\eta\rangle < \sigma_\eta$) even in quasistatic regime, making the efficiency a non-self averaging quantity. This implies that in such a situation mean is not a good physical variable and one must study the behaviour of full probability distributions which in all our cases contain power law behaviour in their tails with varied exponents. This is one of our main result. We have also shown that $\bar{\eta} = \frac{\langle w\rangle}{\langle q_1\rangle} \neq \langle\frac{w}{q_1}\rangle = \langle\eta\rangle$.

Our analysis of model dependence of finite cycle time clearly rules out any simple universal relation (e.g., $\eta_{CA} = 1 - \sqrt{\frac{T_l}{T_h}}$.) between efficiency at maximum power and temperature of the baths. Time asymmetric periodic protocol makes engine less efficient. Only in the quasistatic regime time asymmetry does not play any role.

For given cycle time there are several realizations which do not work as a heat engine. These are referred to as transient second law violating trajectories. Number of these realizations decreases as we increase τ. The fractions of realisations following second law with corresponding τ are reported earlier sections both in underdamped and overdamped regimes. Thus for large cycle time the reliability of the system working as an engine increases. Persistence of these realizations even in quasistatic regime can be attributed to the fluctuation of heat and work distributions. Fluctuations in work are mainly attributed to two adiabatic processes connecting two isotherms, while fluctuations of q_1 result from the relaxation of the system, when brought in direct contact with high temperature reservoir from low temperature bath.

We have shown that in TPSS $P_{ss}(x, v, t)$ exhibit strong correlation between variables x and v in small cycle time limit. However, it becomes uncorrelated as we approach quasistatic limit. For analytical simplicity it had been generally assumed in earlier literature that there is no correlation between x and v in $P_{ss}(x, v, t)$ (see for

example [80]).

In the inertial regime we have also verified the recently proposed fluctuation theorems for heat engines in a TPSS. Our results are amenable to experimental verifications.

Chapter 4

Quantum JE with multiple measurement and feedback

4.1 Introduction

In this chapter we derive the Jarzynski equality (JE) for an isolated quantum system for three different cases: (i) for unitay evolution with no intermediate measurements, (ii) with intermediate measurements of arbitrary observables being performed, and (iii) with intermediate measurements whose outcomes are used to modify the external protocol (feedback). We find that the JE remains unaffected in the second case, but gets modified in the third case where the mutual information between the measured values with the actual eigenvalues must be incorporated into the relation.

In earlier chapters we have already introduced fluctuation theorems [20, 21, 23, 28, 29]. One of the pioneering works was due to Jarzynski [23], who had derived a relation between the nonquilibrium work performed on a system to change in its equilibrium free energy. Let us consider a system that is initially at canonical equilibrium with a heat bath at inverse temperature $\beta = \frac{1}{k_B T}$. Subsequently an external perturbation $\lambda(t)$, called protocol, is applied to the system that takes it out of equilibrium. At time $t = \tau$, the process is terminated when the parameter value reaches $\lambda(\tau)$. The work W done on the system will in general vary for different phase space trajectories, owing to the randomness of the initial state and thermal fluctuations due to coupling with the environment during the evolution. The Jarzynski equality (JE) states that,

$$\langle e^{-\beta W} \rangle = e^{-\beta \Delta F}. \tag{4.1}$$

Here, the angular brackets denote ensemble averaging over a large number of repetitions of the experiment. $\Delta F \equiv F(\lambda(\tau)) - F(\lambda(0))$ is the difference in the equilibrium free energy of the system between the final and the initial states. The JE has been extended to quantum domain [44] in presence of measurement [89] and feedback [90, 91]. JE in presence of feedback has also been verified experimentally [92]. Quantum feedbacks are important in nanosytems or mesoscopic systems and can be applied to

produce the cooling of nanomechanical resonators and atoms [93, 94].

In this chapter we derive quantum extended JE with multiple measurements and feedback for an isolated system. Our treatment is based on path probability in state space for each realization as opposed to formal approach dealing with projection operator and density matrices [90, 91]. All the results are simple extensions of the theorems for fixed protocol, and the latter in turn depends on the principle of microscopic reversibility. It may be noted that only with the choice of von Neumann type measurements, corresponding to the measurement operator $\Pi_j \equiv |j\rangle\langle j|$, the earlier approaches reduce to the present approach. Here, $|j\rangle$ is an eigenstate of the measured observable.

For the quantum case to obtain the work values, we perform measurement (von Neumann type) of system energies (or Hamiltonian $H(t)$) at the beginning and end of protocol. The measured energy eigenvalues are denoted by $E_{i_0}(\lambda(0))$ and $E_{i_\tau}(\lambda(\tau))$ and corresponding instantaneous eigenstates by $|i_0\rangle$ and $|i_\tau\rangle$ respectively. The work done on the system by changing external protocol $\lambda(t)$ is given by

$$W = E_{i_\tau}(\lambda(\tau)) - E_{i_0}(\lambda(0)). \tag{4.2}$$

W is a realization dependent random variable. Initially the system is brought into contact with large reservoir at temperature T, thereby allowing the system to equilibrate. Subsequently the system is decoupled from the bath and the system evolves unitarily with a given Hamiltonian H(t). Our treatment closely follows [95] wherein Hamiltonian derivation of JE under feedback control is derived for classical case.

Probability of system being in state $|i_0\rangle$ is given by

$$p(i_0) = \frac{e^{-\beta E_{i_0}(\lambda(0))}}{Z_0}. \tag{4.3}$$

The partition function is defined as

$$Z_0 = \sum_{i_0} e^{-\beta E_{i_0}(\lambda(0))}. \tag{4.4}$$

Between measurements, the system undergoes unitary evolution with an operator U given by

$$U_\lambda(t_2, t_1) = T \exp\left(-\frac{i}{\hbar}\int_{t_1}^{t_2} H(t, \lambda(t))dt\right), \tag{4.5}$$

where T denotes time ordering and $H(t)$ is the system Hamiltonian. The probability of the system initially in the state $|i_0\rangle$ to be found in state $|i_\tau\rangle$ at time τ is given by

$$P(i_\tau|i_0) = |\langle i_\tau|U_\lambda(\tau, 0)|i_0\rangle|^2. \tag{4.6}$$

Thus the joint probability of state being in $|i_0\rangle$ and $|i_\tau\rangle$ is

$$P(i_\tau, i_0) = P(i_\tau|i_0)p(i_0) \qquad \text{(Bayes' theorem)} \tag{4.7}$$

In section 4.2, we rederive the JE for a quantum particle to make the chapter self consistent. In section 4.3, we derive the same with measurements of arbitrary observables being performed in-between. In section 4.4, we derive the extended JE for a system with the protocol being monitored by a feedback control that changes the protocol according to the outcomes of the measurements performed. In section 4.5 generalized JE involving efficacy parameter is derived.

4.2 Jarzynski Equality

For deriving JE we need to calculate $\langle e^{-\beta W}\rangle$ which is given by

$$\langle e^{-\beta W}\rangle = \sum_{i_\tau, i_0} e^{-\beta W} P(i_\tau, i_0). \tag{4.8}$$

Substituting the expression for realization dependent work (eq.(4.2)) and joint probability $P(i_\tau, i_0)$ (eq.(4.7)) and using eq.(4.3) and eq.(4.6) we get

$$\begin{aligned}\langle e^{-\beta W}\rangle &= \sum_{i_0,i_\tau} e^{-\beta(E_{i_\tau}(\lambda(\tau))-E_{i_0}(\lambda(0))}|\langle i_\tau|U_\lambda(\tau,0)|i_0\rangle|^2\frac{e^{-\beta E_{i_0}(\lambda(0))}}{Z_0}\\ &= \sum_{i_0,i_\tau}\frac{e^{-\beta E_{i_\tau}(\lambda(\tau))}}{Z_0}\langle i_\tau|U_\lambda(\tau,0)|i_0\rangle\langle i_0|U_\lambda^\dagger(\tau,0)|i_\tau\rangle. \end{aligned} \tag{4.9}$$

Making use of completeness relation $\sum_{i_0}|i_0\rangle\langle i_0| = 1$ and normalization condition $\langle i_\tau|i_\tau\rangle = 1$ and unitarity of evolution, $U_\lambda^\dagger U_\lambda = 1$, we have,

$$\langle e^{-\beta W}\rangle = \sum_{i_\tau}\frac{e^{-\beta E_{i_\tau}(\lambda(\tau))}}{Z_0} = \frac{Z_\tau}{Z_0} = e^{-\beta\Delta F}. \tag{4.10}$$

where, $Z_\tau = \sum_{i_\tau} e^{-\beta E_{i_\tau}(\lambda(\tau))}$, is the partition function of the system with the control parameter held fixed at $\lambda(\tau)$ and $\Delta F = \ln\frac{Z_0}{Z_\tau}$ is the equilibrium free energy difference between final and initial states. This is the quantum version of the JE [44]. Using Jensen's inequality, we retrieve the second law from the above relation:

$$\langle W\rangle \geq \Delta F, \tag{4.11}$$

implying second law is valid for average W although for some individual realizations, W can be less than ΔF.

4.3 JE in presence of measurement

This time, one intermediate measurement (of arbitrary observables, not necessarily the Hamiltonian) at time t_1 has been carried out but the entire protocol $\lambda(t)$ is predetermined. At time t_1 the state collapses to one of the eigenstates of the measured observable, say $|i_1\rangle$, after which it evolves according to the unitary operator $U_\lambda(\tau, t_1)$ up to the final time τ. It is to be noted that the projective measurements result in

collapse of the system state to one of the eigenstates and leads to decoherence and dephasing. If along two paths, intermediate measurements are performed, then the interference between alternative paths disappear and quantum effects are suppressed. Hence in presence of measurement, path probabilities in state space obeys simple classical probability rules. For example, the path probability is simply the product of the transition probabilities between subsequent measured states. However, it may be noted that quantum mechanics enters through the explicit calculation of transition probabilities between states. The joint probability of the state trajectory is

$$P(i_\tau, i_1, i_0) = p(i_\tau|i_1)p(i_1|i_0)p(i_0) \tag{4.12}$$

$$= |\langle i_\tau|U_{\lambda_{y_1}}(\tau, t_1)|i_1\rangle|^2|\langle i_1|U_\lambda(t_1, 0)|i_0\rangle|^2 p(i_0). \tag{4.13}$$

Then,

$$\langle e^{-\beta W}\rangle = \sum_{i_\tau, i_1, i_0} e^{-\beta W} P(i_\tau, i_1, i_0).$$

using eq.(4.2), eq.(4.13) and eq.(4.3)

$$\begin{aligned}
\langle e^{-\beta W}\rangle &= \sum_{i_0, i_1, i_\tau} e^{-\beta(E_{i_\tau}(\lambda(\tau)) - E_{i_0}(\lambda(0)))} |\langle i_1|U_\lambda(t_1, 0)|i_0\rangle|^2 |\langle i_\tau|U_\lambda(\tau, t_1)|i_1\rangle|^2 \frac{e^{-\beta E_{i_0}(\lambda(0))}}{Z_0} \\
&= \sum_{i_0, i_1, i_\tau} \frac{e^{-\beta E_{i_\tau}(\lambda(\tau))}}{Z_0} \langle i_1|U_\lambda(t_1, 0)|i_0\rangle\langle i_0|U_\lambda^\dagger(t_1, 0)|i_1\rangle |\langle i_\tau|U_\lambda(\tau, t_1)|i_1\rangle|^2 \\
&= \sum_{i_1, i_\tau} \frac{e^{-\beta E_{i_\tau}(\lambda(\tau))}}{Z_0} \langle i_\tau|U_\lambda(\tau, t_1)|i_1\rangle\langle i_1|U_\lambda^\dagger(\tau, t_1)|i_\tau\rangle \\
&= \sum_{i_\tau} \frac{e^{-\beta E_{i_\tau}(\lambda(\tau))}}{Z_0} = \frac{Z_\tau}{Z_0} = e^{-\beta \Delta F}.
\end{aligned} \tag{4.14}$$

In the above simplification we have used completeness relation, normalization condition and unitarity of U_λ as in section 4.2. Thus, we find that the JE remains unaffected even if measurements are performed on the system in-between $(0, \tau)$. The above treatment can be readily generalized to the case of multiple measurements

(see appendix A). Even though the form of JE is not altered in the presence of measurements, the statistics of the work performed on the system changes (strongly influenced by measurements). This is due to the fact that path probabilities for a given value of work are modified in presence of measurements. This is clearly illustrated in [96], wherein work distribution has been calculated for the Landau-Zener model in presence of measurement.

4.4 Extended JE in presence of feedback

The extended JE in presence of feedback has been given by Sagawa and Ueda for both the classical [45, 95] and the quantum [91] cases. Feedback means that system will be controlled by the the measurement output. After each measurement, the protocol is changed accordingly. Suppose initial protocol was $\lambda(t)$; at time t_1 a measurement of some observable A is performed on the system and outcome y_1 is obtained. We then modify our protocol from $\lambda_0(t)$ to $\lambda_{y_1}(t)$ and evolve the system up to time τ. We assume that the intermediate measurements can involve errors that are purely classical in nature. The error probability is given by $p(y_1|i_1)$, where $|i_1\rangle$ is the actual collapsed eigenstate of A. The final value of the protocol $\lambda_{y_1}(\tau)$ depends on y_1 and hence equilibrium free energy at the end of the protocol depends on y_1. The mutual information between actual state $|i_1\rangle$ and measured value y_1 is

$$I = \ln \frac{p(y_1|i_1)}{p(y_1)}. \tag{4.15}$$

Here, $p(y_1)$ is the probability density of the outcome y_1. The mutual information I quantifies a change in uncertainty about the state of the system upon making measurement [97]. Note that I can be positive or negative for a given realization; however, $\langle I \rangle$ is always positive. The probability of the state trajectory $|i_0\rangle \to |i_1\rangle \to$

$|i_\tau\rangle$ with single measurement is

$$\begin{aligned} P(i_\tau, i_1, i_0, y_1) &= p(i_\tau|i_1)p(y_1|i_1)p(i_1|i_0)p(i_0) \\ &= |\langle i_\tau|U_{\lambda_{y_1}}(\tau, t_1)|i_1\rangle|^2 p(y_1|i_1)|\langle i_1|U_\lambda(t_1, 0)|i_0\rangle|^2 p(i_0). \end{aligned} \tag{4.16}$$

Now we have,

$$\langle e^{-\beta(W-\Delta F)-I}\rangle = \int dy_1 \sum_{i_\tau, i_1, i_0} P(i_\tau, i_1, i_0, y_1) e^{-\beta(W-\Delta F(y_1))-I}. \tag{4.17}$$

Substituting the expressions of joint probability $P(i_\tau, i_1, i_0, y_1)$ (eq.(4.16)), work W (eq.(4.2)), Free energy difference $\Delta F = \frac{Z_0}{Z_\tau(y_1)}$, and mutual information I (eq.(4.15)) and simplifying we get

$$\begin{aligned} &\langle e^{-\beta(W-\Delta F)-I}\rangle \\ &= \int dy_1 \sum_{i_\tau, i_1, i_0} |\langle i_\tau|U_{\lambda_{y_1}}(\tau, t_1)|i_1\rangle|^2 |\langle i_1|U_\lambda(t_1, 0)|i_0\rangle|^2 p(y_1) \frac{e^{-\beta E_{i_\tau}(\lambda_{y_1}(\tau))}}{Z_\tau(y)} \\ &= \int dy_1 \sum_{i_\tau, i_1, i_0} |\langle i_\tau|U_{\lambda_{y_1}}(\tau, t_1)|i_1\rangle|^2 \langle i_1|U_\lambda(t_1, 0)|i_0\rangle\langle i_0|U_\lambda^\dagger(t_1, 0)|i_1\rangle p(y_1) \frac{e^{-\beta E_{i_\tau}(\lambda_{y_1}(\tau))}}{Z_\tau(y)} \\ &= \int dy_1 \sum_{i_\tau, i_1} |\langle i_\tau|U_{\lambda_{y_1}}(\tau, t_1)|i_1\rangle|^2 p(y_1) \frac{e^{-\beta E_{i_\tau}(\lambda_{y_1}(\tau))}}{Z_\tau(y)} \\ &= \int dy_1 \sum_{i_\tau, i_1} \langle i_\tau|U_{\lambda_{y_1}}(\tau, t_1)|i_1\rangle\langle i_1|U_{\lambda_{y_1}}^\dagger(\tau, t_1)|i_\tau\rangle p(y_1) \frac{e^{-\beta E_{i_\tau}(\lambda_{y_1}(\tau))}}{Z_\tau(y)} \\ &= \int dy_1 p(y_1) \sum_{i_\tau} \frac{e^{-\beta E_{i_\tau}(\lambda_{y_1}(\tau))}}{Z_\tau(y)} \\ &= \int dy_1 p(y_1) = 1. \end{aligned} \tag{4.18}$$

In second and fourth step, the modulus squared terms have been rewritten in expanded form and completeness relation is used. The above relation (4.18) constitutes the extended JE in the presence of information. Using Jensen's inequality, one arrives

at the generalized version of the second law in presence of feedback:

$$\langle W \rangle \geq \langle \Delta F \rangle - k_B T \langle I \rangle, \tag{4.19}$$

where the average mutual entropy $\langle I \rangle$ is always non-negative on account of being a relative entropy [43]. Thus, the lower bound of the mean work done on the system can be lowered by a term that is proportional to the average of the mutual information. In other words, with the help of an efficiently designed feedback, we can extract more work from the system. The above treatment can be readily extended to the case of multiple measurements between (0,τ) not necessarily at equal intervals of time. This is given in appendix B.

4.5 Generalized JE and efficacy parameter in presence of feedback

The efficacy parameter γ [45,95,90] provides a measure of how efficiently our feedback is able to extract work from the system. It is defined as

$$\gamma \equiv \langle e^{-\beta(W-\Delta F)} \rangle = \int dy_1 \sum_{i_\tau, i_1, i_0} P(i_\tau, i_1, i_0, y_1) e^{-\beta(W-\Delta F)}. \tag{4.20}$$

Here we have assumed single intermediate measurement. Substituting the expressions of joint probability $P(i_\tau, i_1, i_0, y_1)$ (eq.(4.16)), work W (eq.(4.2)), Free energy difference $\Delta F = \frac{Z_0}{Z_\tau(y_1)}$, and information I (eq.(4.15)), we get

$$
\begin{aligned}
&\langle e^{-\beta(W-\Delta F)}\rangle \\
&= \int dy_1 \sum_{i_\tau,i_1,i_0} |\langle i_\tau|U_{\lambda_{y_1}}(\tau,t_1)|i_1\rangle|^2 |\langle i_1|U_\lambda(t_1,0)|i_0\rangle|^2 p(y_1|i_1)\frac{e^{-\beta E_{i_\tau}(\lambda_{y_1}(\tau))}}{Z_\tau(y)} \\
&= \int dy_1 \sum_{i_\tau,i_1,i_0} |\langle i_\tau|U_{\lambda_{y_1}}(\tau,t_1)|i_1\rangle|^2 \langle i_1|U_\lambda(t_1,0)|i_0\rangle\langle i_0|U^\dagger_\lambda(t_1,0)|i_1\rangle p(y_1|i_1)\frac{e^{-\beta E_{i_\tau}(\lambda_{y_1}(\tau))}}{Z_\tau(y)} \\
&= \int dy_1 \sum_{i_\tau,i_1} |\langle i_\tau|U_{\lambda_{y_1}}(\tau,t_1)|i_1\rangle|^2 p(y_1|i_1)\frac{e^{-\beta E_{i_\tau}(\lambda_{y_1}(\tau))}}{Z_\tau(y)}. \qquad (4.21)
\end{aligned}
$$

For further calculations we need to take into account time reversed path. For this we introduce time reversal operator Θ with the properties $\Theta^\dagger = \Theta$ and $\Theta^\dagger\Theta = 1$. Let $|i_0^*\rangle$ denote the time reversed state of $|i_0\rangle$, i.e, $|i_0^*\rangle = \Theta|i_0\rangle$. It follows [47]

$$
\Theta U_{\lambda_{y_1}}(\tau,t_1)\Theta^\dagger = U_{\lambda^\dagger_{y_1}}(\tilde{\tau},\tilde{t}_1), \qquad (4.22)
$$

where $\tilde{t} = \tau - t$, i.e, the time calculated along reverse process. We assume time-reversibility of measurements, $p(y_1^*|i_1^*) = p(y_1|i_1)$ [90], y_1^* being the time reversed value of y_1. As i^* and i have one to one correspondence, the summation over i_1, i_τ is equivalent to that over i_1^*, i_τ^*. We get

$$
\begin{aligned}
\langle e^{-\beta(W-\Delta F)}\rangle &= \int dy_1 \sum_{i_\tau^*,i_1^*} |\langle i_\tau|\Theta^\dagger\Theta U_{\lambda_{y_1}}(\tau,t_1)\Theta^\dagger\Theta|i_1\rangle|^2 p(y_1|i_1)\frac{e^{-\beta E_{i_\tau}(\lambda_{y_1}(\tau))}}{Z_\tau(y)} \\
&= \int dy_1 \sum_{i_\tau^*,i_1^*} |\langle i_\tau^*|U_{\lambda^\dagger_{y_1}}(\tilde{\tau},\tilde{t}_1)|i_1^*\rangle|^2 p(y_1^*|i_1^*)\frac{e^{-\beta E_{i_\tau}(\lambda_{y_1}(\tau))}}{Z_\tau(y)} \\
&= \int dy_1 \sum_{i_\tau^*,i_1^*} |\langle i_1^*|U^\dagger_{\lambda^\dagger_{y_1}}(\tilde{\tau},\tilde{t}_1)|i_\tau^*\rangle|^2 p(y_1^*|i_1^*)\frac{e^{-\beta E_{i_\tau}(\lambda_{y_1}(\tau))}}{Z_\tau(y)} \\
&= \int dy_1 \sum_{i_\tau^*,i_1^*} |\langle i_1^*|U_{\lambda^\dagger_{y_1}}(\tilde{t}_1,\tilde{\tau})|i_\tau^*\rangle|^2 p(y_1^*|i_1^*)\frac{e^{-\beta E_{i_\tau}(\lambda_{y_1}(\tau))}}{Z_\tau(y)} \\
&= \int dy_1 \sum_{i_\tau^*,i_1^*} P_{\lambda^\dagger_{y_1}}(i_1^*|i_\tau^*) p(y_1^*|i_1^*) P(i_\tau). \qquad (4.23)
\end{aligned}
$$

where

$$P_{\lambda^\dagger_{y_1}}(i_1^*|i_\tau^*) = |\langle i_1^*|U_{\lambda^\dagger_{y_1}}(\tilde{t}_1,\tilde{\tau})|i_\tau^*\rangle|^2, \tag{4.24}$$

is the conditional probability of time reversed trajectory from state $|i_\tau^*\rangle$ to $|i_1^*\rangle$. We also have

$$P(i_\tau^*) = P(i_\tau) = \frac{e^{-\beta E_{i_\tau}(\lambda_{y_1}(\tau))}}{Z_\tau(y_1)}, \tag{4.25}$$

which is the initial probability distribution of the time reversed process with fixed protocol $\lambda^\dagger_{y_1}(\tau)$. Substituting eq.(4.25) in eq.(4.23) and using Bayes' theorem we get

$$\gamma = \langle e^{-\beta(W-\Delta F)}\rangle = \int dy_1 \sum_{i_1^*} p(y_1^*|i_1^*) P_{\lambda^\dagger_{y_1}}(i_1^*) = \int dy_1 P_{\lambda^\dagger_{y_1}}(y_1^*). \tag{4.26}$$

The physical meaning of the efficacy parameter is apparent now: it is the total probability of observing time-reversed outcomes along time-reversed protocols. Thus expression for the efficacy parameter remains the same as in the classical case. For multiple measurements, efficacy parameter is given by $\gamma = \int dy_1 \cdots dy_n P_{\lambda^\dagger}(y_1^* \cdots y_n^*)$. The derivation is simple and we are not reproducing it here.

4.6 Conclusion

In conclusion we have shown that the quantum extension of JE with multiple measurements and measurement accompanied feedback and quantum efficacy parameter retain same expressions as in the classical case. This is mainly due to performed measurements being of von Neumann projective type accompanied by classical errors, and system being isolated. In next chapter we will shown that in quantum case, entropy production fluctuation theorems retain the same form as in the classical case with measurement and feedback.

Chapter 5

Generalized entropy production FTs for quantum systems

5.1 Introduction

Based on trajectory dependent path probability formalism in state space, in this chapter we derive generalized entropy production fluctuation relations for a quantum system in the presence of measurement and feedback. We have obtained these results for three different cases: (i) the system is evolving in isolation from its surroundings; (ii) the system being weakly coupled to a heat bath; and (iii) system in contact with reservoir using quantum Crooks fluctuation theorem. The obtained entropy production fluctuation theorems retain the same form as in the classical case. The inequality of second law of thermodynamics gets modified in the presence of information. These fluctuation theorems are robust against intermediate measurements of any observable performed with respect to von Neumann projective measurements as well as weak or positive operator valued measurements.

In 2005 Seifert introduced a general Fluctuation theorem (FT) [27, 13] which contains the Jarzynski [23] and the Crooks [28, 29] theorems as special cases. It relates the probability of a phase space trajectory along the forward process to that along the reverse process. We have already introduced these theorems in detail in the introduction. In the following, we mention them just for recapitulation. The integral fluctuation theorem (IFT) for total entropy production [13] states that

$$\langle e^{-\Delta s_{tot}} \rangle = 1. \tag{5.1}$$

where ΔS_{tot} is the total entropy production along a given trajectory. If the system is in steady state, one can also obtain detailed entropy production fluctuation theorem (DFT), namely

$$\frac{p(\Delta S_{tot})}{p(-\Delta S_{tot})} = e^{\Delta S_{tot}}. \tag{5.2}$$

The IFT follows directly from the DFT. Using Jensen's inequality in eq.(5.1) we get

$$\langle \Delta S_{tot} \rangle \geq 0. \tag{5.3}$$

This is a statement of second law of thermodynamics, expressed in the form of inequality for the average change in total entropy.

If the systems are driven by the feedback controlled protocols, which in turn depend on the measurement outcomes of the state of the system at intermediate times (information gain), then IFT gets modified a form [47]

$$\langle e^{-\Delta S_{tot} - I} \rangle = 1, \tag{5.4}$$

where I is the mutual information which quantifies the change in uncertainty of state of the system upon making measurements. Application of Jensen's inequality generalizes second law for total entropy production:

$$\langle \Delta S_{tot} \rangle \geq -\langle I \rangle. \tag{5.5}$$

The average mutual information $\langle I \rangle$, is always non negative [43]. Thus the average entropy change can be made negative by feedback control, and the lower bound is given by $-\langle I \rangle$. There are few attempts to extend the IFT (eq.(5.1)) to the quantum domain [31,32,98]. In our present work we extend the IFT for ΔS_{tot} to quantum systems, in presence of multiple measurements and feedback. We assume that measurement procedure involves errors that are classical in nature. We show the robustness of FTs against intermediate measurements of any system observable (both von Neumann projective measurements or generalized positive operator valued measurements (POVM)).

We obtain these theorems for three different cases: (i) the system evolves in

isolation from its surroundings; (ii) it is weakly coupled to a heat bath; and (iii) evolution of system coupled to heat bath is modelled in terms of work steps and heat steps following closely the treatment given Ref [65] and is described in section 5.4. Our treatment is based on path probability in state space. The measurement is assumed to be von Neumann type, i.e, projective measurement which results in the collapse of system state to one of the eigenstates of the corresponding observable. Case (i) namely isolated quantum system is discussed in detail. DFT is obtained for various different situations, i.e., (a) system evolving unitarily, (b) in the presence of measurement and feedback, and finally (c) in the presence of intermediate measurements, of any observables of the system. The IFT follows from DFT. For cases (ii) and (iii) we have derived generalized IFT. In the appendix, we have given a proof of IFT in presence of weak measurements. In passing, we note that all the extended quantum FTs retain the same form as their classical counterparts.

5.2 Isolated quantum system

5.2.1 Unitary evolution

In this section we consider an isolated quantum system given by Hamiltonian $H(\lambda(t))$, where $\lambda(t)$ is some external time dependent protocol. To clarify our notation and for completeness we rederive DFT for this system following the treatment of ref [32]. Initially at time t=0 energy measurement is performed and system is found to be in eigenstate $|i_0\rangle$, with energy eigenvalue E_0. It then evolves unitarily from time 0 to τ under the protocol $\lambda(t)$. The energy measurement at final time τ is performed and system is found to be at state $|i_\tau\rangle$ with energy eigenvalue E_τ. If the initial probability density of the state $|i_0\rangle$ is $p(i_0)$ then the joint probability of $|i_0\rangle$ and $|i_\tau\rangle$ (forward

state trajectory) is given by

$$\begin{aligned} P_F(i_\tau, i_0) &= p(i_\tau|i_0)p(i_0) \\ &= |\langle i_\tau|U_\lambda(\tau,0)|i_0\rangle|^2 p(i_0), \end{aligned} \tag{5.6}$$

where $U_\lambda(t_2,t_1)$ denotes the unitary evolution operator for given $\lambda(t)$ from time t_1 to time t_2. It is defined as

$$U_\lambda(t_2,t_1) = T\exp\left(-\frac{i}{\hbar}\int_{t_1}^{t_2} H(\lambda(t))dt\right). \tag{5.7}$$

Here, T denotes time ordering.

The system entropy is defined as $S(t) = -\ln p(i_t)$. As the system is isolated there is no generation of heat, i.e, Q=0. It leads the total change in entropy production ΔS_{tot} during the evolution from time 0 to τ is equal to the change in system entropy alone.

$$\Delta S_{tot} = -\ln\frac{p(i_\tau)}{p(i_0)}, \tag{5.8}$$

where $p(i_\tau)$ is the final probability of state $|i_\tau\rangle$ at time τ. The probability density $P_F(\Delta S_{tot})$ for the forward path is by definition

$$\begin{aligned} P_F(\Delta S_{tot}) &= \sum_{i_\tau,i_0}\delta\left(\Delta S_{tot} + \ln\frac{p(i_\tau)}{p(i_0)}\right)P_F(i_\tau,i_0) \\ &= \sum_{i_\tau,i_0}\delta\left(\Delta S_{tot} + \ln\frac{p(i_\tau)}{p(i_0)}\right)p(i_\tau|i_0)p(i_0). \end{aligned} \tag{5.9}$$

We now introduce time reversal operator Θ. The time reversed state of $|i\rangle$ is defined as $|\tilde{i}\rangle = \Theta|i\rangle$. It can be readily shown that [47]

$$p(i_2|i_1) = |\langle i_2|U_\lambda(t_2,t_1)|i_1\rangle|^2 = |\langle\tilde{i}_1|U_{\lambda^\dagger}(\tilde{t}_1,\tilde{t}_2)|\tilde{i}_2\rangle|^2 = p(\tilde{i}_1|\tilde{i}_2). \tag{5.10}$$

where $\tilde{t} = \tau - t$ and $\lambda^{\dagger}(\tilde{t}) = \lambda(\tau - t)$ is the time reversed protocol of $\lambda(t)$. The evolution of the system from given time reversed state $\Theta|i_2\rangle$ to the time-reversed state $\Theta|i_1\rangle$, under the time reversed protocol $\lambda^{\dagger}(t)$, is given by the conditional probability $p(\tilde{i}_1|\tilde{i}_2)$. We consider the initial distribution of reverse trajectory to be equal to the final distribution of forward trajectory

$$p(\tilde{i}_\tau) = p(i_\tau). \tag{5.11}$$

The states $|i\rangle$ and $|\tilde{i}\rangle$ have one-to-one correspondence. Multiplying and dividing by $p(i_\tau)$ in the summand in eq.(5.9) and using (5.10) and (5.11), we get

$$\begin{aligned}
P_F(\Delta S_{tot}) &= \sum_{i_\tau, i_0} \delta\left(\Delta S_{tot} + \ln\frac{p(i_\tau)}{p(i_0)}\right) p(\tilde{i}_0|\tilde{i}_\tau) p(\tilde{i}_\tau) \frac{p(i_0)}{p(i_\tau)} \\
&= \sum_{i_\tau, i_0} \delta\left(\Delta S_{tot} + \ln\frac{p(i_\tau)}{p(i_0)}\right) p(\tilde{i}_0|\tilde{i}_\tau) p(\tilde{i}_\tau) e^{\Delta S_{tot}} \\
&= e^{\Delta S_{tot}} \sum_{i_\tau, i_0} \delta\left(\Delta S_{tot} + \ln\frac{p(\tilde{i}_\tau)}{p(\tilde{i}_0)}\right) p(\tilde{i}_0|\tilde{i}_\tau) p(\tilde{i}_\tau) \\
&= e^{\Delta S_{tot}} \sum_{i_\tau, i_0} \delta\left(\Delta S_{tot} - \ln\frac{p(\tilde{i}_0)}{p(\tilde{i}_\tau)}\right) P_R(\tilde{i}_\tau, \tilde{i}_0) \\
&= e^{\Delta S_{tot}} P_R(-\Delta S_{tot}).
\end{aligned} \tag{5.12}$$

To arrive at this result we have used eq.(5.8) in the second step and eq.(5.11) in third step. $P_R(\tilde{i}_\tau, \tilde{i}_0)$ is the joint probability of the corresponding states in the reverse direction. If the ΔS_{tot} is the total entropy change for forward path then the total entropy change in the corresponding reverse path is $-\Delta S_{tot}$. It follows from the fact that $p(\tilde{i}_\tau)$ and $p(\tilde{i}_0)$ is the initial and final probability distribution of state in the time reversed process because of unitary evolution. The eq.(5.12) can be written in the form

$$\frac{P_F(\Delta S_{tot})}{P_R(-\Delta S_{tot})} = e^{\Delta S_{tot}}. \tag{5.13}$$

This is the detailed fluctuation theorem for change in total entropy, extended to the quantum regime. Simple cross multiplication followed by integration over ΔS_{tot} leads to the integral form of the above theorem:

$$\langle e^{-\Delta S_{tot}} \rangle = 1. \tag{5.14}$$

5.2.2 Isolated quantum system with feedback

So far we have been dealing with a predetermined protocol, also known as open loop feedback. Often to increase the efficiency of a physical process (eg. engines at nanoscale, molecular motor etc.), we need to perform intermediate measurements and change the protocol as per the outcomes of these measurements [93,94,99,100,45,46, 101,97]. Such a process is known as closed loop feedback. Let the system evolve under some external protocol $\lambda_0(t)$, from its initial energy eigenstate $|i_0\rangle$ measured at time t_0. At time t_1, we perform a measurement of some arbitrary observable and system collapses to state $|i_1\rangle$. We assume that measurement process leading to information gain involves classical errors. Here y_1 is the measured outcome with a probability $p(y_1|i_1)$, while system's actual state is $|i_1\rangle$. Depending on the value of y_1 the protocol is changed to $\lambda_{y_1}(t)$. Under this new protocol the system evolves unitarily up to time t_2 where another measurement is performed and so on. This process terminates at time τ when the system collapses to its final energy eigenvalue $|i_\tau\rangle$. We should note that initial and final measurements are energy measurements. The joint probability of the corresponding state trajectory for n number of intermediate measurements $y_1, y_2, \cdots y_n$ at times $t_1, t_2, \cdots t_n$ respectively is [47]

$$\begin{aligned} P_F(i_\tau, .., i_1, i_0, y_n, .., y_1) &= p(i_\tau|i_n) \cdots p(y_2|i_2)p(i_2|i_1)p(y_1|i_1)p(i_1|i_0)p(i_0) \\ &= |\langle i_\tau|U_{\lambda_{y_n}}(\tau, t_1)|i_n\rangle|^2 ... p(y_2|i_2)|\langle i_2|U_{\lambda_{y_1}}(t_2, t_1)|i_1\rangle|^2 p(y_1|i_1) \\ &\quad \times |\langle i_1|U_{\lambda_0}(t_1, 0)|i_0\rangle|^2 p(i_0). \end{aligned} \tag{5.15}$$

It may be noted that the joint probability of path is expressed using classical probability rules. This is because we perform projective measurement on the system which collapses to one of the eigenvalues of the measured observables [47, 102]. As a consequence, it wipes out the previous memory of evolution and the post-measurement evolution becomes uncorrelated to the pre-measurement evolution. Thus if one performs intermediate measurements along two paths, the interference effects between the two paths disappear and the quantum effects are suppressed. Hence in the presence of measurement, path probability in state space obeys classical probability rules, and is given by product of transition probability of paths between consecutive measurements. However, it may be noted that quantum mechanics enters through the explicit calculation of transition probability between two consecutive states.

To generate the reverse trajectory of a path in state space given in eq.(5.15), we first choose one of the forward protocols with probability $p(y_n \cdots, y_2, y_1)$, and then blindly time reverse the protocol. We perform measurements at the appropriate times along reverse path to allow the state to collapse to the corresponding time-reversed eigenstates. We do not use these measurements to perform any feedback to respect causality [97]. Then the expression for the joint probability of reverse trajectory is given by

$$P_R(\tilde{i}_\tau \cdots, \tilde{i}_0, y_n, .., y_1) = p(\tilde{i}_N|\tilde{i}_\tau) \cdots p(\tilde{i}_0|\tilde{i}_1)p(i_\tau)p(y_n \cdots, y_1). \tag{5.16}$$

The mutual information gain due to measurements between the measured values and the actual value is defined as [47, 97]

$$I = \ln \frac{p(y_n|i_n)...p(y_2|i_2)p(y_1|i_1)}{p(y_n \cdots, y_2, y_1)}. \tag{5.17}$$

We now calculate the joint probability density $P_F(\Delta S_{tot}, \mathcal{I})$ of the entropy production

and $\mathcal{I}$ along the forward path, which is

$$
\begin{aligned}
P_F(\Delta S_{tot}, \mathcal{I}) &= \int dy_n \cdots dy_1 \sum_{i_\tau \cdots, i_1, i_0} \delta\left(\Delta S_{tot} + \ln \frac{p(i_\tau)}{p(i_0)}\right) \delta\left(\mathcal{I} - I(i_n, .., i_1, y_n, .., y_1)\right) \\
&\qquad \times P_F(i_\tau, .., i_1, i_0, y_n, .., y_1) \\
&= \int dy_n \cdots dy_1 \sum_{i_\tau \cdots, i_1, i_0} \delta\left(\Delta S_{tot} + \ln \frac{p(i_\tau)}{p(i_0)}\right) \delta\left(\mathcal{I} - I(i_n, .., i_1, y_n, .., y_1)\right) \\
&\qquad \times p(i_\tau|i_n) \cdots p(y_2|i_2) p(i_2|i_1) p(y_1|i_1) p(i_1|i_0) p(i_0) \\
&= \int dy_n \cdots dy_1 \sum_{i_\tau \cdots, i_1, i_0} \delta\left(\Delta S_{tot} + \ln \frac{p(i_\tau)}{p(i_0)}\right) \delta\left(\mathcal{I} - I(i_n, .., i_1, y_n, .., y_1)\right) \\
&\qquad \times p(\tilde{i}_N|\tilde{i}_\tau) \cdots p(\tilde{i}_0|\tilde{i}_1) p(i_\tau) p(y_n \cdots, y_1) e^{\Delta S_{tot} + I} \\
&= \int dy_n \cdots dy_1 \sum_{i_\tau \cdots, i_1, i_0} \delta\left(\Delta S_{tot} + \ln \frac{p(i_\tau)}{p(i_0)}\right) \delta\left(\mathcal{I} - I(i_n, .., i_1, y_n, .., y_1)\right) \\
&\qquad \times P_R(\tilde{i}_\tau \cdots, \tilde{i}_0, y_n, .., y_1) e^{\Delta S_{tot} + I} \\
&= e^{\Delta S_{tot} + \mathcal{I}} \int dy_n \cdots dy_1 \sum_{i_\tau \cdots, i_1, i_0} \delta\left(\Delta S_{tot} + \ln \frac{p(i_\tau)}{p(i_0)}\right) \\
&\qquad \times \delta\left(\mathcal{I} - I(i_n, .., i_1, y_n, .., y_1)\right) P_R(\tilde{i}_\tau \cdots, \tilde{i}_0, y_n, .., y_1) \\
&= e^{\Delta S_{tot} + \mathcal{I}} P_R(-\Delta S_{tot}, \mathcal{I}). \qquad (5.18)
\end{aligned}
$$

In deriving above result we have made use eq.(5.15), (5.16), (5.17). The path variable $I(i_n, .., i_1, y_n, .., y_1)$ is given by eq. (5.17), and $\mathcal{I}$ denotes its value. It is important to note that the probability density function $P_R(-\Delta S_{tot}, \mathcal{I})$ gives the probability of reverse trajectories along which the entropy chage is $-\Delta S_{tot}$ and whose corresponding forward trajectory has the mutual information $\mathcal{I}$ between its measured outcomes and actual states. Once again, the initial and final distributions of states along forward trajectory get interchanged in the reverse trajectory because of unitary evolution between measurements. Along the reverse trajectory the change in total entropy is

$-\Delta S_{tot}$. Thus we obtain the DFT

$$\frac{P_F(\Delta S_{tot}, \mathcal{I})}{P_R(-\Delta S_{tot}, \mathcal{I})} = e^{\Delta S_{tot}+\mathcal{I}}. \tag{5.19}$$

From the above equation the extended version of IFT and second law, eqs. (5.4) and (5.5) can be readily obtained as discussed in earlier subsection.

5.2.3 Isolated system under multiple measurements

In this subsection we restrict ourselves on the influence of intermediate measurements of arbitrary observables on the statistics of ΔS_{tot}. To this end we do not involve any feedback. Following closely the discussions in section (5.2.2), of path probability in state space is given by

$$\begin{aligned} P(i_\tau, .., i_1, i_0) &= p(i_\tau|i_n)\cdots p(i_2|i_1)p(i_1|i_0)p(i_0) \\ &= |\langle i_\tau|U_{\lambda_{yn}}(\tau, t_1)|i_n\rangle|^2 ... |\langle i_2|U_{\lambda_{y_1}}(t_2, t_1)|i_1\rangle|^2 |\langle i_1|U_{\lambda_0}(t_1, 0)|i_0\rangle|^2 p(i_0). \end{aligned} \tag{5.20}$$

From preceding section we now calculate the probability density $P_F(\Delta S_{tot})$ of the total entropy change along forward path

$$\begin{aligned} P_F(\Delta S_{tot}) &= \sum_{i_\tau\cdots, i_1, i_0} \delta\left(\Delta S_{tot} + \ln\frac{p(i_\tau)}{p(i_0)}\right) P(i_\tau, .., i_1, i_0) \\ &= \sum_{i_\tau\cdots, i_1, i_0} \delta\left(\Delta S_{tot} + \ln\frac{p(i_\tau)}{p(i_0)}\right) p(i_\tau|i_n)\cdots p(i_2|i_1)p(i_1|i_0)p(i_0) \\ &= \sum_{i_\tau\cdots, i_1, i_0} \delta\left(\Delta S_{tot} + \ln\frac{p(i_\tau)}{p(i_0)}\right) p(\tilde{i}_N|\tilde{i}_\tau)\cdots p(\tilde{i}_0|\tilde{i}_1)p(i_\tau)e^{\Delta S_{tot}} \\ &= \sum_{i_\tau\cdots, i_1, i_0} \delta\left(\Delta S_{tot} + \ln\frac{p(i_\tau)}{p(i_0)}\right) P_R(\tilde{i}_\tau\cdots, \tilde{i}_0)e^{\Delta S_{tot}} \\ &= e^{\Delta S_{tot}} \sum_{i_\tau\cdots, i_1, i_0} \delta\left(\Delta S_{tot} + \ln\frac{p(i_\tau)}{p(i_0)}\right) P_R(\tilde{i}_\tau\cdots, \tilde{i}_0), \end{aligned} \tag{5.21}$$

where $P_R(\tilde{i}_\tau \cdots, \tilde{i}_0)$ is the probability of reverse path. The DFT for ΔS_{tot} follows from the above equation:

$$\frac{P_F(\Delta S_{tot})}{P_R(-\Delta S_{tot})} = e^{\Delta S_{tot}}. \tag{5.22}$$

We observe from eq.(5.22) the robustness of this FT against intermediate measurements [89, 44]. It retains the same form as in the classical case. The path probability, however, gets modified in presence of measurements and statistics of ΔS_{tot} is strongly influenced by the intermediate measurements. In the next section we derive IFT in presence of feedback for a quantum system coupled weakly to a bath. In the appendix, we have shown that the IFT for ΔS_{tot} is also robust against weak or generalized intermediate measurements.

5.3 Weakly coupled quantum system

Consider a driven system which is weakly coupled to a bath. The total Hamiltonian will be

$$H(\lambda(t)) = H_S(\lambda(t)) + H_B + H_{SB}. \tag{5.23}$$

The external time dependent drive $\lambda(t)$ only affects the system Hamiltonian $H_S(\lambda(t))$ while the bath Hamiltonian H_B and interaction Hamiltonian H_{SB} are time independent. As the system is weakly coupled it is assumed that H_{SB} is negligibly small compared to $H_S(\lambda(t))$ and H_B. Initially the super-system (system+bath) is coupled to a large reservoir of inverse temperature β [44, 34]. At time $t = 0$ the large reservoir is decoupled from the super-system. Hence initially the super-system will be in a canonical distribution,

$$\rho(\lambda_0) = \frac{e^{-\beta H(\lambda(0))}}{Y(\lambda(0))}, \tag{5.24}$$

where $Y(\lambda(0)) = \mathrm{Tr}\, e^{-\beta H(\lambda(0))}$. The system and the bath Hamiltonians commute with each other, hence we can measure simultaneously the energy eigenstates for system as

well as bath. At t=0, the measured energy eigenvalues of system and bath are denoted by E_0^S and E_0^B, respectively. We perform N number of intermediate measurements of some arbitrary observable at time $t_1, t_2 \cdots t_N$ between time 0 to τ. Initially the protocol was $\lambda_0(t)$. At t_1 the measured output is y_1, while its actual state is i_1, with probability $p(y_1|i_1)$. Now the protocol is changed to $\lambda_{y_1}(t)$ and system evolves up to time t_2 . Again measurement is performed and protocol is changed according to the output at intermediate times and so on. Finally at t=τ joint measurement is performed on system and bath Hamiltonians, and the measured eigenvalues are E_τ^S and E_τ^B, respectively. The system-reservoir interaction energy can be neglected in the presence of weak coupling. Hence during the evolution process from time $t = 0$ to $t = \tau$ for a single realization the change in the internal energy of the system is given by [34]

$$\Delta U = E_\tau^S - E_0^S \tag{5.25}$$

and the heat dissipated to the bath is

$$Q = E_\tau^B - E_0^B. \tag{5.26}$$

If i_0 and i_τ denote initial and final system energy eigenstates, then system entropy change is

$$\Delta S_{sys} = -\ln \frac{p(i_\tau)}{p(i_0)}, \tag{5.27}$$

and the total entropy change is

$$\Delta S_{tot} = \Delta S_{sys} + \Delta S_B = -\ln \frac{p(i_\tau)}{p(i_0)} + \frac{Q}{T}, \tag{5.28}$$

where T is the temperature of the bath. The mutual information between the state trajectory $\{i_1, i_2, \cdots, i_N\}$ and the measurement trajectory $\{y_1, y_2, \cdots y_N\}$ is

$$I \equiv \ln \left[\frac{p(y_1|i_1) \cdots p(y_N|i_N)}{P(y_1, \cdots, y_N)} \right]. \tag{5.29}$$

Denoting initial and final states of the bath by α_0 and α_τ, it can written from microscopic reversibility [45, 97]

$$p(i_\tau, \alpha_\tau|i_0, \alpha_0) = p(\tilde{i}_0, \tilde{\alpha_0}|\tilde{i}_\tau, \tilde{\alpha}_\tau). \tag{5.30}$$

where $p(i_\tau, \alpha_\tau|i_0, \alpha_0)$ is the total transition probability for system and reservoir to evolve from state $|i_0, \alpha_0\rangle$ to $|i_\tau, \alpha_\tau\rangle$ under the full Hamiltonian. Here $|\tilde{i}, \tilde{\alpha}\rangle \equiv \Theta|i, \alpha\rangle$ is the time-reversed state of $|i, \alpha\rangle$. To generate the reverse trajectory, proper causal protocol has to be used which has been discussed in section 5.2.2. Thus the forward and the reverse path probabilities of trajectories are respectively given by

$$P_F(A \to B) = p(i_\tau, \alpha_\tau|i_N, \alpha_N) \cdots p(y_1|i_1) p(i_1, \alpha_1|i_0, \alpha_0) p(i_0, \alpha_0), \tag{5.31}$$

$$P_R(A \leftarrow B) = p(\tilde{i}_0, \tilde{\alpha_0}|\tilde{i}_1, \tilde{\alpha}_1) \cdots p(\tilde{i}_N, \tilde{\alpha_N}|\tilde{i}_\tau, \tilde{\alpha}_\tau) p(\tilde{i}_\tau, \tilde{\alpha}_\tau) p(y_1, y_2, \cdots y_N). \tag{5.32}$$

The notations A and B denote initial and final values of the forward protocol, respectively. For reverse trajectory we have chosen the outcome of the forward trajectory with probability $p(y_1, y_2, \cdots y_N)$ and have blindly reversed the protocol, but performing measurements (without any feedback) at appropriate time instants. From (5.31)

and (5.32) we get

$$\begin{aligned}\frac{P_F(A\to B)}{P_R(A\leftarrow B)} &= \frac{p(i_\tau,\alpha_\tau|i_N,\alpha_N)\cdots p(y_1|i_1)p(i_1,\alpha_1|i_0,\alpha_0)p(i_0,\alpha_0)}{p(\tilde{i}_0,\tilde{\alpha_0}|\tilde{i}_1,\tilde{\alpha}_1)\cdots p(\tilde{i}_N,\tilde{\alpha_N}|\tilde{i}_\tau,\tilde{\alpha}_\tau)p(\tilde{i}_\tau,\tilde{\alpha}_\tau)p(y_1,y_2,\cdots y_N)} \\ &= \frac{p(y_N|i_N)\cdots p(y_1|i_1)}{P(y_1,\cdots,y_N)}\frac{p(i_0,\alpha_0)}{p(\tilde{i}_\tau,\tilde{\alpha}_\tau)} \\ &= e^I\ \frac{p(i_0)p(\alpha_0)}{p(\tilde{i}_\tau)p(\tilde{\alpha}_\tau)} \\ &.\end{aligned} \tag{5.33}$$

In arriving at (5.33), we have used microreversibility (5.30) and we have assumed that the system and the bath are weakly coupled. The joint probability of system and bath states is approximated as a product of individual state probabilities. Correction to this factorized initial state is at least of second order in system-bath interaction, and therefore they can be neglected in the limit of weak coupling. The bath probability can be considered canonical with inverse temperature β. This leads to

$$\frac{P_F(A\to B)}{P_R(A\leftarrow B)} = e^I\ e^{\Delta S_{sys}}\frac{e^{-\beta E_0^B}/Z_B}{e^{-\beta E_\tau^B}/Z_B} = e^I\ e^{\Delta S_{sys}}e^{Q/T} = e^{\Delta S_{tot}+I}. \tag{5.34}$$

A simple cross multiplication and integration over paths gives the extended IFT. It may be noted that in our framework we can also obtain the DFT, provided the system either begins and ends in equilibrium or in the same nonequilibrium steady state [29]. In the next section, we prove the same IFT for ΔS_{tot} by means of the method developed in [65] by using the quantum mechanical generalization of the Crooks fluctuation theorem.

5.4 IFT using quantum Crooks fluctuation theorem

We consider the system to be coupled to a bath, but there is no assumption made in regard to the strength of the coupling. Each time step in the entire evolution is divided into two substeps. In first substep the protocol is changed while in second, protocol is kept fixed and system relaxes by dissipation of heat. The total evolution is divided into N steps. Each step starts at t_n and ends at t_{n+1}, where $n = 0, 1, 2, \cdots N-1$. We closely follow the treatment in [65].

For a quantum adiabatic process the protocol changes slowly and the system remains in same eigenstate in the work step. However, in the present case the work step is almost instantaneous and the process is non adiabatic. As a consequence the eigenstates before and after work step may be different. The system starts to evolve under a predetermined protocol λ_0. For simplicity, let us consider the observable measured at intermediate times to be the Hamiltonian itself. It can be readily generalized to the case of other observables. We consider that the feedback is applied at the beginning of the each work step and we change the protocol subsequently according to the result obtained from the measurement, as discussed earlier. The conditional probability $p(y_{n-1}|i_{n-1})$ denotes that the measured outcome is y_{n-1} while the actual collapsed state is $|i_{n-1}, \lambda_{n-1}\rangle$, at the beginning of the n^{th} work step. Within the ket notation, i_{n-1} represents the state of the system and λ_{n-1} is the value of the control parameter. After the measurement of t_{n-1}, the protocol is changed to $\lambda_n(y_{n-1})$ from $\lambda_{n-1}(y_{n-2})$. During the work step, the system evolves unitarily from t_{n-1} to t'_{n-1}, where it is measured to be in state $|i'_{n-1}, \lambda_n\rangle$. The time taken in the work substep is considered to be too small for the system to relax. In the n^{th} heat step, the system relaxes from state $|i'_{n-1}, \lambda_n\rangle$ to $|i_n, \lambda_n\rangle$. Therefore, the path followed by the system in state space of the measured eigenstates from state $|i_0, \lambda_0 = A\rangle$ to $|i_\tau, \lambda_\tau = B\rangle$

is represented as $|i_0, \lambda_0\rangle \to |i'_0, \lambda_1\rangle \to |i_1, \lambda_1\rangle \to |i'_1, \lambda_2\rangle \to \cdots \to |i_{N-1}, \lambda_{N-1}\rangle \to |i'_{N-1}, \lambda_N\rangle \to |i_N, \lambda_N\rangle$. Let $E(i_n, \lambda_n)$ be the energy eigenvalue of state $|i_n, \lambda_n\rangle$. By adding the contributions from all the work steps, the total work done on the system is given by

$$W = \sum_{n=0}^{N-1} \left[E(i'_n, \lambda_{n+1}) - E(i_n, \lambda_n) \right], \tag{5.35}$$

while heat dissipated into the bath is

$$Q = -\sum_{n=0}^{N-1} \left[E(i_{n+1}, \lambda_{n+1}) - E(i'_n, \lambda_{n+1}) \right]. \tag{5.36}$$

The change in internal energy of the system along the trajectory is

$$\Delta E = Q + W = E(i_N, \lambda_N) - E(i_0, \lambda_0). \tag{5.37}$$

As before, the mutual information is

$$I = \ln \frac{p(y_n|i_n)...p(y_2|i_2)p(y_1|i_1)}{p(y_n \cdots, y_2, y_1)}. \tag{5.38}$$

The forward and the reverse path probabilities are respectively given by

$$\begin{aligned} &P_F(A \to B) \\ &= p(i_0, \lambda_0) \prod_{n=0}^{N-1} p(y_n|i_n) p_F(|i_n, \lambda_n\rangle \to |i'_n, \lambda_{n+1}\rangle)\ p_F(|i'_n, \lambda_{n+1}\rangle \to |i_{n+1}, \lambda_{n+1}\rangle). \end{aligned} \tag{5.39}$$

and

$$P_R(A \leftarrow B)$$
$$= p(i_N, \lambda_N)p(y_n \cdots, y_1) \prod_{n=0}^{N-1} p_R(|\tilde{i}_n, \lambda_n\rangle \leftarrow |\tilde{i}'_n, \lambda_{n+1}\rangle) p_R(|\tilde{i}'_n, \lambda_{n+1}\rangle \leftarrow |\tilde{i}_{n+1}, \lambda_{n+1}\rangle). \tag{5.40}$$

As mentioned earlier, during the work step, the system can be regarded as an isolated quantum system and evolution is completely determined by the time-dependent Hamiltonian $H_S(\lambda(t))$. Thus the evolution is unitary. Microscopic reversibility for work step gives [65]

$$p_F(|i_n, \lambda_n\rangle \rightarrow |i'_n, \lambda_{n+1}\rangle) = p_R(|\tilde{i}_n, \lambda_n\rangle \leftarrow |\tilde{i}'_n, \lambda_{n+1}\rangle). \tag{5.41}$$

The heat steps or relaxation steps are assumed to be microscopically reversible and obey the local detailed balance for all the fixed values of the external parameter λ. The detailed balance condition in relaxation substep implies

$$\frac{P_F(|i'_n, \lambda_{n+1}\rangle \rightarrow |i_{n+1}, \lambda_{n+1}\rangle)}{P_R(|\tilde{i}'_n, \lambda_{n+1}\rangle \leftarrow |\tilde{i}_{n+1}, \lambda_{n+1}\rangle)} = \exp[-\beta(E_{n+1}, \lambda_{n+1} - E(i'_n, \lambda_{n+1})]. \tag{5.42}$$

Using above two equations we get

$$\frac{P_F(A \rightarrow B)}{P_R(A \leftarrow B)}$$
$$= \frac{p(y_n|i_n)...p(y_2|i_2)p(y_1|i_1)}{p(y_n \cdots, y_2, y_1)} \frac{p(i_0, \lambda_0)}{p(i_N, \lambda_N)} \prod_{0}^{N-1} \exp[-\beta(E_{n+1}, \lambda_{n+1} - E(i'_n, \lambda_{n+1})]. \tag{5.43}$$

The total entropy change along the trajectory, $\Delta S_{tot} = \Delta S + \Delta S_B$, which is a trajectory dependent random variable, where $\Delta S \equiv -\ln \frac{P(i_N, \lambda_N)}{P(i_0, \lambda_0)}$ is the change in system entropy, and $\Delta S_B \equiv Q/T$ is the entropy change of the bath, along a single trajectory.

Using (5.36) and (5.38), eq. (5.43) simplifies to

$$\frac{P_F(A \to B)}{P_R(A \leftarrow B)} = e^I \; e^{\Delta S_{sys}} e^{Q/T} = e^{\Delta S_{tot}+I} \tag{5.44}$$

This immediately leads to the generalized integral fluctuation theorem for total entropy change, in the presence of measurement and feedback. In the above derivation, we have taken measurements for feedback at the beginning of the work steps for simplicity. These measurements can be performed at any time in-between the work steps. The result will not be affected. It would only make the notations more complicated and would not provide any new physical insight. Feedback cannot be performed within the heat step which be definition requires protocol to be held constant.

As in case (ii), the DFT for ΔS_{tot} can be obtained if the initial and final distributions are in the equilibrium or in the same nonequilibrium steady state [29].

5.5 Conclusions

Based on the path probability formulation in state space, we have derived generalized total entropy production fluctuation theorems for quantum systems in presence of measurement and feedback, for three different cases. They retain the same form as in classical case. The second law of thermodynamics gets modified in the presence of information and feedback (eq. (5.5)). For isolated quantum system with feedback, we have derived the generalized DFT for the total entropy. For this case DFT retains the same form in presence of multiple measurements of any system observable, thus showing the robustness of these fluctuation theorems against measurements (von Neumann type or generalized measurements (for generaliged measurement see appendix C)). For the case (ii) of a weakly coupled quantum system under feedback, we have derived the extended IFT for total entropy. In case (iii), we have derived the extended IFT for ΔS_{tot}, using the quantum Crooks fluctuation theorem, where

quantum trajectory is characterized by a sequence of alternating work and heat steps. IFT is valid for any initial arbitrary state of a system. DFT in cases (ii) and (iii) can be obtained only when the system either begins or ends in equilibrium or remains in the same nonequilibrium steady state. By using our approach, the generalized DFT can be proved, but we have not provided the details. The derivation of the robustness of the fluctuation theorems against intermediate measurements is given only for case (i), namely, for the isolated quantum system. Following the same treatment, the robustness of fluctuation theorems can be readily demonstrated for cases (ii) and (iii) as well.

In conclusion, we have generalized total entropy production fluctuation theorem in presence of feedback to the quantum domain using three different approaches.

Chapter 6

FTs in inhomogeneous media under coarse graining

6.1 Introduction

In this chapter we compare the fluctuation relations for work and entropy in underdamped and overdamped systems, when the friction coefficient of the medium is space-dependent. We find that these relations remain unaffected in both cases. We have restricted ourselves to Stratonovich discretization scheme for the overdamped case.

The Crooks Fluctuation theorem (CFT) for heat [28, 29] relates the ratio of the probabilities of forward trajectory and the corresponding reverse trajectory for given initial states and is given by

$$\frac{P[X|x_0]}{\tilde{P}[\tilde{X}|x_\tau]} = e^{\beta Q}. \tag{6.1}$$

Here, X is the short form of the phase space trajectory along the forward process $x_0, x_1, ..., x_\tau$ generated by the protocol $\lambda(t)$. x_i represents the phase space point at time t_i. $\tilde{X}$ is the corresponding reverse trajectory generated by the time reversed protocol $\lambda(\tau - t)$, where τ is the time of observation. x_0 is a given initial state of the forward process. The reverse process begins from the state $\tilde{x}_\tau$, which is the time-reversal of the final state x_τ of the forward process. Using CFT, several other theorems like the Jarzynski equality and entropy production FT, can be easily derived [28, 29].

In this chapter, we study the validity of these FTs in the presence of coarse-graining, when we transform the underdamped Langevin equation to the overdamped one, in the limit of high friction. We find that a prominent difference in the analysis is observed between the overdamped (coarse-grained) and the underdamped systems, when the friction coefficient is space-dependent [103, 104, 105, 106]. It should be noted that space-dependent friction does not alter the equilibrium state. However, Langevin dynamics of the system gets modified especially for the overdamped case. There are several physical systems wherein friction is space-dependent (see [106] and the references therein).

6.2 Crooks theorem in presence of space-dependent friction

In the presence of space-dependent friction $\gamma(x)$, the equation of motion of the underdamped system of mass m moving in a time-dependent potential $U(x,t)$ is given by

$$m\dot{v} = -\gamma(x)v - U'(x,t) + \sqrt{2\gamma(x)T}\xi(t). \tag{6.2}$$

Note that the above equation contains multiplicative noise term. Here, T is the temperature of the bath, while $\xi(t)$ is the delta-correlated Gaussian noise with zero mean: $\langle\xi(t)\rangle = 0; \langle\xi(t)\xi(t')\rangle = \delta(t-t')$. The overhead dot denotes time-derivative, whereas prime represents space derivative. Eq. (6.2) has been derived microscopically by invoking system and bath coupling [104, 105]. It is shown that the high damping limit of eq. (6.2) is not equivalent to ignoring only inertial term [103, 104, 105, 106]. The detailed treatment leads to an extra term that is crucial for system to reach equilibrium state in absence of time-dependent perturbations (see eq. 6.19 below).

Roughly speaking, this happens in the overdamped case because the random forces $\xi(t)$ appear as delta-function pulses that cause jumps in x. It then becomes unclear what value of x must be provided in the argument of the function g, because the value of the position at the time the delta-peak appears becomes undefined [6]. It does not converge to a unique value even in the limit of small time step Δt. In fact, we can plug in any value of position in-between $x(t)$ (position before the jump) and $x(t+\Delta t)$ (position after the jump). These different values of position lead to different discretization schemes. The case is simpler in case of underdamped Langevin equation. There, the jumps are caused in the velocities, while the position is a much smoother variable (being an integral over the velocities). In other words, it does not feel the noise as delta peaks, but instead as a more well-behaved function. In that case, in the limit of small Δt, the argument of g is given by the unambiguous value

$x(t)$. Thus, in this case, an update in the values of x and v will be unique in each time step.

Let us now check the validity of CFT in both the underdamped and overdamped cases.

6.2.1 Underdamped case

At first we want to calculate the ratio of path probabilities between forward and reverse process. In a given process, let the evolution of the system in phase space be denoted by the phase space trajectory $X(t) \equiv \{x_0, x_1, \cdots, x_\tau\}$. Here, x_k represents the phase point at time $t = t_k$. In general, the phase point includes both the position and the velocity coordinates of the system. In the overdamped case, however, it would consist of the position coordinate only. Now, a given path $X(t)$, for a given initial point x_0, would be fully determined if the sequence of noise terms for the entire time of observation is available (this happens because there is no unambiguity in either the positions or the velocities, while updating their values by using the underdamped Langevin equation, as discussed above): $\boldsymbol{\xi} \equiv \{\xi_0, \xi_1, \cdots, \xi_{\tau-1}\}$. The probability distribution of ξ_k is given by

$$P(\xi_k) \propto e^{-\xi_k^2 dt/2}. \tag{6.3}$$

Therefore, the probability of obtaining the sequence $\boldsymbol{\xi}$ will be [26, 107]

$$P[\boldsymbol{\xi(t)}] \propto \exp\left[-\frac{1}{2}\int_0^\tau \xi^2(t)dt\right]. \tag{6.4}$$

Now, from the probability $P[\boldsymbol{\xi(t)}]$ of the path $\boldsymbol{\xi(t)}$ in noise space, we can obtain the probability $P[X(t)|x_0]$. These two probability functionals are related by the Jacobian

$|\frac{\partial \xi}{\partial x}|$. Thus, we can as well write [26]

$$P[X(t)|x_0] \propto \exp\left[-\frac{1}{2}\int_0^\tau \xi^2(t)dt\right], \tag{6.5}$$

where the proportionality constant is different from that in eq. (6.4). In eq. (6.5), we then substitute the expression for $\xi(t)$ from the Langevin equation (eq.(6.2)):

$$P[X(t)|x_0] \propto \exp\left[-\frac{1}{4}\int_0^\tau dt\frac{(m\dot{v} + U'(x,t) + \gamma(x)v)^2}{\gamma(x)T}\right]. \tag{6.6}$$

For the reverse process, $v \to -v$, but the Jacobian is same. The ratio of probability of the forward to the reverse path can be readily shown to be [26, 108]

$$\begin{aligned}
&\frac{P[X(t)|x_0]}{\tilde{P}[\tilde{X}(t)|\tilde{x}_\tau]} \\
&= \frac{\exp\left[-\int_0^\tau dt(m\dot{v} + U'(x,t) + \gamma(x)v)^2/4\gamma(x)T\right]}{\exp\left[-\int_0^\tau dt(m\dot{v} + U'(x,t) - \gamma(x)v)^2/4\gamma(x)T\right]} \\
&= \exp\left[-\int_0^\tau dt\frac{4m\gamma(x)\dot{v}v + 4U'(x,t)\gamma(x)v}{4\gamma(x)T}\right] \\
&= \exp\left[-\beta\int_0^\tau dt\left(m\dot{v}v + U'(x,t)v\right)\right] \\
&= e^{\beta Q},
\end{aligned} \tag{6.7}$$

where Q is the heat dissipated by the system into the bath, defined as

$$\begin{aligned}
Q \quad &\equiv \int_0^\tau \{\gamma(x)v - \sqrt{2\gamma(x)T}\xi(t)\}v\ dt \\
&= -\int_0^\tau \{m\dot{v} + U'(x,t)\}\ v\ dt.
\end{aligned} \tag{6.8}$$

This definition follow from the stochastic energetics developed by Sekimoto [12, 11] from the definition of first Law using Langevin dynamics. Eq.(6.7) is the celebrated CFT, from which several FT follow.

6.2.2 Integral and detailed fluctuation theorems

We have,

$$\frac{P[X(t)|x_0]}{\tilde{P}[\tilde{X}(t)|\tilde{x}_\tau]} = e^{\beta Q}, \tag{6.9}$$

where Q is the heat dissipated, as obtained from the first law. Multiplying by the ratio of the initial equilibrium distributions, for forward and reverse processes, namely by $p_0(x_0)/p_1(x_\tau)$, we get [28]

$$\begin{aligned}\frac{P[X(t)|x_0]p_0(x_0)}{\tilde{P}[\tilde{X}(t)|\tilde{x}_\tau]p_1(x_\tau)} = \frac{P[X]}{\tilde{P}[\tilde{X}]} &= e^{\beta Q}\cdot\frac{e^{-\beta E_0}}{Z(\lambda_0)}\cdot\frac{Z(\lambda_\tau)}{e^{-\beta E_\tau}} \\ &= e^{\beta(Q+\Delta E-\Delta F)} = e^{\beta(W-\Delta F)}.\end{aligned} \tag{6.10}$$

We have used the expression for equilibrium initial distribution $p_0(x_0) = \frac{e^{-\beta E_0}}{Z(\lambda_0)}$ and $p_1(x_\tau) = \frac{e^{-\beta E_\tau}}{Z(\lambda_\tau)}$. Here, $\Delta E \equiv E_\tau - E_0$, and we have made use of the relation $Z = e^{-\beta F}$, between the partition function and the free energy. $Z(\lambda_0)$ and $Z(\lambda_\tau)$ are the partition functions corresponding to the protocol values at the initial time and the final time, respectively. In the final step, the first law for the work done on the system, $W = Q + \Delta E$, has been invoked. The above relation can be readily converted to the Crooks work theorem [29], given by

$$\frac{P(W)}{\tilde{P}(-W)} = e^{\beta(W-\Delta F)}. \tag{6.11}$$

Here, $P(W)$ is the probability of work done W on the system in the forward process. $\tilde{P}(-W)$ is the probability of W amount of work extracted from the system in the reverse process. By cross-multiplication and integration over W, we get the Jarzynski equality [23]:

$$\left\langle e^{-\beta W}\right\rangle = e^{-\beta\Delta F}. \tag{6.12}$$

If the initial distributions for the forward and reverse processes are not equilibrium

ones and $p_1(x_\tau)$ is the solution of the Fokker-Planck Equation at the final time τ of the forward process, we get, instead of eq. (6.10), the relation [27, 13]

$$\frac{P[X]}{\tilde{P}[\tilde{X}]} = e^{\beta Q + \ln(p_0(x_0)/p_1(x_\tau))} = e^{\Delta s_{tot}}. \tag{6.13}$$

We then arrive at the relations for change of total entropy Δs_{tot} which is nothing but sum of change of system entropy $\Delta s_{sys} = \ln(p_0(x_0)/p_1(x_\tau))$ (in the units of Boltzmann constant k_B) and entropy production in the bath $s_B = \beta Q$.

$$\Delta s_{tot} = \ln(p_0(x_0)/p_1(x_\tau)) + \beta Q. \tag{6.14}$$

From eq.(6.13) integral fluctuation theorem follows, which hold for all times, namely,

$$\left\langle e^{-\Delta s_{tot}} \right\rangle = 1. \tag{6.15}$$

From the integral forms of the fluctuation theorems, given by eqs. (6.12) and (6.15), using Jensen's inequality we easily obtain the second law inequalities [23, 13]

$$\langle W \rangle \geq \Delta F; \tag{6.16}$$

$$\langle \Delta s_{tot} \rangle \geq 0. \tag{6.17}$$

Thus, in the underdamped limit second law retains same form for a system in presence of space-dependent friction. This completes our treatment for some FTs in the underdamped case for a particle moving in space dependent friction.

Above exact FTs do not give any information about probability distribution of work ($P(W)$), entropy $P(\Delta s_{tot})$ etc. These distributions depend crucially on the specific problem being investigated.

Here, we study these distributions for the case of driven particle in harmonic

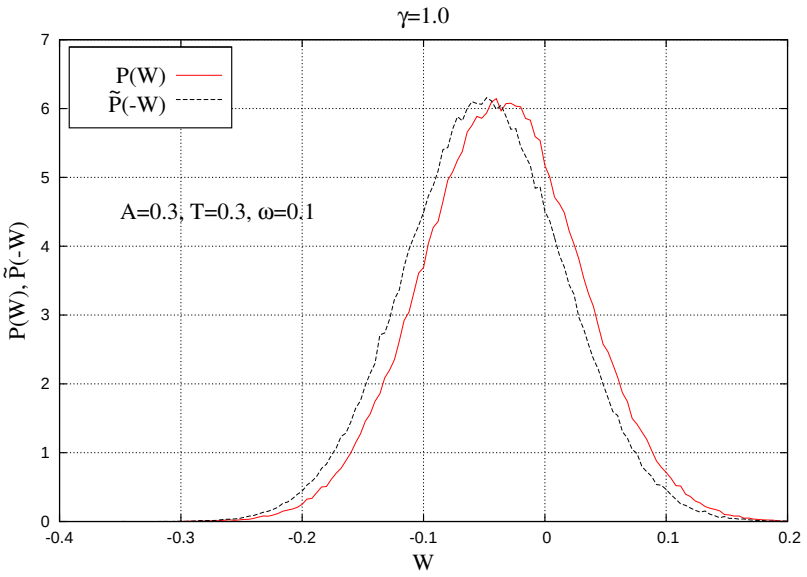

Figure 6.1: Transient work distribution for underdamped case

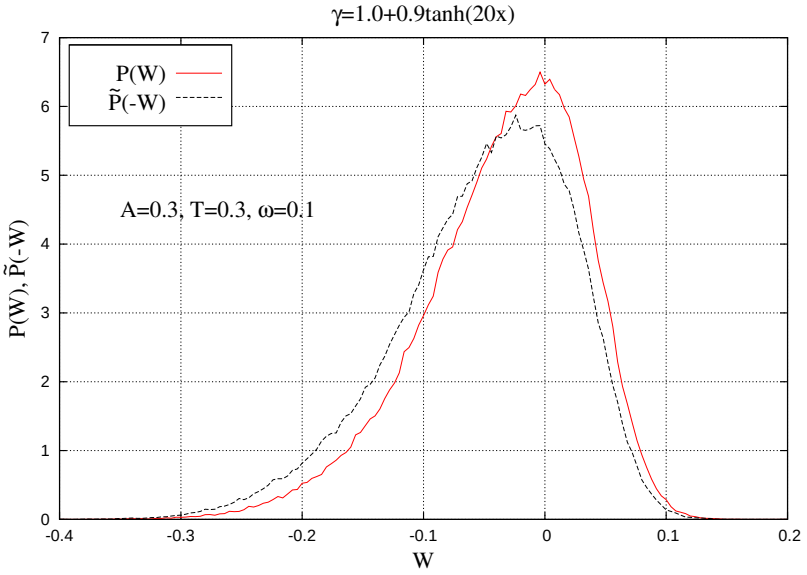

Figure 6.2: Transient work distribution for underdamped case with space dependent friction

trap. Apart from verifying FTs we also see how the space dependent friction modifies the distribution of $(P(W))$, and $P(\Delta s_{tot})$ as compared to the particle moving in a space independent frictional coefficient γ (which is the space average of $\gamma(x)$). The

underdamped Langevin equation is given by

$$m\dot{v} = -\gamma(x)v - kx + A\sin(\omega t) + \sqrt{2\gamma(x)T}\xi(t). \tag{6.18}$$

$A\sin(\omega t)$ is driven sinusoidal force of frequency ω and amplitude A. For this model analytical solution can be obtained for space independent case only for both overdamped and underdamped case [109, 110].

For simplicity in our study, we restrict ourselves to two cases of space dependent friction (i) $\gamma(x) = \gamma =$ constant (ii) $\gamma(x) = \gamma + c\tanh(\alpha x)$

In figure 6.1 we have plotted the transient work distribution obtained after driving a system for one-fourth of a cycle for forward ($P(W)$) and corresponding reverse ($\tilde{P}(-W)$) protocol. Initially the system is equilibrated at appropriate initial values of protocol for forward and reverse process. In all our simulations, we have used the Heun's method of numerical integration [84], and have generated $\sim 10^5$ realizations. Implementing the Heun's method tantamounts to using the Stratonovich discretization scheme [111]. Henceforth we have used all the quantities in dimensionless form and taken k=1, m=1 and $\gamma = 1$. For case (i), both distributions are Gaussian nature, and they cross each other at $\Delta F = -0.044$, which is the free energy difference over one-fourth cycle. This is obtained numerically from $\left\langle e^{-\beta W}\right\rangle = e^{-\beta\Delta F}$, while theoretically we have $\Delta F = -0.045$. This is well within our numerical accuracy.

In figgure 6.2 we have plotted the same for space dependent friction $\gamma(x) = 1.0 + 0.9\tanh(20x)$. Here the distributions are non-Gaussian but the crossing point is same as in space independent case. This is because the equilibrium distribution remain same in both cases.

In figure 6.3 we have plotted distribution of total entropy production of a driven Brownian particle confined in a harmonic trap for one-fourth cycle. Here the underlying dynamics is underdamped and we find that the distribution is Gaussian for

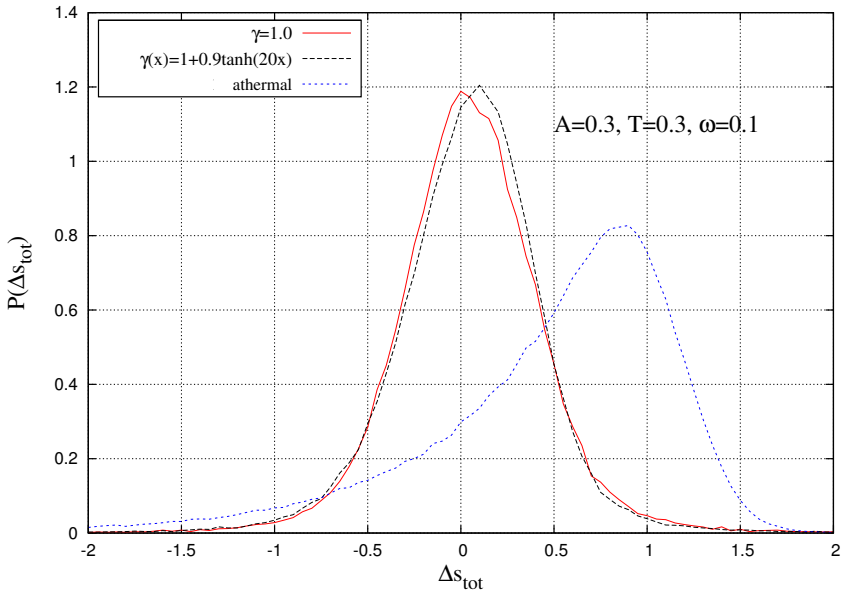

Figure 6.3: Distribution for total entropy production for underdamped dynamics

space independent case, while it is non-Gaussian for space dependent case. If we take particle to be initially equilibrated at different temperature $T = 0.1$ and then connected instantaneously to the given bath of temperature $T = 0.3$, and driven by same external force (i.e, for athermal case), we find that the distribution of total entropy production is non-Gaussian even for space independent case. This is consistent with the results in [88]. Numerically we find $\langle e^{-\Delta s_{tot}} \rangle = 1.002$ which is well within our numerical accuracy. In all these distributions, we find that there is a finite weight for realizations having $W < \Delta F$ and $\Delta s_{tot} < 0$, although the mean values follow the second law inequalities. These realizations are called transient second Law violating trajectories. This finite weight is necessary to satisfy the fluctuation theorems [42].

After establishing the well known FTs in the underdamped case, we turn our attention to the overdamped dynamics of the particle, in a space-dependent frictional medium. Going to the overdamped regime implies coarse-graining. Instead of evolution in full phase space (coordinates and momenta), we restrict the evolution of the system to the position space only. This is equivalent to ignoring the information

contained in the velocity variables.

6.2.3 Overdamped case

The treatment of overdamped case is more subtle and a proper methodology must be followed (see appendix D). In order to obtain a unique Fokker-Planck equation (which is needed for a unique equilibrium distribution), the overdamped Langevin equation must be modified, depending on the discretization process that is being used. It can be written as

$$\begin{aligned} \dot{x} &= f(x,t) + g(x)\xi(t) \\ &= -\Gamma(x)U'(x,t) + (1-\alpha)g(x)g'(x) + g(x)\xi(t). \end{aligned} \tag{6.19}$$

For detail we refer to [106]. Such ambiguity of discretization process does not arises in the underdamped case as discussed in detail in [6, 112]. Here, $g(x) = \sqrt{2T\Gamma(x)} = \sqrt{2T/\gamma(x)}$. $\alpha \in [0,1]$. $\alpha = 0$ for Ito convention, while $\alpha = 1/2$ and $\alpha = 1$ for Stratonovich and and isothermal conventions, respectively. In earlier literature [103], the underdamped Langevin equation in a Stratonovich prescription is derived. In [106], it has been shown that for all values of α, the same equilibrium distribution is obtained for a given value of the protocol. Now we closely follow the treatment given in [106]. From eq.(6.19), the path probability for a single trajectory in position space can be shown to be given by

$$P[X(t)|x_0] \sim e^{-S[X]}, \tag{6.20}$$

where

$$S[X] = \int_0^\tau dt \left(\frac{1}{2g^2}[\dot{x} - f(x,t) + \alpha g g']^2 + \alpha f'(x,t) \right). \tag{6.21}$$

Using $f(x,t) = -U'(x,t)\Gamma(x) + (1-\alpha)g(x)g'(x)$, we get

$$S[X] = \int_0^\tau dt \left(\frac{1}{2g^2}[\dot{x} + U'\Gamma + (2\alpha - 1)gg']^2 \right.$$
$$\left. +\alpha[-U''\Gamma - U'\Gamma' + (1-\alpha)(gg'' + g'^2)] \right). \tag{6.22}$$

For reverse path, (see eq. (22) of [113],[1]) one has to replace $\dot{x} \to -\dot{x}$, and $\alpha \to 1-\alpha$. Thus the action for reverse path is given by,

$$\tilde{S}[\tilde{X}] = \int_0^\tau dt \left(\frac{1}{2g^2}[-\dot{x} - f(x,t) + (1-\alpha)gg']^2 + (1-\alpha)f'(x,t) \right). \tag{6.23}$$

Once again, substituting $f(x,t) = -U'(x,t)\Gamma(x) + \alpha g(x)g'(x)$, we get

$$\tilde{S}[\tilde{X}] = \int_0^\tau dt \left(\frac{1}{2g^2}[-\dot{x} + U'\Gamma - (2\alpha - 1)gg']^2 \right.$$
$$\left. +(1-\alpha)[-U''\Gamma - U'\Gamma' + \alpha(gg'' + g'^2)] \right). \tag{6.24}$$

However we restrict our analysis to $\alpha = 1/2$, i.e, Stratonovich discretization scheme. For this we have

$$S[X] = \int_0^\tau dt \left(\frac{1}{2g^2}[\dot{x} + U'\Gamma]^2 + \frac{1}{2}\left[-U''\Gamma - U'\Gamma' + \frac{1}{2}(gg'' + g'^2) \right] \right). \tag{6.25}$$

Similarly,

$$\tilde{S}[\tilde{X}] = \int_0^\tau dt \left(\frac{1}{2g^2}[-\dot{x} + U'\Gamma]^2 + \frac{1}{2}[-U''\Gamma - U'\Gamma' + \frac{1}{2}(gg'' + g'^2)] \right). \tag{6.26}$$

[1]However, note that in our case (see appendix D), the equilibrium distribution is independent of discretization scheme, unlike in [113]

Thus, the path ratio become simply

$$\frac{P[X|x_0]}{\tilde{P}[\tilde{X}|x_\tau]} = e^{\tilde{S}[\tilde{X}]-S[X]}$$
$$= \exp\left[-\int_0^\tau dt\ \dot{x}U'\right] = e^{\beta Q}, \tag{6.27}$$

where $Q \equiv -\int_0^\tau dt\dot{x}U'(x,t)$. Thus, under Stratonovich scheme, the Crooks fluctuation theorem for trajectories remains unaffected in the overdamped regime, even in the presence of multiplicative noise. Since the Stratonovich scheme is considered to be the physically correct one for a Brownian particle in a heat bath [6], we may conclude that all the fluctuation theorems retain their forms as in the underdamped case [2].

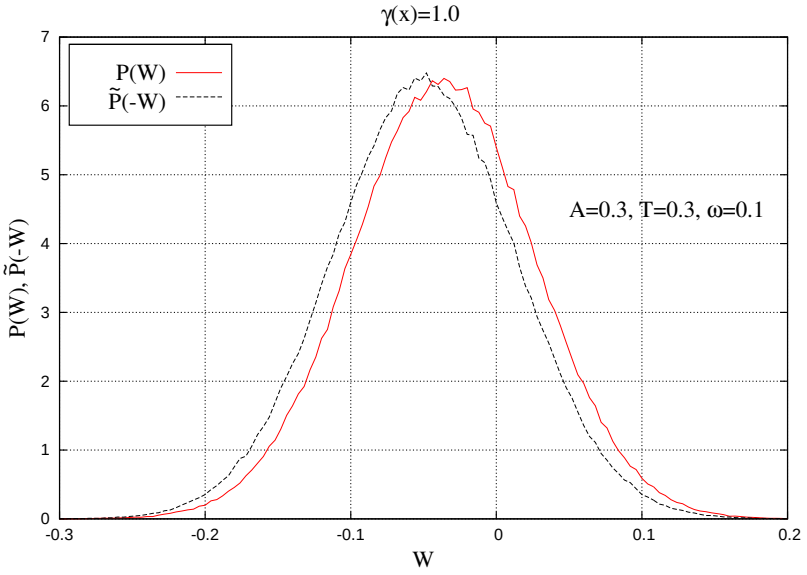

Figure 6.4: Transient work distribution for overdamped case with space-independent friction

As in the underdamped case we study the nature of probability distribution for

[2]The above reasoning is correct for systems where the noise is not exactly delta-correlated, but has a very short correlation time. Now if we take the limit of correlation time going to zero, we get the Fokker-Planck equation that corresponds to the Stratonovich discretization scheme. As is evident, this is the case with most stochastic systems in nature.

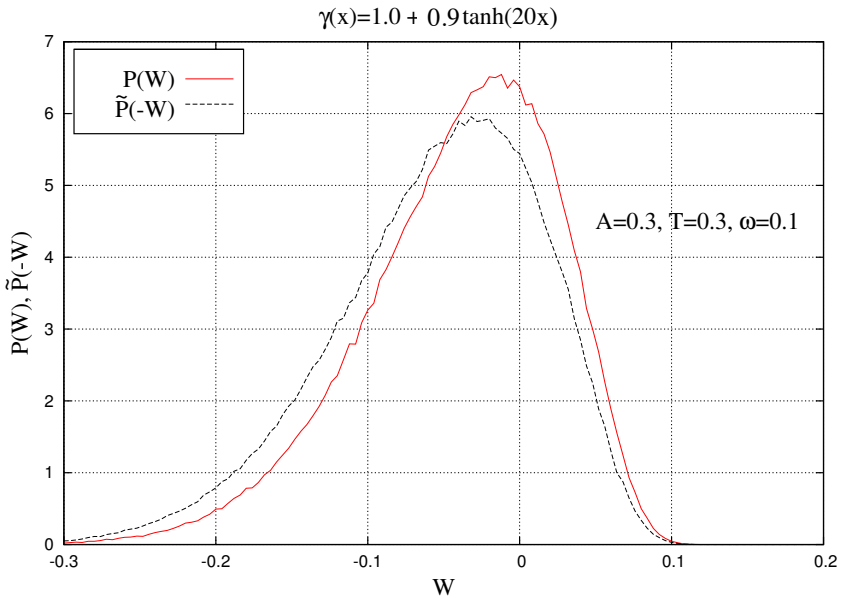

Figure 6.5: Transient work distribution for overdamped case with space dependent friction

work and entropy for simple model of driven harmonic oscillator for both space independent and space dependent case and verifying FTs numerically using Heun's method (which is equivalent to following Stratonovich description as discussed earlier). The corresponding Langevin equation is given by

$$\gamma(x)\dot{x} = -kx + A\sin(\omega t) - \frac{\gamma'(x)}{2\gamma(x)}T + \sqrt{2\gamma(x)T}\;\xi(t). \tag{6.28}$$

In figure 6.4 and figure 6.5, we have plotted the transient work distributions for forward and reverse processes, for space-independent and space-dependent friction, respectively. The functional form of $\gamma(x)$ are same as studied in underdamped case. All the units are in dimensionless form and we take $k = 1$, $\gamma = 1$. We find that the distributions are Gaussian for space independent case while for space dependent it is non-Gaussian. But, the crossing point is same. From $\left\langle e^{-\beta W}\right\rangle = e^{-\beta\Delta F}$, the numerically obtained free energy difference $\Delta F = -0.045$, which is equal to the theoretical value, thus reassuring that space dependent friction does not alter the

equilibrium distribution.

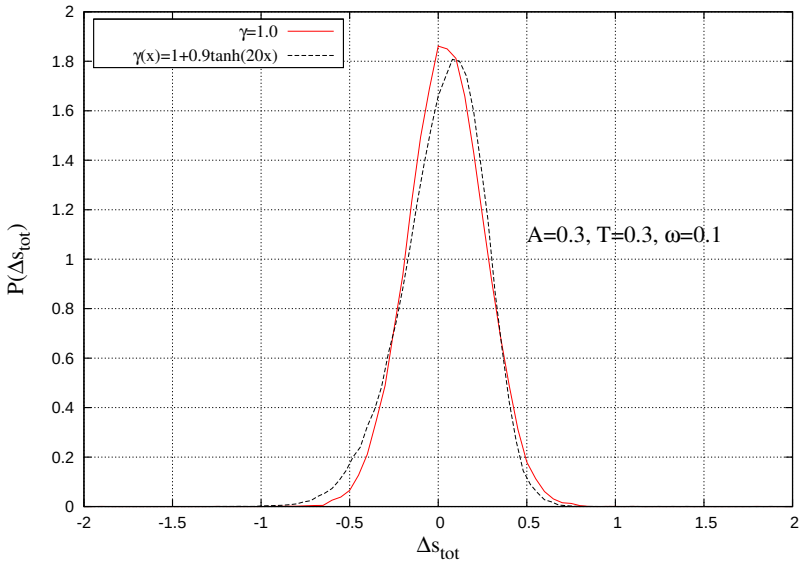

Figure 6.6: Distribution for total entropy production for overdamped dynamics

In figure 6.6 we have plotted the distribution of total entropy production for the overdamped particle. We found that for space independent case the distribution is Gaussian. This is true only if initial distribution is the thermal one. We have verified separately that for initial nonequilibrium distribution, $P(\Delta s_{tot})$ is non Gaussian. But for space dependent case $P(\Delta s_{tot})$ is non-Gaussian even initial equilibrium distribution. Numerically we find $\langle e^{-\Delta s_{tot}} \rangle = 1.002$ which is well within our numerical accuracy.

6.3 Definition of heat in overdamped case

We can, following Sekimoto [11], derive the expression for dissipated heat using the overdamped Langevin dynamics (substituting $\alpha = 1/2$ in eq. (6.19)):

$$\dot{x} = -\Gamma(x)U'(x,t) + \frac{1}{2}g(x)g'(x) + g(x)\xi(t). \tag{6.29}$$

We found that microscopic reversibility gives (see eq. (6.27))

$$Q = -\int_0^\tau dt\ \dot{x}U'(x,t). \tag{6.30}$$

The above two equations then give

$$\begin{aligned} Q &= \int_0^\tau dt\ \frac{\dot{x}}{\Gamma(x)}\left[\dot{x} - \frac{1}{2}g(x)g'(x) - g(x)\xi(t)\right] \\ &= \int_0^\tau dt\ \dot{x}\left[\gamma(x)\dot{x} + \frac{\gamma'(x)T}{2\gamma(x)} - \sqrt{2\gamma(x)T}\ \xi(t)\right] \\ &= \int_0^\tau dt\ \dot{x}[\gamma(x)\dot{x} - \sqrt{2\gamma(x)T}\ \xi(t)] + \frac{T}{2}\ln\frac{\gamma(x_\tau)}{\gamma(x_0)} \\ &= Q_{conv} + \frac{T}{2}\ln\frac{\gamma(x_\tau)}{\gamma(x_0)}, \end{aligned} \tag{6.31}$$

where Q_{conv} is the conventional definition of heat. We thus get an extra boundary term in the definition, which assigns the logarithm of $\sqrt{\gamma(x)}$ with the physical meaning of an entropy term. The presence of this term implies that if the particle begins from a given position x_0 with a small friction coefficient, then it dissipates more heat into the bath if it travels to a position x_τ with a greater friction coefficient.

6.4 Conclusion

In this work, we have considered the validity of FTs in presence of space-dependent friction, for both underdamped and overdamped limit. We find that, although no conceptual difficulties arise when the system is underdamped, the derivation of the FTs are more involved for overdamped system. In latter case, where we have dealt with the Stratonovich scheme of discretization, the Langevin equation contains extra terms and although Crooks theorem remains valid, the definition of heat gets altered. Thus, we conclude that the FTs remain valid for the case of dynamics of a particle in space dependent frictional medium, even under coarse graining, i.e, reducing the

description of the system of two phase space variable (x,v,underdamped case), to a single phase space variable (x, overdamped case).

As an illustration, we have analyzed the nature of $P(\Delta s_{tot})$ and $P(W)$ for the simple case of a driven harmonic oscillator in presence of space dependent friction, both in underdamped and the overdamped regime (in Stratonovich prescription). Distributions for constant friction are compared with that of a particle moving in a space dependent frictional medium. Moreover, several FTs have been verified. This model system is amenable to experimental verification [109].

Chapter 7

The effect of confinement on SR in continuous bistable systems

7.1 Introduction

Using the input energy per cycle as a quantifier of stochastic resonance (SR), we show that SR is observed in superharmonic (hard) potentials. However, it is not observed in subharmonic (soft) potentials, even though the potential is bistable. These results are consistent with recent observations based on amplitude of average position as a quantifier. In both soft and hard potentials, we observe resonance phenomenon as a function of the driving frequency. The nature of probability distributions of average work are qualitatively different for soft and hard potentials.

SR is an exclusively nonlinear phenomenon where the combined effect of the noise and the nonlinearity gives rise to an enhanced response of the system at a particular frequency of an external periodic drive. It has been found to be of fundamental importance not only in physics [59, 60, 61, 62] but also in biological systems, from the mechanoreceptor cells in crayfish to the functioning of sensory neurons in humans. This is in sharp contrast to the general trend of a noise to cause the effect of a signal to fade. A typical model used to study this behaviour consists of a bistable potential in which a Brownian particle is present. The particle is in contact with a thermal bath of temperature T. This system is driven by a periodic drive with a given frequency, $f(t) = A \sin \omega t$. Now, the initial system without the drive has an intrinsic escape rate of going from one minimum of the potential ($V(x)$) to the other. This is given by the *Kramers escape rate* [7, 4]:

$$r_K = Ce^{-\beta \Delta V}, \tag{7.1}$$

where $\beta \equiv 1/k_B T$, k_B being the Boltzmann Constant, C is a constant that depends on the system parameters, and ΔV is the barrier height (height difference between the minimum and the maximum of $V(x)$). The escape time will then be given by the inverse of the escape rate: $\tau_K = r_K^{-1}$. As the external periodic drive is switched on, in general its time period τ_ω will not be in synchronization with the escape time of

the particle over the barrier. However, if the noise strength or temperature is varied, at a certain value of temperature, τ_ω will be exactly equal to $2\tau_K$. Now we will have proper synchronization of the dynamics: when the right well becomes deeper compared to the left well, the particle hops into the right well with a high probability, and vice versa. Under this condition, the system absorbs maximum energy from the drive. This phenomenon is termed as *stochastic resonance*. Various quantifiers of SR have been proposed in literature [59]: signal-to-noise ratio (SNR), hysteresis loop area (HLA), spectral power amplification (SPA), position amplitude of the particle ($\bar{x}$), phase lag of the response with the external drive ($\bar{\phi}$), etc. In [63], a relation has been derived between SNR, HLA and SPA which is given by:

$$\text{SNR} \times \text{HLA} = -\frac{\pi^2 A^4 \omega}{4k_B T}\text{SPA} \tag{7.2}$$

The above relation shows that some of the above quantifiers are related to each other. We observe that a similar relation is present that connects the quantifiers mean thermodynamic work, $\bar{x}$ and $\bar{\phi}$, and as a result the three cannot act as independent quantifiers of SR.

In the present work we use the mean input energy per drive period as a quantifier for SR [64, 114, 115, 77]. As a function of noise strength, we observe suppression of SR in soft potentials and distinct peak signifying SR in hard potentials.

Since it has been established that SR is a bonafide resonance it should show maximum in the quantifiers as a function of drive frequency as well. Interestingly, whereas the mean input energy per period, $\langle W \rangle$, shows peaking behaviour, the average amplitude, $\overline{x}$ does not. As opposed to the behaviour of $\langle W \rangle$ as a function of noise strength, for soft and hard potentials, its behaviour with frequency is same for both kinds of potentials. In particular, $\langle W \rangle$ shows peaking behaviour and $\bar{x}$ decreases monotonically as a function of frequency for both hard and soft potentials. We further

investigate the probability distributions of work for various temperatures [115,77], for both hard and soft potentials, and point out the qualitative differences between the nature of these distributions.

7.2 The system

We consider a Brownian particle described by the overdamped Langevin equation:

$$\gamma\dot{x} = -V'(x) + f(t) + \xi(t), \tag{7.3}$$

where $V'(x) = \frac{\partial V(x)}{\partial x}$, $\xi(t)$ is Gaussian distributed white noise having the properties $\langle\xi(t)\rangle = 0$ and $\langle\xi(t)\xi(t')\rangle = 2\gamma k_B T\delta(t-t')$, γ being the viscous drag in the medium. The strength of the noise is described by the thermal energy $k_B T$. The expression for the bistable potential is given by [116]

$$V(x) = e^{-x^2} + k\frac{|x|^q}{q}, \tag{7.4}$$

where the parameter k has been set equal to 0.2 throughout the manuscript, which sets the barrier height at approximately $\Delta V = 0.67$ (all variables are dimensionless). The parameter q is used to modulate the steepness of the walls of the potential. In other words, as q is increased, the slope of the potential wall increases as shown in figure 7.1, so that the particle is more confined in-between the two minima. The external drive is given by $f(t) = A\sin\omega t$.

If we plot the amplitude of mean position as a function of temperature, i.e., $\bar{x}(T)$ vs T, then the resonance gets suppressed when $q \leq 2$. Analytically, this follows from the following approximate expression for $\langle x\rangle$ in the nonequilibrium steady state

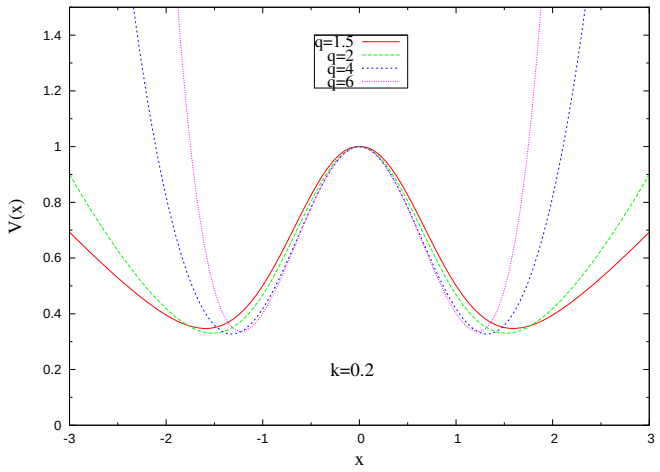

Figure 7.1: The shapes of the potential for different values of q, with $k = 0.2$.

(where the intrawell dynamics has been ignored) [59]:

$$\langle x(t)\rangle = \bar{x}\sin(\omega t - \bar{\phi}), \tag{7.5}$$

where

$$\bar{x}(T) = \frac{A\langle x^2\rangle_0}{T}\frac{2r_K}{\sqrt{4r_K^2+\omega^2}}. \tag{7.6}$$

$$\bar{\phi}(T) = \tan^{-1}\left(\frac{\omega}{2r_K}\right). \tag{7.7}$$

Here, the angular brackets $\langle\cdots\rangle$ represent ensemble averaging over a large number of phase space trajectories. $\langle x^2\rangle_0$ is the variance of the position of the particle in *absence* of any drive, i.e., subjected to the unperturbed potential. r_K is the Kramers escape rate whose expression is given by [7, 4]

$$r_K = \left(\frac{\gamma\sqrt{V''(x_m).|V''(0)|}}{2\pi}\right)e^{-\beta\Delta V}, \tag{7.8}$$

where $\pm x_m$ and 0 are the positions of the minima and of the maximum of the potential, ΔV is the barrier height, and V'' is double derivative of the potential function with

respect to x.

It can then be shown from (7.6) that as $T \to \infty$, the behaviour of the amplitude of mean position is given by [116]

$$\lim_{T\to\infty} \bar{x}(T) \sim T^{2/q-1}. \tag{7.9}$$

Now it can easily be seen that if $q > 2$, then $\bar{x}(T)$ goes to zero for large T. Of course, as $T \to 0$, $\bar{x} \to 0$ as well, because the particle hardly deviates from its equilibrium position (for details refer to [116]). This means that there must be a maximum in-between these two limits - a signal for resonance. However, if $q < 2$, the particle travels large distances away from the minima, so that the $\bar{x}$ grows monotonically with temperature, and stochastic resonance is not observed. The case $q = 2$ is the marginal case.

Following stochastic energetics [12], the thermodynamic work done on the system is given by

$$W = \int_0^\tau \frac{\partial V(x,t)}{\partial t} dt = -\int_0^\tau x(t) \frac{df(t)}{dt} dt, \tag{7.10}$$

where $V(x,t) = V(x) - xf(t)$. The average work done over time τ is

$$\langle W \rangle = -\int_0^\tau \langle x(t) \rangle \frac{df(t)}{dt} dt.$$

Now, using the approximate expression for $\langle x(t) \rangle$ (eq. (7.5)), we get

$$\begin{aligned}
\langle W \rangle &= -\int_0^\tau \langle x(t) \rangle \dot{f}(t) dt \\
&= -A\omega \int_0^\tau \bar{x} \sin(\omega t - \bar{\phi}) \cos \omega t dt \\
&= A \, \frac{2\pi}{\tau} \, \bar{x} \, \sin \bar{\phi} \, \frac{\tau}{2} \\
&= A\pi \bar{x} \sin \bar{\phi}.
\end{aligned} \tag{7.11}$$

Thus, we have arrived at a relation that connects three of the proposed quantifiers of SR: $\langle W \rangle$, $\bar{x}$ and $\bar{\phi}$. Plugging in the expressions for $\bar{x}(T)$ (eq. (7.6)) and $\bar{\phi}(T)$ (eq.(7.7)), we find

$$\langle W \rangle = \frac{2\pi A^2 \langle x^2 \rangle_0 \ \omega r_K}{T(4r_K^2 + \omega^2)}. \tag{7.12}$$

Eq. (7.12) predicts SR as a function of temperature. Later on we use this to analyze our numerical results.

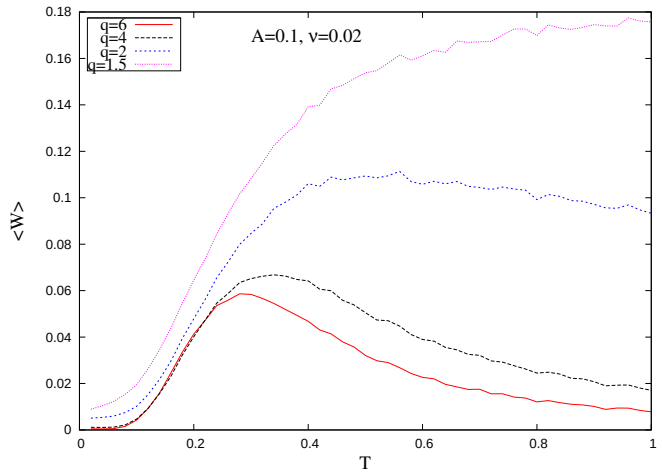

Figure 7.2: Average work as a function of temperature for $A = 0.1$ and $\nu = 0.02$ for different values of q. SR is observed for all values of q excepting $q = 1.5$.

7.3 Results and discussions

The plots of average thermodynamic work done on the particle by the drive per period τ_ω have been shown, for different values of the parameter q in figure 7.2. These plots have been obtained numerically by using the Heun's method [84]. We have ignored the initial transients and have evaluated the work over many cycles ($\sim 10^5$) using a single long trajectory of the particle. We find that the plots qualitatively show the same features as shown by the position amplitude with temperature [116]. The parameters used have been given in the figure captions. At very low temperature, the particle

can see only a single well, the barrier height being too large for it to cross. Thus, only intrawell dynamics is dominant under this condition and as a result the work done on the particle is very small and goes to zero as $T \to 0$. At the other extreme, $T \to \infty$, the barrier becomes negligible compared to the thermal energy of the particle. Now the random motion of the particle becomes so large that the synchronization gets washed away. This happens only for strong confining potential with $q > 2$. Thus for the hard potentials, we get a clear resonance peak. Moreover, our numerical result shows that the temperature at which SR peak occurs is consistent with the condition $\tau_\omega = 2\tau_K$.

However, for values of $q \leq 2$, the particle travels far from the left(right) of left(right) minimum and takes a long time to return. So it is expected that the distribution of passage time above the barrier will be very broad, so that the mean passage time ceases to be a good variable, being dominated by a large dispersion. As a result, the synchronization condition of escape rate with drive period is never satisfied. Thus these plots do not show the characteristic maxima of SR.

In figure 7.3, the numerically obtained plot for $\langle W \rangle$ vs T has been compared for the superharmonic potential with $q = 6$ with the following two analytical expressions for average work in steady state that are commonly used in the literature [116]:

$$\langle W_1 \rangle = \frac{2\pi A^2 \langle x^2 \rangle_0}{T} \frac{\omega r_K}{4r_K^2 + \omega^2}. \tag{7.13a}$$

$$\langle W_2 \rangle = \frac{2\pi A^2 x_m^2}{T} \frac{\omega r_K}{4r_K^2 + \omega^2}. \tag{7.13b}$$

In the expression for $\langle W_2 \rangle$, we have replaced $\langle x^2 \rangle_0$ by x_m^2, where x_m is the position of the minimum of the potential. However, from the figure we find that $\langle W_1 \rangle$ matches the simulated curve reasonably well, whereas $\langle W_2 \rangle$ deviates by a larger extent. This can be understood as follows [116]. In the derivation of the expression for $\langle W_2 \rangle$, one

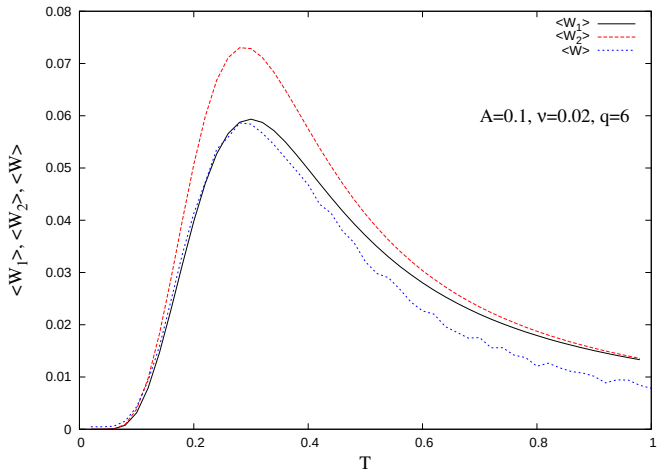

Figure 7.3: Comparison of temperature dependence of $\langle W \rangle$ obtained numerically with the analytical results. $\langle W_1 \rangle$ (the smooth solid line) is the expression obtained by taking into account the temperature dependence of the variance in position of the particle, $\langle x^2 \rangle_0$. $\langle W_2 \rangle$ (the smooth dashed line) is the expression for average work obtained with the variance replaced by x_m^2. The curve labelled $\langle W \rangle$ is the numerically generated one.

assumes that we are dealing with a *strictly* two-state system, where the particle's position distribution is the summation of two delta functions. x_m^2 then becomes the variance of the distribution having two δ-functions equidistant from the origin: $\langle x_m - 0 \rangle^2 = x_m^2$. Evidently, at any finite temperature the above distribution will be incorrect, owing to the softness of the double well potential. Thus, we need to incorporate into our expression the temperature dependence of the variance in particle position, which has been done in deriving the expression for $\langle W_1 \rangle$.

Previously the phase lag $\bar{\phi}$ of the response with drive (eq. (7.5)) has been used to detect stochastic resonance [118]. The variation of $\bar{\phi}$ with temperature has been shown in figure 7.4. We find that the curves for $q = 2$, 4 and 6 show prominent maxima, whereas the curve for $q = 1.5$ monotonically increases from zero and then saturates to an upper limit. Systems exhibiting SR show a peak in the phase lag $\bar{\phi}$ as a function of noise strength. However, the optimum value of noise intensity at which peak occurs does not coincide with SR peak for different quantifiers. The bell-shaped

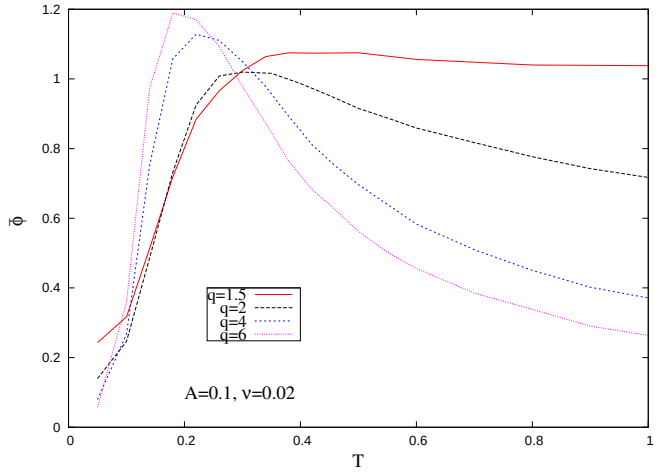

Figure 7.4: Phase difference $\bar{\phi}$ between drive and response, as a function of bath temperature. The peak in the curve becomes less distinct as the value of q is lowered.

dependence reflects the competition between hopping and intrawell dynamics [59]. However, for $q = 1.5$, we do not see a bell-shaped curve, implying no clear-cut time scale separation between hopping and intrawell motion.

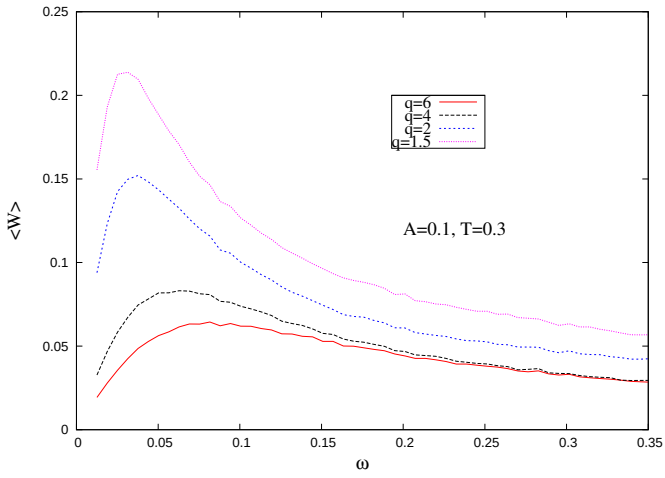

Figure 7.5: Average work as a function of frequency for $A = 0.1$ and $T = 0.3$ for different values of q. SR is observed for all values of q.

We now study the SR quantifiers $\langle W \rangle$ and $\bar{x}$ as a function of frequency of drive. The major difference between $\bar{x}$ and $\langle W \rangle$ as quantifiers is observed as a function of frequency of external drive. In figure 7.5 we have plotted the mean work versus

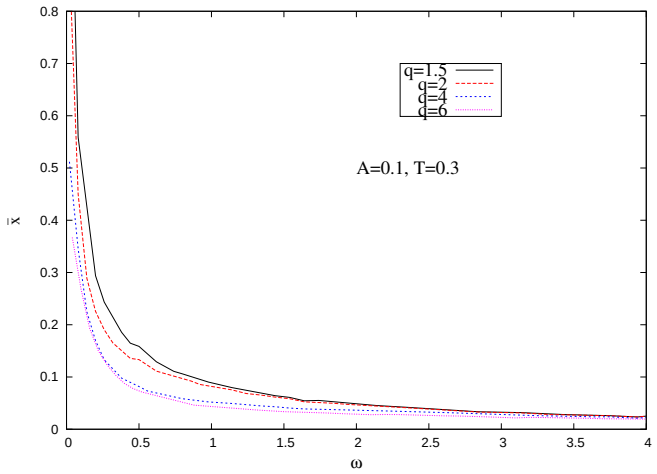

Figure 7.6: position amplitude as a function of frequency for different values of q. The monotonic decrease in $\bar{x}$ is apparent.

driving frequency. Whereas $\langle W \rangle$ shows a peak for all values of q (figure 7.5), $\bar{x}$ *decreases* monotonically with frequency for any value of q (see eq. (7.6)), as can be seen in figure 7.6. It may be emphasized here that the general trends of $\langle W \rangle$ and $\bar{x}$ as a function of ω do not depend on the nature of the confining potential. This is in contrast to the behaviour of $\langle W \rangle$ and $\bar{x}$ as a function of temperature, which crucially depends on the softness of $V(x)$.

Computing the derivative of $\langle W \rangle$ with respect to ω from the expression (7.12), we find the maximum to occur precisely at $\omega = 2r_K$:

$$\left.\frac{\partial \langle W \rangle}{\partial \omega}\right|_{\omega_{max}} = 0 \quad \Rightarrow \quad \omega_{max} = 2r_K. \tag{7.14}$$

However, the proper condition for synchronization is

$$\tau_\omega = 2\tau_K \quad \Rightarrow \quad \omega_{SR} = \pi r_K. \tag{7.15}$$

On calculating the escape rate for the superharmonic ($q = 4$) potential at $T = 0.3$, we find $r_K \approx 0.03$. Figure 7.5 shows the peak to occur at $\omega \approx 0.06 \approx 2r_K$, consistent

with eq. (7.14).

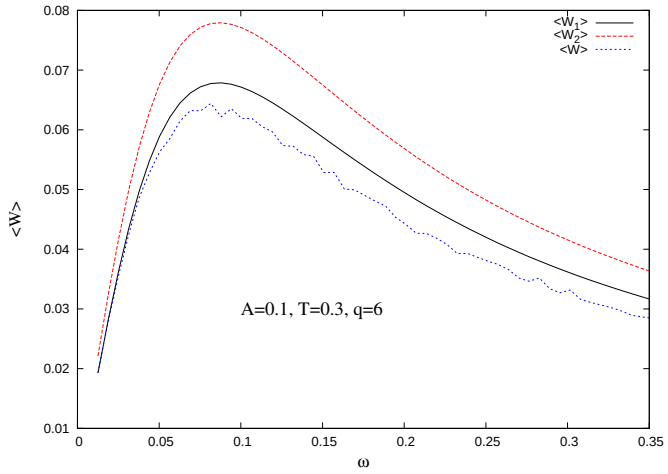

Figure 7.7: Comparison of frequency dependence of $\langle W \rangle$ obtained numerically with the analytical results. $\langle W_1 \rangle$ (the smooth solid line) is the expression obtained by taking into account the variance in position of the particle, $\langle x^2 \rangle_0$, at the fixed temperature $T = 0.3$. $\langle W_2 \rangle$ (the smooth dashed line) is the expression for average work obtained with the variance replaced by x_m^2. The curve labelled $\langle W \rangle$ is the numerically generated one.

In figure 7.7, the numerically obtained plot for $\langle W \rangle$ vs ω is compared with the analytical expressions (7.13a) and (7.13b). For this we have used the superharmonic potential with $q = 6$. We observe that the analytical expression using eq. (7.13a) fits better compared to (7.13b), the reason being the same as explained earlier in the context of figure (7.3). Now we turn our attention to the power applied to the system.

In figure 7.8, we have plotted the power applied to the system by the drive versus the drive frequency. We find that for all values of q, the curves are monotonically increasing. From figure 7.2 (scaling the y-axis by the constant parameter ω), we observe that the average power exhibits peak for $q > 2$ as a function of temperature. Thus, power cannot be used as a quantifier of bona fide SR [117] for $q > 2$.

In figure 7.9, we have plotted the real time trajectory of the particle at $T = 0.3$ (around SR for q=4). In (a), because of subharmonic potential, the particle travels large distances away from the minima and spends more time in the wings of the

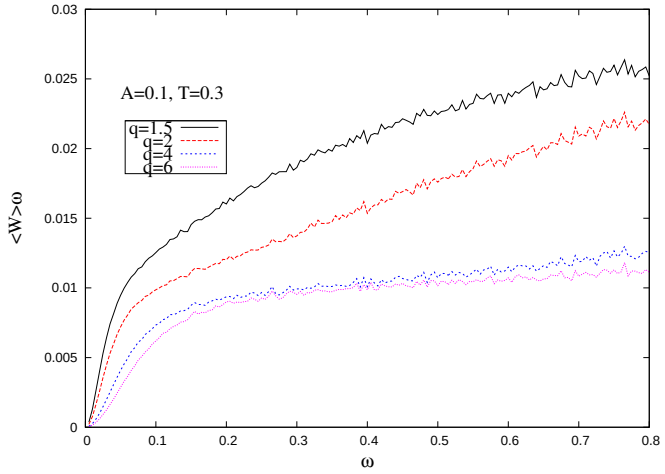

Figure 7.8: Average power as a function of frequency for $A = 0.1$ and $T = 0.3$ for different values of q. The curves are all monotonically increasing with frequency.

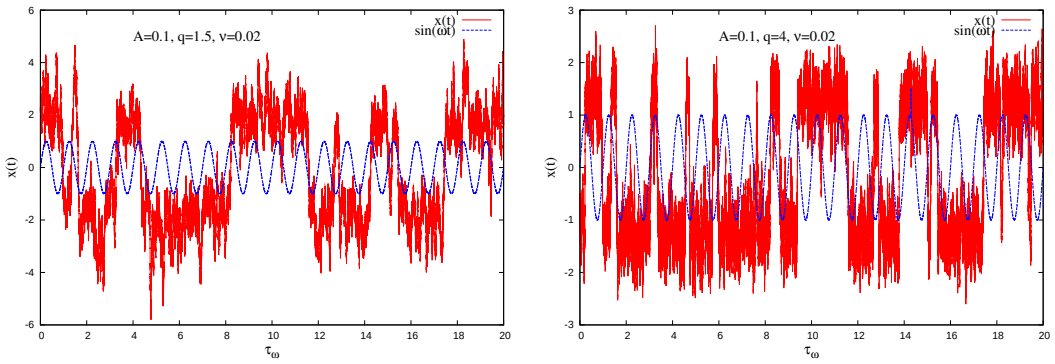

(a) (b)

Figure 7.9: (a) Position as a function of time for a given trajectory is shown, for the $q = 1.5$ potential. We find that the particle travels large distances from either minima due to softer confinement. (b) Similar plot for $q = 4$. The hard confinement effectively contains the particle in a smaller region, and the motion is more synchronized.

potential ($x > x_m$ or $x < -x_m$) over a duration of many cycles of the applied force without passing over the barrier. This is clear from the figure. Thus, the question of synchronization between the applied force and particle hopping does not arise, hence the absence of SR. On the other hand, in (b), the superharmonic potential ($q = 4$) helps in more efficient confinement of the particle so that the proper synchronization between the drive and the particle trajectory is attained.

In figure 7.10, we show how the work distribution $P(W)$ changes as a function

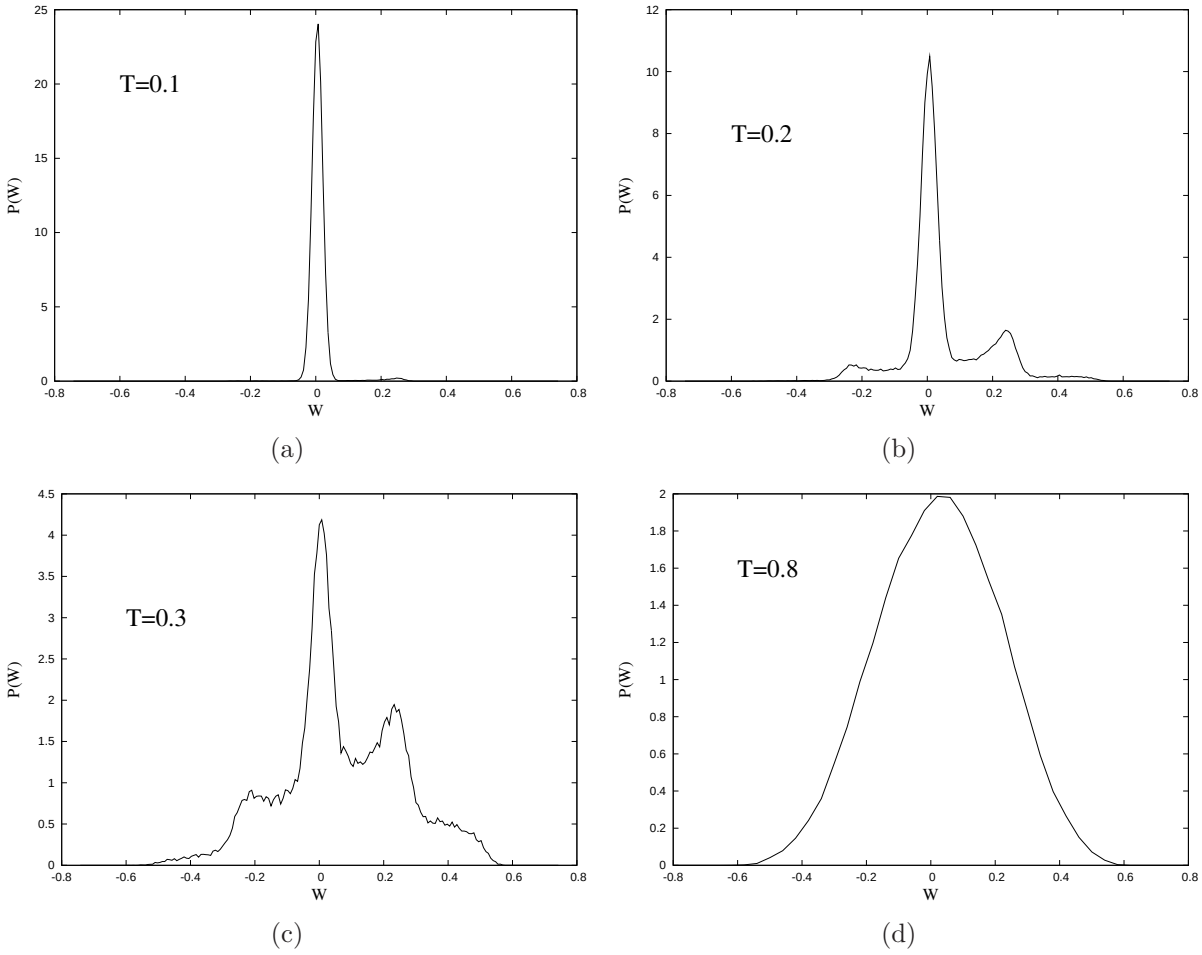

Figure 7.10: Work distributions at different temperatures for q=4. Other parameters are $A = 0.1$ and $\nu = 0.02$.

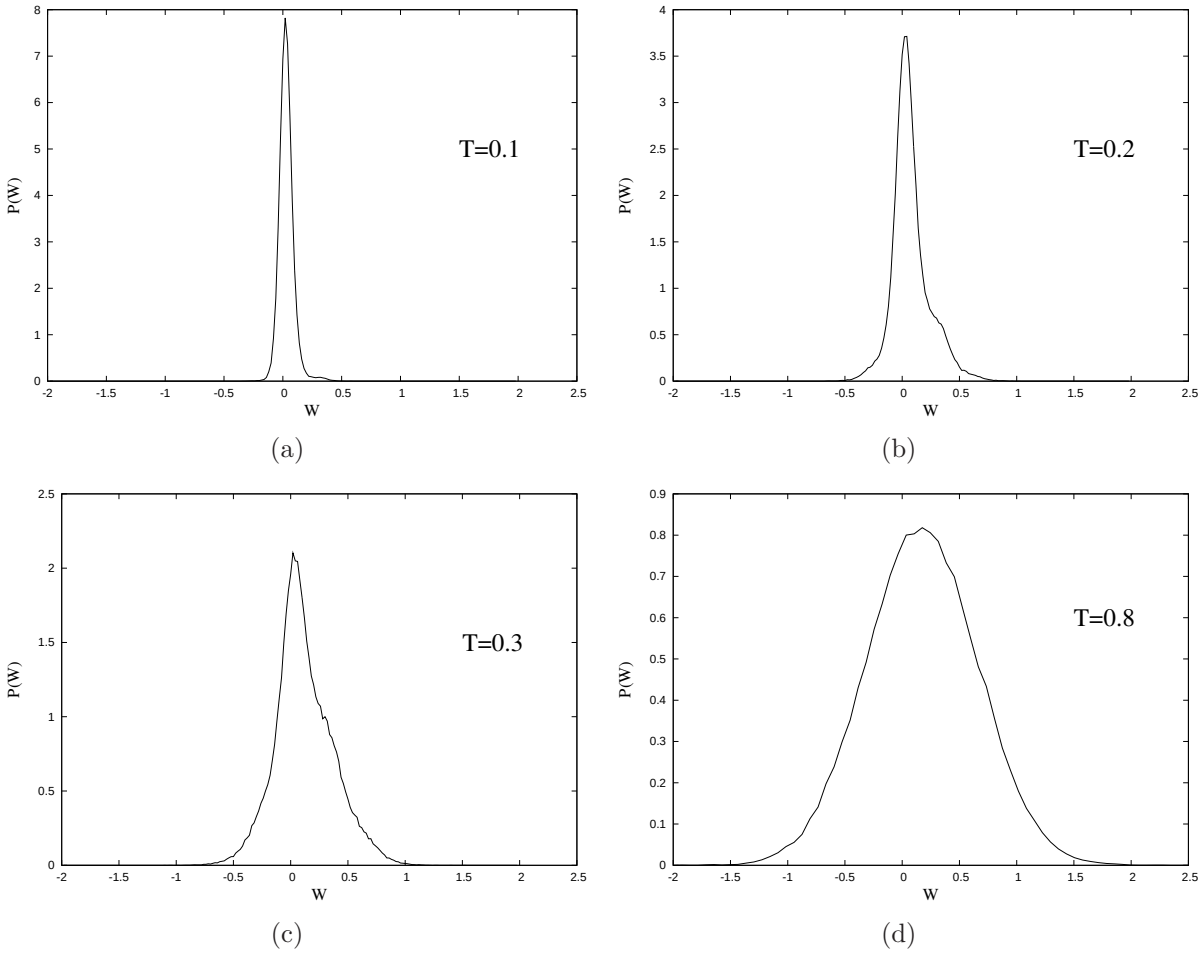

Figure 7.11: Work distributions at different temperatures for q=1.5. Other parameters are $A = 0.1$ and $\nu = 0.02$.

of T for the superharmonic potential with $q = 4$. At small temperature ($T = 0.1$, figure 7.10 (a)), the particle sees only a single well, the barrier height being too large for it to cross. Thus the work done is entirely due to intrawell dynamics and the distribution is almost Gaussian. Occasional excursion of the particle into the other well is clearly reflected as a small hump at higher values of W. As T increases, interwell dynamics starts playing dominant role and hence the distribution becomes broader (figures 7.10 (b) and (c)). Additional peak appears towards right mainly due to the interwell motion. A third peak also appears in the negative side. For large values of temperature beyond SR point, the dynamics is dominated by interwell motion and $P(W)$ tends towards a Gaussian distribution (figure 7.10 (d)).

The probability distribution for work has finite weight for negative values of W. These negative values correspond to the trajectories where the particle moves against the perturbing ac field over a cycle. The existence of finite weight for negative work values is essential to satisfy the recently discovered fluctuation theorems.

In figure 7.11, we have plotted the variations in the work distribution with temperature, for the subharmonic potential ($q = 1.5$). This time, however, we do not find the appearance of prominent double and multiple peaked distribution as was observed for the superharmonic potential. This is because the particles travel higher distances during intrawell as well as interwell motion, which gives rise to work values varying over a wide range. Moreover there is no clear-cut time scale separation between intrawell and interwell motion.Thus the two distinct peaks that were observed for $q = 4$ have got merged in $q = 1.5$ case.

7.4 Discussion and conclusions

In this chapter, we have studied the phenomenon of stochastic resonance in a bistable potential, using the mean input energy per cycle (or the mean work done per cycle)

$\langle W \rangle$ as a quantifier of resonance. We find that the system exhibits SR as a function of temperature for $q > 2$, but does not show SR for subharmonic potentials. This behaviour is further verified by studying the phase lag $\bar{\phi}$. Thus bistability is necessary but not sufficient condition for the observation of stochastic resonance. This result is consistent with the findings in [116]. However, in both the superharmonic and subharmonic potentials, the work exhibits resonance peak whereas the average amplitude of mean position decreases monotonically as a function of frequency. This is quite different from the trends of $\langle W \rangle$ and $\bar{x}$ as a function of temperature, which is sensitive to the nature of the confining potential. We have shown that the average power delivered to the system is not a good quantifier for bonafide resonance [117]. Our further investigation reveals qualitative differences in the nature of distributions for hard and soft potentials.

Chapter 8

Conclusions

Non-equilibrium processes are common in nature, but a general framework to understand them is lacking as compared to equilibrium systems. Recent development in the field of non-equilibrium statistical mechanics, had led for the discovery of fluctuation theorems (FT), which are exact equalities that are valid even when the system of interest is driven far away from equilibrium. For such a non-equilibrium system, the statistical distribution of thermodynamic quantities such as work, entropy etc. exhibit universal relations. These thermodynamic quantities have now been generalized to a single trajectory of system evolving in phase space. They are random variables depending on the phase space trajectory (stochastic thermodynamics). In this thesis we have mainly focused on the extensions of FTs to different scenarios and effects of thermal fluctuations on small system in different model systems.

We have generalized the fluctuation relation for heat engines (FRHE) to time-periodic steady states, which leads to the generalized Carnot's theorem. The FRHE in different limits results in Seifert's theorem and the generalized exchange fluctuation theorem. Our FRHE has been verified numerically in a simple realistic heat engine.

We have carried out an extensive analysis of a single particle stochastic heat engine by manipulating a Brownian particle in a harmonic trap with a periodically time dependent stiffness constant as a protocol. The cycle consists of two isothermal steps and two adiabatic steps similar to that of Carnot engine. The proposed model is studied taking into account both the inertial and overdamped Langevin equations. We have observed thermodynamic quantities, defined over microscopic phase space trajectory of our system, fluctuate from one cycle of operation to another in time periodic steady states. Our analytical results of average thermodynamic quantities in the quasistatic regime are consistent with the corresponding numerical results. We have reported several new results which were not addressed in earlier literature.

The full phase diagram for operation of a system is given for both inertial and high friction regime. It is found that they differ from each other qualitatively. In both cases

it is also shown that, unlike Carnot engine, system acts as an engine provided the temperature difference is greater than a critical value. The mean of the stochastic efficiency is dominated by its fluctuations ($\langle\eta\rangle < \sigma_\eta$) even in quasistatic regime, making the efficiency a non-self averaging quantity. This is one of our main result. We have also shown that $\bar{\eta} = \frac{\langle w\rangle}{\langle q_1\rangle} \neq \langle\frac{w}{q_1}\rangle = \langle\eta\rangle$. Our analysis of model dependence of finite cycle time clearly rules out any simple universal relation between efficiency at maximum power and temperature of the baths. We have also found time asymmetric periodic protocol makes engine less efficient. For given cycle time there are several realizations which do not work as a heat engine. The fraction of such realisations decreases as we increase τ. Thus for large cycle time the reliability of the system working as an engine increases.

Based on the path probability formulation of state space, we have extended Jarzynsky equality to quantum regime with multiple measurements and accompanying feedback. The quantum efficacy parameter retain same expressions as in the classical case. We have also derived generalized total entropy production FTs for quantum systems in presence of measurement and feedback, for three different cases. The second law of thermodynamics gets modified in the presence of information and feedback. For isolated quantum system with feedback, we have derived the generalized detailed fluctuation theorem (DFT) for the total entropy. The DFT retains the same form in presence of multiple measurements of any system observables, thus showing the robustness of these fluctuation theorems against measurements (von Neumann type or generalized measurements). The integral fluctuation theorem is valid for any initial arbitrary state of a system. However, DFT can be obtained only when the system either begins or ends in equilibrium or remains in the same nonequilibrium steady state.

The validity of FTs in presence of space-dependent friction is considered for both underdamped and overdamped limit. We find that, although no conceptual difficulties

arise when the system is underdamped, the derivation of the FTs are more involved for overdamped system. In latter case, where we have dealt with the Stratonovich scheme of discretization, the Langevin equation contains extra terms and the definition of heat gets modified. However, Crooks theorem remains unaltered. Thus, we conclude that the FTs remain valid for the case of dynamics of a particle in space dependent frictional medium, even under coarse graining. We have analyzed the nature of $P(\Delta s_{tot})$ and $P(W)$ for the simple case of a driven harmonic oscillator in presence of space dependent friction, both in underdamped and the overdamped regime (in Stratonovich prescription) numerically and verified the FTs.

We have also studied the phenomenon of stochastic resonance(SR) in a bistable potential, using the mean input energy per cycle (or the mean work done per cycle) $\langle W \rangle$ as a quantifier of resonance. We find that the system exhibits SR as a function of temperature for superharmonic potentials, but does not show SR for subharmonic potentials. This behavior is further verified by studying the phase lag $\bar{\phi}$. Thus bistability is necessary but not sufficient condition for the observation of stochastic resonance. However, in both the superharmonic and subharmonic potentials, we have observed resonance phenomenon as a function of driving frequency. We have shown that the average power delivered to the system is not a good quantifier for bonafide resonance. Our investigation reveals qualitative differences in the nature of work distributions for hard and soft potentials.

Appendix A

JE in presence of multiple measurements

We consider n number of intermediate measurements of any observable being performed at time $t_1, t_2, ..., t_n$ and the system collapses to its corresponding eigenstate at $|i_1\rangle, |i_2\rangle, ...|i_n\rangle$ respectively. Here we have considered the system evolves with the predetermined protocol $\lambda(t)$. The probability of the corresponding state trajectory

$$\begin{aligned} P(i_\tau, ...i_2, i_1, i_0) &= p(i_\tau|i_n)...p(i_2|i_1)p(i_1|i_0)p(i_0) \\ &= |\langle i_\tau|U_\lambda(\tau, t_n)|i_n\rangle|^2...|\langle i_2|U_\lambda(t_2, t_1)|i_1\rangle|^2|\langle i_1|U_\lambda(t_1, 0)|i_0\rangle|^2 p(i_0) \end{aligned} \tag{A.1}$$

$$\begin{aligned} &\langle e^{-\beta W}\rangle \\ &= \sum_{i_0, i_1, ..., i_\tau} e^{-\beta(E_{i_\tau}(\lambda(\tau)) - E_{i_0}(\lambda(0)))} P(i_\tau, ...i_2, i_1, i_0) \\ &= \sum_{i_0, i_1, ..., i_\tau} e^{-\beta(E_{i_\tau}(\lambda(\tau)) - E_{i_0}(\lambda(0)))} |\langle i_\tau|U_\lambda(\tau, t_n)|i_n\rangle|^2...|\langle i_2|U_\lambda(t_2, t_1)|i_1\rangle|^2 \\ &\qquad \times |\langle i_1|U_\lambda(t_1, 0)|i_0\rangle|^2 p(i_0). \end{aligned} \tag{A.2}$$

Using completeness and normalization of eigenstates $|i_0\rangle, |i_1\rangle, ...|i_n\rangle$ and unitarity of evolution, we get after simplification

$$\langle e^{-\beta W} \rangle = \sum_{i_\tau} \frac{e^{-\beta E_{i_\tau}(\lambda(\tau))}}{Z_0} = \frac{Z_\tau}{Z_0} = e^{-\beta \Delta F}. \tag{A.3}$$

Thus JE retain the same classical form even in presence of multiple measurements.

Appendix B

Multiple measurement and feedback

Let the outcome of measurement values at time $t_1, t_2, ..., t_n$ is $y_1, y_2, ..., y_n$ with a classical measurement error $p(y_1|i_1), p(y_2|i_2)\ , ..., p(y_n|i_n)$ respectively when actual intermediate states are $|i_1\rangle,\ |i_2\rangle \cdots |i_n\rangle$. The state $|i_0\rangle$ and $|i_\tau\rangle$ are observed projected eigenstates of energy observable in the beginning and end of the protocol. The total path probability can be expressed as

$$P(i_\tau, .., i_1, i_0, y_n, .., y_1) = |\langle i_\tau|U_{\lambda_{y_n}}(\tau, t_1)|i_n\rangle|^2 ... p(y_2|i_2)|\langle i_2|U_{\lambda_1}(t_2, t_1)|i_1\rangle|^2 p(y_1|i_1) \times|\langle i_1|U_\lambda(t_1, 0)|i_0\rangle|^2 p(i_0). \tag{B.1}$$

Now,

$$\langle e^{-\beta(W-\Delta F)-I}\rangle = \int dy_n, .., dy_1 \sum_{i_\tau,..,i_1,i_0} P(i_\tau, .., i_1, i_0, y_n, .., y_1) e^{-\beta(W-\Delta F)-I}. \tag{B.2}$$

Substituting value of work W (eq.(4.2)), mutual information $I = \ln \frac{p(y_n|i_n)...p(y_2|i_2)p(y_1|i_1)}{p(y_n,...y_2,y_1)}$, Free energy difference $\Delta F = \frac{Z_0}{Z_\tau(y_n)}$, and simplifying we get

$$
\begin{aligned}
&\left\langle e^{-\beta(W-\Delta F)-I}\right\rangle \\
&= \int dy_n \cdots dy_1 \sum_{i_\tau,..,i_1,i_0} |\langle i_\tau|U_{\lambda_{y_n}}(\tau,t_1)|i_n\rangle|^2 ...|\langle i_2|U_{\lambda_1}(t_2,t_1)|i_1\rangle|^2 |\langle i_1|U_\lambda(t_1,0)|i_0\rangle|^2 \\
&\qquad\qquad \times p(y_n,...,y_2,y_1)\frac{e^{-\beta E_{i_\tau}(\lambda_{y_n}(\tau))}}{Z_\tau(y_n)}, \\
&= \int dy_n \cdots dy_1 p(y_n,...,y_2,y_1) \sum_{i_\tau} \frac{e^{-\beta E_{i_\tau}(\lambda_{y_n}(\tau))}}{Z_\tau(y_n)}, \\
&= \int dy_n \cdots dy_1 p(y_n ... y_2,y_1) = 1. \qquad \text{(B.3)}
\end{aligned}
$$

Appendix C

Isolated system under weak measurements

In this appendix we derive IFT for ΔS_{tot} under weak measurement (POVM), as opposed to projective von Neumann type measurements considered in sec.5.2.1. We follow the mathametical treatment given in [96]. For simplicity we consider only one weak measurement is performed at intermediate time. The genaralization to multiple weak measurements is straight forward. Consider an isolated quantum system is controlled externally through time dependent protocol $\lambda(t)$. Initially at $t = 0$ energy measurement is performed and the system is found to be in state $|n, 0\rangle$ with probability density p_n. The density matrix becomes

$$\rho_n(0^+) = \frac{\Pi_n^0 \rho_0 \Pi_n^0}{p_n} \tag{C.1}$$

where ρ_0 is the density matrix of the system before measurement and Π_n^0 denotes von Neumann projective measurement operator and $p_n = \text{Tr } \Pi_n^0 \rho_0$. The system then evolves unitarily up to time t_1 and a weak measurement is performed and we get the density matrix

$$\rho_n(t_1^+) = \sum_r M_r U_\lambda(t_1, 0) \rho_n(0^+) U_\lambda^\dagger(t_1, 0) M_r^\dagger. \tag{C.2}$$

M_r is the weak measurement operator with property $\sum_r M_r M_r^\dagger = 1$. The system undergoes further unitarily evolution and finally the projective measurement is performed and the system is found to be in state $|m, \tau\rangle$ at time τ. The conditional

probability $P_\lambda(m,\tau|n,0)$ for system initially in state $|n,0\rangle$ and finally in state $|m,\tau\rangle$ is given by

$$P_\lambda(m,\tau|n,0) = \text{Tr } \Pi_m^f U_\lambda(\tau,t_1)\rho_n(t_1^+)U_\lambda^\dagger(\tau,t_1). \tag{C.3}$$

Thus the probability of the change in total entropy,

$$\Delta S_{tot} = -\ln p_m + \ln p_n, \tag{C.4}$$

for a given pre-determined protocol $\lambda(t)$ is

$$P_\lambda(\Delta S_{tot}) = \sum_{m,n} \delta(\Delta S_{tot} + \ln p_m - \ln p_n) P_\lambda(m,\tau|n,0) p_n. \tag{C.5}$$

where p_m is the probability of the system to stay at the end of protocol at final time τ. The Fourier Transform of this probability is

$$G_\lambda(u) = \int d\Delta S_{tot} P_\lambda(\Delta S_{tot}) e^{iu\Delta S_{tot}}. \tag{C.6}$$

Substituting the expression for $P_\lambda(\Delta S_{tot})$ from eq.(C.5) and using eqs.(C.3),(C.2),(C.1) we get

$$\begin{aligned}
G_\lambda(u) &= \sum_{m,n,r} e^{iu(-\ln p_m + \ln p_n)} \text{Tr } \Pi_m^f U_\lambda(\tau,t_1) M_r U_\lambda(t_1,0) \Pi_n^0 \rho_0 \Pi_n^0 U_\lambda^\dagger(t_1,0) M_r^\dagger U_\lambda^\dagger(\tau,t_1) \\
&= \sum_{m,n,r} \text{Tr } \Pi_m^f e^{-iu\ln\rho_f} U_\lambda(\tau,t_1) M_r U_\lambda(t_1,0) \Pi_n^0 e^{iu\ln\rho_0} \rho_0 U_\lambda^\dagger(t_1,0) M_r^\dagger U_\lambda^\dagger(\tau,t_1) \\
&= \sum_r \text{Tr } e^{-iu\ln\rho_f} U_\lambda(\tau,t_1) M_r U_\lambda(t_1,0) e^{iu\ln\rho_0} \rho_0 U_\lambda^\dagger(t_1,0) M_r^\dagger U_\lambda^\dagger(\tau,t_1) \\
&= \sum_r \text{Tr } U_\lambda^\dagger(t_1,0) M_r^\dagger U_\lambda^\dagger(\tau,t_1) e^{-iu\ln\rho_f} U_\lambda(\tau,t_1) M_r U_\lambda(t_1,0) e^{iu\ln\rho_0} \rho_0
\end{aligned} \tag{C.7}$$

ρ_f is the final density matrix which is diagonal in the energy basis. In the second step we have used the completeness relation $\sum_m \Pi_m^f = 1$ and $\sum_n \Pi_n^0 = 1$ for the projective operator. Substituting $u = i$, for the Fourier Transform variable, we get

from eq.(C.6) $G_\lambda(i) = \langle e^{-\Delta S_{tot}} \rangle$ and hence

$$\begin{aligned}
\langle e^{-\Delta S_{tot}} \rangle &= \sum_r \text{Tr } U_\lambda^\dagger(t_1,0) M_r^\dagger U_\lambda^\dagger(\tau,t_1) e^{\ln \rho_f} U_\lambda(\tau,t_1) M_r U_\lambda(t_1,0) e^{-\ln \rho_0} \rho_0 \\
&= \sum_r \text{Tr } U_\lambda^\dagger(t_1,0) M_r^\dagger U_\lambda^\dagger(\tau,t_1) e^{\ln \rho_f} U_\lambda(\tau,t_1) M_r U_\lambda(t_1,0) \\
&= \sum_r \text{Tr } U_\lambda(\tau,t_1) M_r U_\lambda(t_1,0) U_\lambda^\dagger(t_1,0) M_r^\dagger U_\lambda^\dagger(\tau,t_1) e^{\ln \rho_f} \\
&= \sum_r \text{Tr } U_\lambda(\tau,t_1) M_r M_r^\dagger U_\lambda^\dagger(\tau,t_1) e^{\ln \rho_f} \\
&= \text{Tr } U_\lambda(\tau,t_1) U_\lambda^\dagger(\tau,t_1) e^{\ln \rho_f} \\
&= \text{Tr } e^{\ln \rho_f} = \text{Tr } \rho_f = 1. \qquad \text{(C.8)}
\end{aligned}$$

In the second line , we make use of $e^{-\ln \rho_0} \rho_0 = 1$, while the cyclic property of trace is used in the third line. operator identity $\sum_r M_r M_r^\dagger = 1$ is used in fourth step.

We have proved that the IFT holds in the same form as in eq.(5.1) under intermediate weak measurements. This can be readily generalized to the multiple intermediate weak measurements, which corroborates the robustness of fluctuation theorems under weak or generalized measurements.

Appendix D

Space dependent friction in overdamped limit

The general form of overdamped Langevin equation is

$$\dot{x} = -\Gamma(x)\frac{\partial V(x)}{\partial x} + f_1(x) + g(x)\xi(t) = f(x) + g(x)\xi(t), \tag{D.1}$$

where $\Gamma(x) = \frac{1}{\gamma(x)}$ and $g^2(x) = 2\Gamma(x)k_BT$. Note that one extra term $f_1(x)$ is added into the ordinary overdamped equation. This extra term arises due to the correlations of noise with the state dependent diffusion constant. In the following, this term will be determined. Now, integrating between t and $t + \Delta t$ one can obtain,

$$x(t + \Delta t) - x(t) \equiv \Delta x(t + \Delta t) = \int_t^{t+\Delta t} ds\{f[x(s)] + g[x(s)]\xi(s)\}. \tag{D.2}$$

Since, $\xi(s)$ is not continuous, we define

$$\int_t^{t+\Delta t} dsg[x(s)]\xi(s) = g[(1-\alpha)x(t) + \alpha x(t + \Delta t)] \int_t^{t+\Delta t} ds\xi(s), \tag{D.3}$$

where $\alpha \in [0, 1]$. Now, one can rewrite

$$(1-\alpha)x(t) + \alpha x(t + \Delta t) = x(t) + \alpha(x(t + \Delta t) - x(t)) = x(t) + \alpha\Delta x(t + \Delta t)). \tag{D.4}$$

Setting $x(t) = x_0$, we can write as $\Delta t \to 0$

$$\Delta x = f[x_0 + \alpha \Delta x]\Delta t + g[x_0 + \alpha \Delta x] \int_t^{t+\Delta t} ds\xi(s). \tag{D.5}$$

Expanding upto the first order of Δt, one can obtain

$$\begin{aligned}
\Delta x \quad &\approx f(x_0)\Delta t + \{g(x_0) + \alpha \Delta x g'(x_0)\} \int_t^{t+\Delta t} ds\xi(s) \\
&= f(x_0)\Delta t + g(x_0) \int_t^{t+\Delta t} ds\xi(s) \\
&\quad + \alpha g'(x_0) \left[f(x_0)\Delta t + \{g(x_0) + \alpha \Delta x g'(x_0)\} \int_t^{t+\Delta t} ds'\xi(s') \right] \int_t^{t+\Delta t} ds\xi(s) \\
\Rightarrow \langle \Delta x \rangle \quad &= f(x_0)\Delta t + \alpha g(x_0) g'(x_0) \int_t^{t+\Delta t} ds' \int_t^{t+\Delta t} ds \langle \xi(s)\xi(s') \rangle + O(\Delta x \Delta t) \\
&\approx f(x_0)\Delta t + \alpha g(x_0) g'(x_0) \Delta t.
\end{aligned} \tag{D.6}$$

From (D.5) one can also gets

$$\begin{aligned}
(\Delta x)^2 \quad &= \left[f(x_0)\Delta t + \{g(x_0) + \alpha \Delta x \; g'(x_0)\} \int_t^{t+\Delta t} ds\xi(s) \right]^2 \\
\Rightarrow \langle (\Delta x)^2 \rangle \quad &\approx \left[g^2(x_0) + 2\alpha \Delta x \; g(x_0) g'(x_0) \right] \int_t^{t+\Delta t} ds \int_t^{t+\Delta t} ds' \langle \xi(s)\xi(s') \rangle \\
&= \left[g^2(x_0) + 2\alpha \Delta x \; g(x_0) g'(x_0) \right] \Delta t \\
&\approx g^2(x_0)\Delta t
\end{aligned} \tag{D.7}$$

Let us now derive the Fokker Planck equation corresponding to the general Langevin equation (D.1). The Chapman-Kolmogorov equation for Markov processes simply determines the probability of the particle that can reach x in time $t + \Delta t$ from any other point x_0 at time t and is given by

$$P(x, t + \Delta t) = \int dx_0 \; P(x, t + \Delta t | x, t) P(x_0, t). \tag{D.8}$$

Now, from the basic definition of the probability

$$\begin{aligned}
&P(x,t+\Delta t|x,t)\\
&=\langle\delta[x-x(t+\Delta t)]\rangle_{x_0,t}\\
&=\delta(x-x_0)-\langle\Delta x\rangle\frac{\partial}{\partial x}\delta(x-x_0)+\frac{1}{2}\langle(\delta x)^2\rangle\frac{\partial^2}{\partial x^2}\delta(x-x_0)+\ldots
\end{aligned}\tag{D.9}$$

In second line we made a Taylor expansion. Using this one can write

$$\begin{aligned}
&P(x,t+\Delta t)\\
&=\int dx_0\left[\delta(x-x_0)-\langle\Delta x\rangle\frac{\partial}{\partial x}\delta(x-x_0)+\frac{1}{2}\langle(\delta x)^2\rangle\frac{\partial^2}{\partial x^2}\delta(x-x_0)+\ldots\right]P(x_0,t)\\
&=P(x,t)-\int dx_0\langle\Delta x\rangle\{\frac{\partial}{\partial x}\delta(x-x_0)\}P(x_0,t)+\frac{1}{2}\int dx_0\langle(\delta x)^2\rangle\{\frac{\partial^2}{\partial x^2}\delta(x-x_0)\}P(x_0,t)\\
&=P(x,t)-\int dx_0\left[f(x_0)\Delta t+\alpha g(x_0)g'(x_0)\Delta t\right]\{\frac{\partial}{\partial x}\delta(x-x_0)\}P(x_0,t)\\
&\quad+\frac{1}{2}\int dx_0\left[g^2(x_0)\Delta t\right]\{\frac{\partial^2}{\partial x^2}\delta(x-x_0)\}P(x_0,t)\\
&=P(x,t)-\frac{\partial}{\partial x}\int dx_0\left[f(x_0)\Delta t+\alpha g(x_0)g'(x_0)\Delta t\right]\delta(x-x_0)P(x_0,t)\\
&\quad+\frac{\partial^2}{\partial x^2}\frac{1}{2}\int dx_0\left[g^2(x_0)\Delta t\right]\delta(x-x_0)P(x_0,t).
\end{aligned}\tag{D.10}$$

Thus from the definition

$$\frac{\partial P(x,t)}{\partial t}=\frac{P(x,t+\Delta t)-P(x,t)}{\Delta t},\tag{D.11}$$

we get the Fokker-Planck equation

$$\frac{\partial P(x,t)}{\partial t}=-\frac{\partial}{\partial x}\{\left[f(x)+\alpha g(x)g'(x)\right]P(x,t)\}+\frac{1}{2}\frac{\partial^2}{\partial x^2}\{g^2(x)P(x,t)\}.\tag{D.12}$$

If we put the expression of $f(x)$ into the above equation,we get

$$\frac{\partial P(x,t)}{\partial t}=\frac{\partial}{\partial x}\left(\left[\Gamma(x)V'(x)-f_1(x)+(1-\alpha)g(x)g'(x)+\frac{1}{2}g^2(x)\frac{\partial}{\partial x}\right]P(x,t)\right)\tag{D.13}$$

For a system in equilibrium, the distribution must be canonical and must follow $P(x,t) \sim e^{-\beta H}$ where β is the inverse temperature and H is the corresponding Hamiltonian. Then in equilibrium

$$\begin{aligned}
& \frac{\partial}{\partial x}\left(\left[\Gamma(x)V'(x) - f_1(x) + (1-\alpha)g(x)g'(x) + \frac{1}{2}g^2(x)\frac{\partial}{\partial x}\right]P(x,t)\right) = 0 \\
\Rightarrow \quad & \left[\Gamma(x)V'(x) - f_1(x) + (1-\alpha)g(x)g'(x) + \frac{1}{2}g^2(x)\frac{\partial}{\partial x}\right]P(x,t) = C \\
\Rightarrow \quad & \frac{1}{2}g^2(x)\frac{\partial}{\partial x}P(x,t) + \left[\Gamma(x)V'(x) - f_1(x) + (1-\alpha)g(x)g'(x)\right]P(x,t) = C \\
\Rightarrow \quad & \frac{\partial P(x,t)}{\partial x} + \frac{2}{g^2(x)}\left[\Gamma(x)V'(x) - f_1(x) + (1-\alpha)g(x)g'(x)\right]P(x,t) = \frac{2C}{g^2(x)} \\
\Rightarrow \quad & \frac{\partial P(x,t)}{\partial x} + \lambda(x)P(x,t) = \frac{2C}{g^2(x)}.
\end{aligned} \tag{D.14}$$

The integrating factor of the above equation is $\exp[\int \lambda(x)dx]$. Now to fulfill the criterion for equilibrium distribution, we must have

$$\int \lambda(x)dx = \beta V(x) \Rightarrow \lambda(x) = \beta V'(x). \tag{D.15}$$

which implies

$$g^2(x) = 2k_B T\Gamma(x) \tag{D.16}$$

$$f_1(x) = (1-\alpha)g(x)g'(x) = (1-\alpha)k_B T\Gamma'(x) \tag{D.17}$$

Now, Putting the expression of $f_1(x)$, the general overdamped equation become:

$$\dot{x} = -\Gamma(x)V'(x) + (1-\alpha)k_B T\Gamma'(x) + g(x)\xi(t) \tag{D.18}$$

Substituting $\gamma(x) = \frac{1}{\Gamma(x)}$ and using the expression of $g(x)$ and rearranging we get

$$\gamma(x)\dot{x} = -V'(x) - (1-\alpha)k_B T\frac{\gamma'(x)}{\gamma(x)} + \sqrt{2k_B T\gamma(x)}\xi(t). \tag{D.19}$$

For Forward evolution we already have

$$\int_t^{t+\Delta t} dsg[x(s)]\xi(s) = g[(1-\alpha)x(t) + \alpha x(t+\Delta t)] \int_t^{t+\Delta t} ds\xi(s). \tag{D.20}$$

Now the backward evolution can be simply obtained by changing the initial and final integral limits (for normal integrals $\int_a^b = -\int_b^a$). However as the integral is Wiener integrals we can write for backward evolution with variable $\bar{x}$ as

$$\begin{aligned} \int_{t+\Delta t}^{t} dsg[\bar{x}(s)]\xi(s) \quad &= g[(1-\alpha)\bar{x}(t+\Delta t) + \alpha\bar{x}(t)] \int_{t++\Delta t}^{t} ds\xi(s) \\ &= g[\alpha\bar{x}(t) + (1-\alpha)\bar{x}(t+\Delta t)] \int_{t++\Delta t}^{t} ds\xi(s). \end{aligned} \tag{D.21}$$

Therefore, the backward evolution for the space dependent friction is characterized by

$$\begin{aligned} &x(t) \to \bar{x}(t) = x(-t) \\ &\alpha \leftrightarrow (1-\alpha). \end{aligned} \tag{D.22}$$

Bibliography

[1] H. B. Callen, Thermodynamics and an Introduction to Thermostatistics (John Wiley & Sons, 2006).

[2] L. D. Landau, E. M. Lifsitz, Statistical Physics, Butterworth-Heinemann, 3rd Ed., (1980).

[3] L. E. Reichl A modern course in statistical physics. 1998. Edward Arnold, London, 1986.

[4] S. Chandrasekhar, Rev. Mod. Phys. **15**, 1 (1943).

[5] R. Zwanzig, Nonequilibrium Statistical Mechanics, Oxford University Press, USA, 1st Ed. (2001).

[6] N. G. Van Kampen, Stochastic Processes in Physics and Chemistry, North Holland, 3rd Ed. (2007).

[7] H.Risken, *The Fokker-Planck equation*, second edition, Springer (1989).

[8]] C. Gardiner, Handbook of Stochastic Methods: for Physics, Chemistry and the Natural Sciences, Springer, 3rd Ed. (2004).

[9] J. R. Dorfman, An Introduction to Chaos in Nonequilibrium Statistical Mechanics, Cambridge University Press, (1999).

[10] P. C. Hohenberg, B. I. Halperin, Rev. Mod. Phys. **49**, 435 (1977).

[11] K. Sekimoto, Stochastic Energetics (Springer, 2010).

[12] K. Sekimoto, Prog. Theor. Phys. Suppl. **130**, 17 (1998).

[13] U. Seifert, Eur. Phys. J. B **64**, 423 (2008).

[14] V. Holubec, arXiv: 1404.2030.

[15] D. J. Evans and D. J. Searles, Adv. Phys. **51**, 1529 (2002).

[16] R. J. Harris and G. M. Schütz, J. Stat. Mech. **07**, 07020 (2007).

[17] F. Ritort, Sem. Poincare **2**, 63 (2003).

[18] F. Ritort, J. Phys. Condens. Matter **18**, R531 (2006).

[19] J. Kurchan, J. Stat. Mech. **07**, 07005 (2007).

[20] D. J. Evans, E. G. D. Cohen and G. P. Morriss, Phys. Rev. Lett. **71**, 2401 (1993); **71**, 3616 (1993) [errata].

[21] D. J. Evans and D. J. Searles, Phys. Rev. E **50**, 1645 (1994).

[22] G. Gallavotti and E. G. D. Cohen, Phys. Rev. Lett. **74**, 2694 (1995); J. Stat. Phys. **80**, 31 (1995).

[23] C. Jarzynski, Phys. Rev. Lett. **78**, 2690 (1997).

[24] R. van Zon and E. G. D. Cohen, Phys. Rev. E **67**, 046102 (2003).

[25] R. van Zon and E. G. D. Cohen, Phys. Rev. E **69**, 056121 (2004).

[26] O. Narayan and A. Dhar, J. Phys. A: Math Gen **37**, 63 (2004).

[27] Udo Seifert, Phys. Rev. Lett. **95**, 040602 (2005).

[28] G. E. Crooks, J. Stat. Phys. **90**, 1481 (1998).

[29] G. E. Crooks, Phys. Rev. E **60**, 2721 (1999).

[30] U. Seifert, Rep. Prog. Phys. **75**, 126001 (2012).

[31] M. Esposito and S. Mukamel, Phys. Rev. E **73**, 046129 (2006).

[32] T. Monnai, Phys. Rev. E **72**, 027102 (2005).

[33] S. Deffner and E. Lutz Phys. Rev. E **77**, 021128 (2007).

[34] P. Talkner, M. Campisi and P. Hänggi, J. Stat. Mech. **02**, 02025 (2009).

[35] S. Deffner and E. Lutz Phys. Rev. Lett. **107**, 140404 (2011).

[36] R. van Zon and E. G. D. Cohen, Phys. Rev. Lett. **91**, 110601 (2003).

[37] C. Bustamante, Z. Bryant, S. Smith et al.: Nature pages 423426 (2003).

[38] C. Bustamante, J. Liphardt and F. Ritort, Phys. Today **58**, 43 (2005).

[39] K. Visscher, M. Schnitzer and S. Block: Nature **400**, 184 (1999).

[40] W. Ducker, T. Senden and R. Pashley: Nature **353**, 239 (1991).

[41] L. P. Pitaevskii, Phys.-Usp. **54**, 625 (2011).

[42] M. Sahoo, S. Lahiri and A. M. Jayannavar, J. Phys. A: Math. Theor. **44**, 205001 (2011).

[43] T. M. Cover and J. A. Thomas, *Elements of Information Theory*, 2nd. Ed. (Wiley-Interscience, Hoboken, NJ, 2006).

[44] M. Campisi, P. Hänggi and P. Talkner, Rev. Mod. Phys. **83**, 771 (2011).

[45] T. Sagawa and M. Ueda, Phys. Rev. Lett. **104**, 090602 (2010).

[46] T. Sagawa and M. Ueda, Phys. Rev. E **85**, 021104 (2012).

[47] S. Lahiri, S. Rana and A. M. Jayannavar, J. Phys. A: Math theor **45**, 065002 (2012).

[48] T. Sagawa and M. Ueda, Phys. Rev. Lett. **102**, 250602 (2009).

[49] J.M.R. Parrondo, J. M. Horowitz, T. Sagawa, Nature Physics **11**, 131 (2015).

[50] S. Deffner and C. Jarzynski, Phys. Rev. X **3**, 041003 (2013).

[51] N. A. Sinitsyn, J. Phys. A: Math theor **44**, 405001 (2011).

[52] G Verley, M Esposito, T Willaert, C Van den Broeck, Nature comm. **5**, 4721 (2014).

[53] Y. Oono and M. Paniconi, Prog. Theor. Phys. Suppl. **130**, 29, (1998).

[54] T. Hatano and S. Sasa, Phys. Rev Lett. **86**, 3463, (2001).

[55] C. Jarzynski, Eur. Phys. J. B **64**, 331 (2008).

[56] T. Speck and U seifert, J. Phys. A: Math theor **38**, 581 (2005).

[57] M. Esposito and C. Van Den Broeck Europhys. Lett. **95**, 40004 (2011).

[58] R. Landauer, Phys. Today **44**, 23 (1991).

[59] L. Gammaitoni, P. Hänggi, P. Jung, and F. Marchesoni, Rev. Mod. Phys. **70**, 223 (1998).

[60] L. Gammaitoni, P. Hänggi, P. Jung and F. Marchesoni, Eur. Phys. J. B **69**, 13 (2009).

[61] K. Wiesenfeld and F. Moss, Nature **373** 33 (1995).

[62] F. Moss and K. Wiesenfeld, Scientific American **273**, 66 (1995).

[63] M. Evstigneev, P. Reimann, C. Schmitt and C. Bechinger, J. Phys. Condens. Matter **17**, S3795 (2005).

[64] T. Iwai, J. Phys. A: Math theor **300**, 350 (2001).

[65] H. T. Quan and H. Dong, arxiv/cond-mat: 0812.4955.

[66] V. Blickle and C. Bechinger, Nature Phys. **8**, 143 (2012).

[67] P. Chvosta et al, J. Stat. Mech. **03**, 03002 (2010).

[68] C. Jarzynski and D. K. Wojcik, Phys. Rev. Lett. **92**, 230602 (2004).

[69] O. Mazonka and C. Jarzynski, arxiv: cond-mat/9912121.

[70] T. Speck, J. Phys. A: Math theor **44**, 305001 (2011).

[71] F. L. Curzon and B. Ahlborn, Am. J. Phys. **43**, 22 (1975).

[72] T. Schmiedl and U. Seifert, Europhys. Lett. **81**, 20003 (2008).

[73] C. Van den Broeck, Phys. Rev. Lett. **95**, 190602 (2005).

[74] M. Esposito, R. Kawai, K. Lindenberg and C. Van den Broeck, Phys. Rev. Lett. **105**, 150603 (2010).

[75] S. Sheng and Z. C. Tu, arXiv: 1404.7008.

[76] D. Dan and A. M. Jayannavar, Physica A. **345**, 404 (2005).

[77] S. Saikia, R. Roy and A. M. Jayannavar. Phys. Lett. A. **369**,, 367 (2007)

[78] P. Jop, A. Petrosyan and S. Ciiberto. Europhys. Lett. **81**, 50005 (2008).

[79] J. Hoppenau, M. Niemann, and A. Engel, Phys. Rev. E **87**, 062127 (2013).

[80] Z. C. Tu, Phys. Rev. E **89**, 052148 (2014).

[81] S. Lahiri, S. Rana, A. M. Jayannavar, J. Phys. A: Math theor **45**, 465001 (2012).

[82] M. Campisi, J. Phys. A: Math theor **47**, 245001 (2014).

[83] W. T. Coffey, Yu. P. Kalmykov and J. T. Waldorn, The Langevin Equatin (World Scientific 2004).

[84] R. Mannela, in: J.A. Freund and T. Poschel (Eds), Stochastic Process in Physics, Chemistry and Biology, Lecture Notes in Physics, vol. 557 Springer-Verlag, Berlin(2000) p353.

[85] E. Boksenbojm, B. Wynants and C. Jarzynski, Physica A. **389**, 4406 (2010).

[86] G. M. Wang, E. M. Sevick, E. Mittag, D. J. Searles, and D. J. Evans, Phys. Rev. Lett. **89**, 050601 (2002).

[87] S. Lahiri and A. M. Jayannavar Eur. Phys. J. B **69**, 87 (2009).

[88] A. Saha, S. Lahiri and A. M. Jayannavar, Phys. Rev. E **80**, 011117 (2009).

[89] M. Campisi, P. Talkner and P. Hänggi, Phys. Rev. Lett. **105**, 140601 (2010).

[90] T. Sagawa and M. Ueda, Phys. Rev. Lett. **100**, 080403 (2008).

[91] Y. Morikuni and H. Tasaki, J. Stat. Phys. **143**, 1 (2011).

[92] S. Toyabe, T. Sagawa, M. Ueda, E. Muneyuki and M. Sano, Nature Physics **6**, 988 (2010).

[93] A. Hopkins, K. Jacobs, S. Habib and K. Schwab, Phys. Rev. B **68**, 235328 (2003).

[94] D. Steck, K. Jacobs, H. Mabuchi, T. Bhattacharya and S. Habib, Phys. Rev. Lett. **92**, 223004 (2004).

[95] T. Sagawa, J. Phys.: Conf. Ser. **297**, 012015 (2011).

[96] M. Campisi, P. Talkner and P. Hänggi, Phys. Rev. E **83**, 041114 (2011).

[97] J. M. Horowitz and S. Vaikuntanthan, Phys. Rev. E **82**, 061120 (2010).

[98] S. Deffner and E. Lutz, arXiv/cond-mat: 1201.3888.

[99] K. Jacobs, arxiv: quant-ph/0605015.

[100] K. Jacobs and A. Shabani, Contemp. Phys. **49**, 435 (2008).

[101] M. Ponmurugan, Phys. Rev. E **82**, 031129 (2010).

[102] S. Rana, S. Lahiri and A. M. Jayannavar, Pramana J. Phys. **79**, 233 (2012).

[103] J. M. Sancho, M. San Miguel and D. Durr, J. Stat. Phys. **28**, 291 (1982).

[104] A. M. Jayannavar and M. C. Mahato, Pramana J. Phys. **45**, 369 (1995)

[105] A. M. Jayannavar, arXiv:cond-mat/0107079.

[106] A. W. C. Lau and T. C. Lubensky, Phys. Rev. E **76**, 011123 (2007).

[107] A. Imparato, L. Peliti, Phys. Rev. E **74**, 026106 (2006).

[108] R. D. Astumian Am. J. Phys. **74**, 683 (2006).

[109] S. Joubaud, N. Garnier and S. Ciliberto, Journal of Statistical Mechanics: Theory and Experiment. **09**, 09018, (2007).

[110] M. Sahoo and A. M Jayannavar,Indian Journal of Physics **84**, 1421 (2010).

[111] D. Stauffer, *Annual reviews of computational physics IX*, World Scientific.

[112] R. Mannella, P. V. E. McClintock, Fluctuation and Noise Letters, **11** 1240010 (2010).

[113] Z. G. Arenas and D. G. Barci, J. Stat. Mech. **12**, 12005 (2012).

[114] D. Dan and A. M. Jayannavar, Physica A **345**, 404 (2005).

[115] M. Sahoo, S. Saikia, M. C. Mahato and A. M. Jayannavar, Physica A **387**, 6284 (2008).

[116] E. Heinsalu, M. Patriarca and F. Marchesoni, Eur. Phys. J. B **69**, 19 (2009).

[117] P.Jung and F.Marchesoni, CHAOS, **21**, 047516 (2011).

[118] M. I. Dykman and R. Mannella, Phys. Rev. Lett. **68**, 2985 (1992).